Investigation of Low Molecular Weight Chitosan Nanoparticles for CpG ODN 1826 Delivery

by

Oksana Babii

A thesis submitted in partial fulfillment of the requirements for the degree of

Master of Science

in

Food Science and Technology

Department of Agricultural, Food and Nutritional Science
University of Alberta

Abstract

Synthetic oligonucleotides containing unmethylated CpG motifs (CpG ODNs) are powerful stimulators of innate and adaptive immune responses, exerting their activity through the interaction with endolysosomal Toll-like receptor 9 (TLR9) expressed by antigen presenting cells (APCs). The strong immunopotency and a wide range of activity support the use of CpG ODNs as an effective treatment and prevention strategy to combat various infectious diseases. Recent evidence suggested that CpG ODNs might be a potent candidate for Bovine respiratory disease immunotherapy in the livestock. Nevertheless, their stimulatory activity is often transient due to the high susceptibility of free CpG ODNs to the serum nuclease degradation, poor targeting capacity, and inefficient cellular uptake. The overall objective of this research was to develop a vector system based on chitosan nanoparticles suitable for the efficient CpG ODN delivery to the target APCs, with minimal cellular toxicity. In particular, the influence of molecular structure of chitosan, such as the molecular weight, the degree of deacetylation and mannose grafting on the properties of CpG ODN-loaded nanoparticles was investigated.

Chitosan samples with the molecular weights of 5 and 15 kDa and the degree of deacetylation of 50 and 80 % were prepared. Additionally, mannosylated chitosans with a substitution degree of 15% were synthesized. The self-assembled chitosan nanoparticles were produced by ionic gelation method using poly (L-glutamic acid) as a cross-linking agent. The CpG ODN – loaded nanoparticles had the encapsulation efficiency over 88%, average hydrodynamic diameters ranging from 101.8 to 184.5 nm, and zeta potential values from +20.1 to +30.1 mV, providing desirable size and charge for targeting APCs.

It was found that physicochemical properties and *in vitro* immunostimulatory effect of CpG ODN-loaded nanoparticles were strongly dependent on the chitosan molecular weight and degree

of deacetylation. The size of nanoparticles was significantly reduced by lowering the chitosans molecular weight from 15 to 5 kDa. Moreover, chitosan with the molecular weight of 15 kDa formed more stable nanoparticles compared to 5 kDa sample due to the stronger chain entanglement effect. Chitosans with the molecular weight of 5 kDa tent to dissociate at pH 5.9 and prematurely release their cargo, which compromised their efficacy as a vector for the CpG ODN delivery. At the same time, increasing the degree of deacetylation facilitated the formation of nanoparticles with smaller sizes and higher surface charges due to the increased cationic charge density on the chitosan backbone. Samples with a higher degree of deacetylation exhibited a better CpG ODNs binding ability and were able to assemble into more stable nanoparticles when cross-linked by poly (L-glutamic acid).

There was no evidence of cellular toxicity of chitosan nanoparticles regardless of the molecular weight, degree of deacetylation or mannose grafting towards the RAW 264.7 cells. Furthermore, CpG ODN-loaded nanoparticles were biologically active, showing successful stimulation of IL-6 secretion in RAW 264.7 cells. The most efficient immunostimulatory effect was observed while using 50% acetylated and mannosylated chitosan samples with the molecular weight of 15 kDa. The decreased charge density of the chitosan backbone resulted in enhanced intracellular CPG ODN release, which promoted cytokine secretion *in vitro*. Overall, these finding extended the application of chitosan-based nanoparticles as efficient vectors for the intracellular delivery of CpG ODNs and revealed their potential use for the Bovine respiratory disease immunotherapy.

Preface

This thesis is an original work by Oksana Babii. A manuscript has been generated based on Chapter 2. Soon, it will be submitted to a peer-reviewed journal by Oksana Babii, Guangyu Liu, Elisa C. Martinez, Sylvia van Drunen Littel-van den Hurk, and Lingyun Chen. I was responsible for the study design, its conduct, data collection and analysis as well as for manuscript writing. Dr. Guangyu Liu and Elisa C. Martinez assisted with the experimental design and technical training. Dr. Sylvia van Drunen Littel-van den Hurk was a supervisory committee member and co-corresponding author. She contributed to the experimental design, data discussion, and manuscript editing. Dr. Lingyun Chen, as a supervisor and a co-corresponding author, she contributed to the experimental design, data discussion and was responsible for manuscript revision and submission.

Dedication

This thesis is dedicated to the memory of my loving parents,

Olga and Peter,

You taught me to never give up.

Acknowledgements

Firstly, I would like to express a sincere gratitude to my supervisor, Dr. Lingyun Chen, for giving me a chance to work in her lab and pursue my master's degree. I greatly appreciate her endless support, motivation and guidance throughout the course of my studies. Thank-you for her patience, focus and ability to keep me on track. I also would like to thank Dr. Sylvia van Drunen Littel-van den Hurk for serving as my supervisory committee member and for her constructive suggestions to my research project. Thank-you for always pushing me beyond my limits. Also, I would like to express my genuine gratitude to the late Dr. Lech Ozimek; this research would not be possible without his guidance and support.

I would like to acknowledge great people from the 3-52 and 3-30 for all your moral and scientific support during those years. Special thanks to Dr. Guangyu Liu, Dr. Jingqi Yang, and Dr. Ewelina Eckert for their helpful suggestions and troubleshooting my experiments. I also would like to thank Dr. Aja Rieger for her help with Multi-Spectral Imaging Flow Cytometry. Special thanks to both Dr. Mark Miskolzie and Nupur Dabral for their help in completing the NMR test. Many thanks to Arlene Oatway for her helping with obtaining TEM images and Geraldine Barron for her assistance with confocal microscopy. I cannot thank enough Elisa Catalina Martinez Peña, for her helping me with experiments at the University of Saskatchewan.

Finally, I am eternally grateful for the support of my family, friends and loved ones. Your encouragement pushed me to the heights I never thought would be possible. Especial thanks to my husband, Maksym Kononenko. Without your endless love, support, and enormous patience this work would not have been done. Thank you for constantly holding my back. Also, I would like to thank my grandma for always standing by my side. I, honestly, do not know what I would have achieved without you in my life.

Table of Contents

List of Tables

List of Figures

List of Abbreviations and Symbols

ACIDF	Alberta Crop Industry Development Fund Ltd.
AI Bio	Alberta Innovates Bio Solutions
ALMA	Alberta Livestock and Meat Agency
ALR	Absent in melanoma 2 (AIM2)-like receptor
ANOVA	Analysis of variance
AP-1	Activating protein-1
Anti-PD-1	Anti-programmed death 1
APC	Antigen presenting cell
ATCC	American Type Culture Collection
ATF1	Activating transcription factor 1
BCG	*Mycobacterium bovis* Bacillus Calmette-Guerin
BHV-1	Bovine herpes virus-1
BRD	Bovine respiratory disease
BVDV	Bovine viral diarrhea virus
CD	Cluster of differentiation
cDC	Conventional dendritic cell
CE	Cellulose ester
CLR	C-type lectin receptor
CpG motif	Region of DNA containing unmethylated cytosine-phosphate-guanosine dinucleotides
CpG ODN	Synthetic oligodeoxynucleotide containing unmethylated CpG motifs
DAMP	Damage-associated molecules pattern
DAPI	4′,6-diamidino-2-phenylindole
DC	Dendritic cell
DDA	Degree of deacetylation
DLS	Dynamic light scattering

DMEM	Dulbecco's modified Eagle's medium
DMSO	Dimethyl sulfoxide
dsDNA	Double -stranded DNA
dsRNA	Double-stranded RNA
EE	Encapsulation efficiency
ELISA	Enzyme-linked immunosorbent assay
FACS	2% FBS in PBS buffer
FBS	Certified fetal bovine serum
FcR	Fc receptor
FDA	Food and Drug Administration
FITC	Fluorescein isothiocyanate
HBsAg	Yeast-derived surface antigen
HBV	Hepatitis B virus
^{1}H NMR	Proton nuclear magnetic resonance spectroscopy
IgA	Immunoglobulin A
IL	Interleukin
INF	Interferon
IRAK	Interleukin-1 receptor- activated kinase
JNKK1	c-JUN N-terminal kinase (JNK) kinase 1
LF	Lipofectamine 2000 transfection reagent,
LMW chitosan	Low molecular weight chitosan
M01	Default mask
M01,4	Erode mask
MAMP	Microbe-associated molecular pattern
MAPK	Mitogen-activated protein kinase
MFI	Median fluorescence intensity
MHC	Major histocompatibility complex

MIFC	Multi-spectral imaging flow cytometry
M_n	Number average molecular weight
M_n/M_w	Polydispersity index
MTT	3-[4,5-dimethylthiazol-2-yl]-2,5-diphenyltetrazolium bromide
M_w	Weight average molecular weight
MWCO	Molecular weight cut-off
MyD88	Myeloid differentiation primary response 88 adaptor protein
N/C ratio	Charge ratio of chitosan to nucleic acids
NF- κB	Nuclear factor-κB
NIK	NF-κB-inducing kinase
NK	Natural killer cell
NLR	Nucleotide-binding oligomerization domain-like receptor
nMFI	Normalized MFI
NP	Nanoparticle
NSERC	Natural Sciences and Engineering Research Council of Canada
PAMP	Pathogen-associated molecular pattern
PBS	Phosphate buffered saline
pDC	Plasmacytoid dendritic cell
pDNA	Plasmid DNA
PEC	Polyelectrolyte complex
PEI	Polyethyleneimine
PGA	Poly (L-glutamic acid)
PPR	Pattern-recognition receptor
RID	Refractive index detector
RLR	Retinoic acid-inducible gene-I-like receptor
RNAi	Double stranded RNA-mediated interference
SD	Standard deviation

SEC-HPLC	High-Performance Liquid Chromatography – Size Exclusion Chromatography
siRNA	Small interfering RNA
ssDNA	Single-stranded DNA
ssRNA	Single-stranded RNA
TAE	Tris-acetate-EDTA buffer
tgD	Truncated secreted version of glycoprotein D
TEM	Transmission electron microscopy
Th1-type cytokines	Proinflammatory cytokines produces by the type I T helper cells
Th2-type cytokines	Cytokines associated with IgE production, eosinophil activation and anti-inflammatory response, produced by Type II helper cells
TIR	Toll–interleukin-1 receptor domain
TLR	Toll-like receptor
TNF-α	Tumor necrosis factor alpha
TPP	Sodium tripolyphosphate
TRAF6	Tumour-necrosis factor receptor-associated factor 6

Chapter 1

Literature review

1.1. Immune system and its role in the recognition of danger and pathogen signals

The vertebrate innate and adaptive immune systems have evolved to detect and eliminate invading infectious agents and protect the host from diseases (Krieg, 2002; Krieg, 2006; Klinman, 2004). Upon infection, vertebrates employ the innate immune system as the first line of defence to limit the spread of pathogens. The innate immunity is triggered by evolutionally conserved molecular structures expressed by invading pathogens. These structures are known as pathogen- or microbe-associated molecular patterns (PAMPs or MAMPs), and they are specifically recognized by several distinct classes of host pattern-recognition receptors (PRRs) (Krieg, 2006; Kawasaki & Kawai, 2014; Roers, Hiller, & Hornung, 2016). PRRs also recognize self-derived molecules obtained from the host damaged cells as a consequence of infection, cellular stress, damage or injury, known as damage-associated molecules patterns (DAMPs) (Mogensen, 2009). Currently, five families of PRRs have been identified including Toll-like receptors (TLRs), C-type lectin receptors (CLRs), nucleotide-binding oligomerization domain-like receptors (NLRs), retinoic acid-inducible gene-I-like receptors (RLRs), and the Absent in melanoma 2 (AIM2)-like receptors (ALRs) (Brubaker, Bonham, Zanoni, & Kagan, 2015).

TLRs are the most understood and characterized family of PRRs and expressed by a variety of antigen presenting cells (APCs), including macrophages, B cells and dendritic cells (DC) (Miyake, et al., 2018; Kawai & Akira, 2011). They are type 1 transmembrane glycoprotein receptors that contain cytoplasmic, transmembrane, and extracellular or luminal ligand binding domains (Christmas, 2010). Recent studies have notably identified 10 human and 12 murine TLRs

(Kawasaki & Kawai, 2014). All TLRs are primarily classified into two subfamilies based on their cellular localization. Mainly, the cell surface TLRs are most sensitive to extracellular pathogen, whereas the intracellular TLRs recognize nucleic acids derived from viral and bacterial pathogens and are localized inside the endolysosomal compartments (Christmas, 2010). For instance, TLR1 associated with TLR2 can recognize bacterial lipopeptides (Kumar, Kawai, & Akira, 2009). TLR 4 and TLR 2 respond to lipopolysaccharide and lipoprotein that are commonly expressed on the cell walls of bacteria (Alexander & Rietschel, 2001). The intracellular TLR3 senses viral double-stranded RNA (dsRNA), while TLR 7 and TLR 8 recognize bacterial single-stranded RNA (ssRNA) (Kumar, Kawai, & Akira, 2009). Unmethylated CpG motifs, abundantly present in bacterial and viral DNA, are recognized by TLR9 (Krieg A. M., 2006). TLR5 explicitly recognizes flagellin, an extremely abundant protein in flagellated bacteria (Kumar, Kawai, & Akira, 2009).

Following PAMP and DAMP recognition, stimulated TLRs trigger the downstream activation of an appropriate intracellular signalling pathway (Shirota & Klinman, 2014). The TLR-mediated signal transduction ultimately induces the expression of a broad range of proinflammatory cytokines, chemokines, and co-stimulatory molecules, that together orchestrate early host immune responses to the pathogen infection (Hanagata, 2012; Krieg, 2006; Wei, et al., 2012). Consequently, these responses direct the induction of a strong adaptive immunity, leading to the generation of antigen-specific antibodies, elimination of pathogens in the later stages, and development of a long-lasting adaptive immunological memory (Shirota & Klinman, 2014).

The discovery of TLRs and their role in the modulation of immune responses have attracted much attention into the development of ligands that can specifically bind to the receptor and perform agonistic or antagonistic functions (Mifsud, Tan, & Jackson, 2014). These agents target the host rather than the microbial or viral pathogens, and thus they would not induce bacterial

resistance even after repeated administration. Moreover, the rapid and broad nature of stimulated immune responses indicates that these agents can be utilized as a promising new approach to combat infectious diseases (Krieg, 2012).

1.2. CpG motif as a ligand for the Toll-like 9 receptors

In 1984, Tokunaga and colleagues demonstrated that the purified fractions of 97% single-stranded DNA (ssDNA) extracted from *Mycobacterium bovis* BCG caused regression of established solid tumours and/or were very effective in metastasis prevention in a guinea pig model (Tokunaga, et al., 1984). Besides the potent antitumor activity, these DNA fractions possessed distinct immunostimulatory properties. They stimulated *in vitro* proliferation of murine lymphocytes and induced proinflammatory cytokine production (Messina, Gilkeson, & Pisetsky, 1991; Lipford, et al., 1997). Subsequently, the immunostimulatory properties of bacterial DNA were extended to other bacterial and viral strains (Messina, Gilkeson, & Pisetsky, 1991; Neujahr, Reich, & Pisetsky, 1999; Rathinam & Fitzgerald, 2011). In 1995, Krieg et al. concluded that the high immunostimulatory activity of pathogen DNA is attributed to the presence of unmethylated cytosine-phosphate-guanosine dinucleotides flanked by two 5' purines and two 3' pyrimidines (CpG motifs) (Krieg A. M., 1995). Whereas CpG motifs are widely present in the pathogen genome, they are highly suppressed and predominantly methylated in the vertebrate DNA (Krieg, 2002; Krieg, 2006; Klinman, Yi, Beaucage, Conover, & Krieg, 1996; Roberts, et al., 2005). In 2000, Hemmi et al. (2000) discovered TLR9 as a first PRR capable of sensing CpG DNA. TLR9 recognizes unmethylated CpG motifs as ligands and elicits a robust innate immune response, which promotes the development of a long-lasting pathogen-specific adaptive immune response (Takeda, Kaisho, & Akira, 2003).

1.3. CpG motif recognition

TLR9 is an intracellular, transmembrane receptor that is synthesized and assembled in the endoplasmic reticulum, trafficked to the Golgi apparatus, and then transported to endosomes and lysosomes of innate immune cells (Kawasaki & Kawai, 2014). TLR9 contains a C-terminal cytoplasmic signalling domain, a single transmembrane helix, and an intra-endosomal leucine-rich N-terminal domain that mediates the ligand binding (Christmas, 2010). TLR9 shares a high degree of structural homology (>71%) across different species including human, mouse, rat, cow, pig, sheep, cat and dog, with the greatest degree of homology shared between human TLR9 and TLR9 of domestic animals (Griebel, et al., 2005). These investigations also revealed conserved structures of TLR9 protein domains among these species with minor variations in the length of protein and the number of leucine-rich repeats.

Nevertheless, previous investigations demonstrated a species-specific immune response to CpG motifs, which was determined by the specific base sequence flanking CpG dimers and the cellular pattern of TLR9 expression (Griebel, et al., 2005). The innate immune cells from different mammalian species are stimulated by CpG dimers flanked by different surrounding bases (Krieg, 2002; Griebel, et al., 2005). The optimal sequence for human cells stimulation was reported to be 5'-GTCGTT-3', whereas the murine immune cells are being activated by the DNA containing the 5'-GACGTT-3' sequence (Nichani, et al., 2004; Vollmer & Krieg, 2009). Furthermore, the human 5'-GTCGTT-3' motifs also have an optimal stimulatory effect among other domestic species including cattle, sheep, goat, horse, and chicken (Nichani, et al., 2004; Krieg, 2002; Griebel, et al., 2005). On the other hand, 5'-GACGTT-3' sequence was optimal for stimulation of B-cells proliferation and APC maturation only in mice and rabbits but displayed little activity in cattle and other domestic animals (Griebel, et al., 2005).

Moreover, the extent of the CpG-mediated immune response also differs based on the interspecies differences in the cellular pattern of TLR9 expression (Griebel, et al., 2005). For instance, the expression of human TLR9 is mostly restricted to the B cells and plasmacytoid dendritic cells (pDCs) (Kawai & Akira, 2011; Roers, Hiller, & Hornung, 2016). In contrast, murine TLR9 is detected in various cells of the myeloid lineages including B cells, pDCs, monocytes/macrophages, and conventional dendritic cells (cDCs) (Kawai & Akira, 2011; Zhang, et al., 2015; Hemmi, et al., 2000). A cellular pattern of TLR9 expression in cattle was reported to be similar to mice (Griebel, et al., 2005). Despite the differences in the cellular and species-dependent TLR9 expression and stimulation, the results derived from rodent experiments could be reasonably transferred to other animals and humans to predict the biological response and assess the therapeutic potential.

1.4. The mechanism of TLR9-mediated immune system activation

The innate immune cells employ receptor-mediated or sequence-independent endocytosis to facilitate the internalization and trafficking of viral and bacteria CpG DNA to the early endosomes (Lahoud, et al., 2011; Song & Liu, 2015; Vollmer & Krieg, 2009). Subsequent endosomal maturation facilitates the digestion of double-stranded CpG DNA into the short single-stranded fragments and enables their interaction of TLR9 (Häcker, Redecke, & Häcker, 2002; Hemmi, et al., 2000; Miyake, et al., 2018). Following this binding, the TLR9 recruits the myeloid differentiation primary response 88 (MyD88) adaptor protein, which initiates the distinct signalling pathway (Figure 1-1) (Klinman, 2004; Wittig, Schmidt, Scheithauer, & Schmoll, 2015). The activated transduction molecules include the interleukin-1 receptor-associated kinase (IRAK) and tumour-necrosis factor receptor-associated factor 6 (TRAF6) complex. Subsequently, this leads to the recruitment of mitogen-activated protein kinases (MAPKs) and several transcription

factors including nuclear factor-κB (NF-κB) and activating protein-1 (AP1) (Bode, Zhao, Steinhagen, Kinjo, & Klinman, 2011). These transcription factors directly stimulate the cellular gene expression, which can be detected within 30 min of its *in vivo* administration, followed by a peak at 3 h, and a progressive decline thereafter over a 3-day period (Klaschik, Tross, & Klinman, 2009). The gene upregulation in B-cell results in the proliferation, extensive production of immunoglobulins, interleukin-6 (IL-6), IL-12, and as expression of their Fc receptors (FcR) and surface markers including a major histocompatibility complex (MHC) class II, cluster of differentiation 40 (CD40), CD80 and CD86 (Krieg, et al., 1995; Bode, Zhao, Steinhagen, Kinjo, & Klinman, 2011). The *in vitro* stimulation of macrophages, monocytes and dendritic cells by CpG DNA induces synthesis and secretion of proinflammatory Th1-type cytokines, including tumor necrosis factor alpha (TNF- a), IL-1, IL-6, IL-12, IL-18, interferon- a/β (IFN- a/β), as well as expression of 'maturation' surface markers including CD40, CD54, CD80, CD86 and MHC class II costimulatory molecules (Ivory, Prystajecky, Jobin, & Chadee, 2008; Hanagata, 2012; Krieg, 2006; Wei, et al., 2012; Bode, Zhao, Steinhagen, Kinjo, & Klinman, 2011). These events further trigger the maturation, differentiation and proliferation of B-cells, natural killer (NK) cells, T cells and activation of adaptive immune responses.

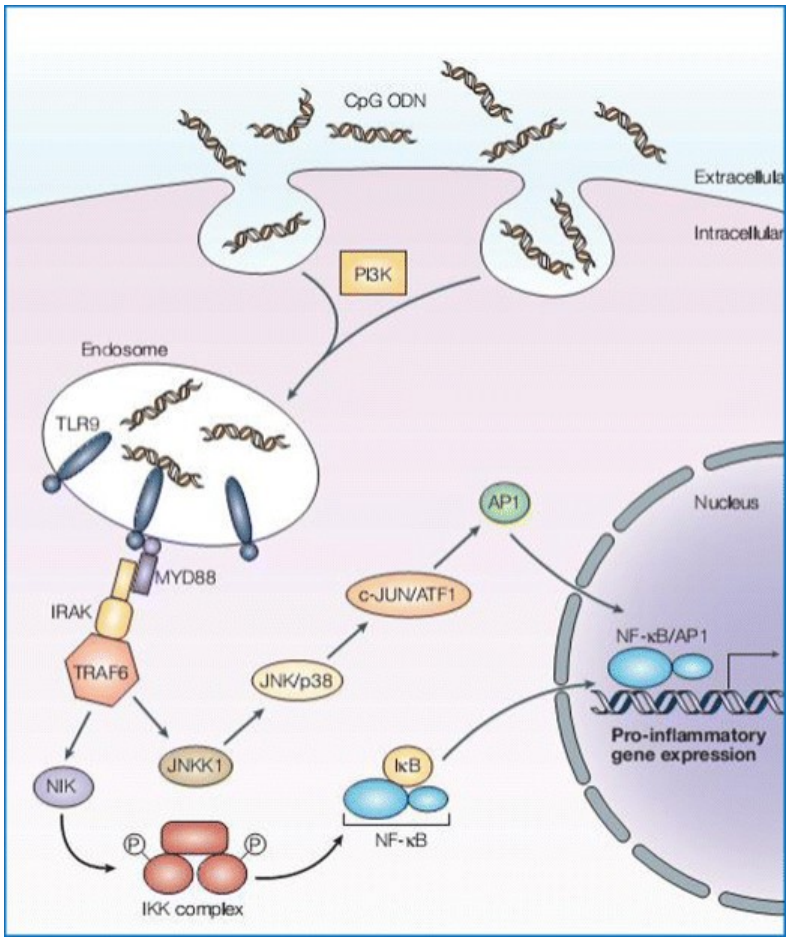

Figure 1-1. The TLR9-activated signaling pathway (Klinman, 2004). Upon internalization, nucleic acids containing CpG motifs interact with the endosomal TLR9 receptor, which transduces the intracytoplasmic activation signal. Firstly, the adapter protein MyD88 is recruited to the Toll–interleukin-1 receptor (TIR) domain of TLR9, following by the activation of IRAK–TRAF6 complex, which leads to the activation of both the mitogen-activated protein kinase JNK/p38 and inhibitor of nuclear factor-κB (NF-κB) kinase (IKK) complexes, resulting in stimulation of transcription factors, including NF-κB and activating protein 1 (AP1). ATF1, activating transcription factor 1; IRAK, IL-1 receptor-activated kinase; JNKK1, c-JUN N-terminal kinase (JNK) kinase 1; NIK, NF-κB-inducing kinase; TRAF6, tumour-necrosis factor receptor-associated factor 6.

1.5. CpG ODNs and their structure–activity relationships

Pathogenic DNA containing unmethylated CpG motifs is a native ligand for TLR9, and synthetic oligodeoxynucleotides that mimic the pathogen DNA structure (CpG ODNs) can duplicate its behaviour and induce similar immune response activation (Krieg, 2006; Klinman, Yi,

Beaucage, Conover, & Krieg, 1996; Roberts, et al., 2005). Currently, four classes of CpG ODN have been developed: A-Class (also referred to as D-type), B-Class (also referred to as K-type), C-Class, and P-Class (Vollmer, et al., 2004). Each class contains at least one CpG dinucleotide and possesses distinct structural differences, which induce different TLR9 responses (Samulowitz, et al., 2010). The nature of backbone modification, its lengths and sequence composition, as well as the formation of secondary and tertiary structures were reported to mediate the immunostimulatory capacity of CpG ODNs (Vollmer, et al., 2004; Samulowitz, et al., 2010). Several examples of commonly used CpG ODNs are present in Table 1-1.

Class	Example ODNs	Sequence
Class-A/Type D	ODN 2216, human	5'-ggGGGACGA:TCGTCgggggg-3' (20 mer)
	ODN 1585, mouse	5'-ggGGTCAACGTTGAgggggg-3' (20 mer)
Class-B/Type K	ODN 2006, human	5'-tcgtcgttttgtcgttttgtcgtt-3' (24 mer)
	ODN 1826, mouse	5'-tccatgacgttcctgacgtt-3' (20 mer)
	ODN 2007, bovine / porcine	5'-tcgtcgttgtcgttttgtcgtt-3' (22 mer)
Class-C	ODN 2395, human/ mouse	5'-tcgtcgttttcggcgc:gcgccg-3' (22 mer)
Class-P	ODN 21798, human/ mouse	5'-tcGtcGacGatcggcgcgcgccg -3' (23 mer)

Table 1-1. Examples of different classes of CpG ODN. Bases in the capital letters are phosphodiester; bases in lower cases are phosphorothioate (nuclease resistant); palindrome sequences are underlined; CpG dinucleotides are in red.

The A-class ODNs contain a central palindromic phosphodiester sequence with a single CpG motif surrounded by phosphorothioated poly-G tails (Vollmer & Krieg, 2009). These ODNs were explicitly designed to form higher-order structures via intrastrand base pairing (e.g. hairpins or stem-loop) (Hanagata, 2017). An altered structure of A-class ODNs contributes to the improved stability and uptake efficiency, as well as prolonged retention time in the early endosomes, which

results in upregulated levels of type I IFN secretion (Shirota & Klinman, 2014). Although this class of ODNs strongly activates pDC, it is not strong enough to induce the pDC maturation or B-cells proliferation (Vollmer & Krieg, 2009).

The B-class ODNs have been extensively used in preclinical and clinical trials (Bode, Zhao, Steinhagen, Kinjo, & Klinman, 2011). B-class ODNs are typically defined as short linear ssDNA of about 18-25 bases that contain one or more CpG motifs on a fully phosphothiolate backbone (Hanagata, 2012). The interaction between B-class ODNs and TLR9 leads to the formation of a complex, which tends to be rapidly transported from the early into late endosomes. This translocation induces a rapid B-cell proliferation and activates secretion of proinflammatory cytokines in DCs/macrophages (Shirota & Klinman, 2014). So far, murine CpG ODN 1826 and human CpG ODN 2006 are the most widely studied B-class TLR9 ligands for *in vitro* and *in vivo* applications.

The C-class ODNs resemble the characteristics of both A-class and B-class ODNs (Bode, Zhao, Steinhagen, Kinjo, & Klinman, 2011; Jurk, et al., 2004). They typically contain stimulatory hexametric CpG motifs linked to GC-rich palindromic sequences by a T-rich spacer (Vollmer, et al., 2004). C-class CpG ODNs can effectively activate Natural killer cells, pDCs, and B cells, and strongly induce high levels of type I IFNs (Pohar, Kužnik Krajnik, Jerala, & Benčina, 2015; Jurk, et al., 2004).

P-class ODN is a new class of TLR9 agonist that can induce the strongest type I IFN secretion (Samulowitz, et al., 2010; Scheiermann & Klinman, 2014). P-class ODN contain two palindromic sequences that can form secondary and tertiary structures, which immediately improve their stability and uptake (Samulowitz, et al., 2010). These structural modifications extend

the retention time of P-class CpG ODNs in the early endosomal compartments and stimulate type I IFNs secretion (Bode, Zhao, Steinhagen, Kinjo, & Klinman, 2011).

1.6. Therapeutic applications of synthetic CpG ODNs

1.6.1. Immunoprotection against infectious diseases

Since synthetic TLR9 agonists can elicit a strong activation of innate immune response and trigger the proinflammatory cytokine production, they may be utilized as a potent treatment and prevention strategy to combat infectious diseases (Krieg, 2012). Hence, CpG ODNs can be used as a broad-spectrum monotherapy to increase the host resistance to bacterial and viral infections. Recent studies revealed that the prophylactic administration of B-class CpG ODNs prior the pathogen challenge could provide effective transient protection of mice against a broad-spectrum of intracellular pathogens, including the lethal dosage of *Listeria monocytogenes*, *Francicella tularensis*, *Bacillus anthracis*, vaccinia virus, and Ebola virus (Krieg, 2006). The activation of defence mechanisms was achieved following an oral, inhalation or injection route of administration. The duration of CpG ODN-induced protection varies greatly on the pathogen and can last form one day as for the vaginal herpes simplex virus up to two - four weeks as for the *L. monocytogenes* and *F. tularensis* models (Ray & Krieg, 2003). Furthermore, it can be prolonged by a repeated administration of CpG ODN.

Besides monotherapy, CpG ODNs have demonstrated good vaccine adjuvating properties. The co-administration of CpG ODNs together with antigens strongly improves functions of APCs and enhances the development of an antigen-specific adaptive immune response (Krieg, 2012). Its adjuvant properties have been evaluated in several human clinical trials for the promotion of immunogenicity of administrated antigens for preventing malaria, hepatitis B virus (HBV), pneumococcus, influenza and anthrax infections (Shirota & Klinman, 2014). Recently,

HEPLISAV-B™ was approved for use by the FDA, as a new HBV vaccine containing a recombinant yeast-derived surface antigen (HBsAg) combined with a synthetic CpG ODN 1018 (Hyer, McGuire, Xing, Jackson, & Janssen, 2018). Addition of TRL9 agonists to the antigens in the in HEPLISAV-B™ was found to enhance the HBV-specific cellular and humoral immune responses and allowed to reduce the number of immunizations compared to the currently licensed alum-adjuvanted vaccines (Shirota & Klinman, 2014; Hyer, McGuire, Xing, Jackson, & Janssen, 2018).

Apart from the preclinical and clinical trials on mice and humans, CpG ODN-mediated immunoprotection has been actively examined in other animal models. For instance, *in ovo* injection as well as needle-free intrapulmonary delivery of CpG ODNs demonstrated significant protection against *Escherichia coli* and *Salmonella enteritidis* infection in neonatal chickens (Goonewardene, et al., 2017; Gomis, et al., 2004; MacKinnon, et al., 2009). Additionally, treatment of piglets with CpG ODNs-adjuvanted vaccine against *Bordetella pertussis* was capable of inducing generation of antigen-specific antibodies and developing a long-lasting immunity (Polewicz, et al., 2013).

Moreover, the adjuvant capacity of CpG ODNs was frequently investigated for immunization of cattle against Bovine herpes virus-1(BHV-1) and Bovine viral diarrhea virus (BVDV). These viral pathogens cause a variety of clinical manifestations in cattle, including fever, difficult breathing, repetitive coughing, nasal and/or eye discharge, diarrhea, dehydration, loss of appetite, abortions, and death (Jelinski & Janzen, 2016; Klima, et al., 2014). Both viruses contribute to the bovine respiratory disease (BRD) complex, which is a leading cause of the significant morbidity and mortality rates in both beef and dairy cattle in the North American industry (Jelinski & Janzen, 2016). Recently, the adjuvant capacity of CpG ODN was studied to

aid in the generation of specific protective immune responses against BHV-1 (Rankina, et al., 2002). Calves were immunized intramuscularly with a truncated secreted version of glycoprotein D (tgD) of BHV-1 combined with the CpG ODNs have shown activation of strong and balanced immune responses. The administration of CpG ODNs as a component TriAdj adjuvant combined with the BVDV-E2 glycoprotein elicited the development of a strong and balanced protective immune response in lambs (Snider, Garg, Brownlie, van den Hurk, & van Drunen Littel-van den Hurk, 2014). Similarly, the effectiveness of CpG ODN as a vaccine adjuvant was examined using the plasmid encoding the BVDV-E2 protein (Liang, van den Hurk, Babiuk, & van Drunen Littel-van den Hurk, 2006). The proposed DNA immunization vaccination strategy with a CpG-formulated subunit has demonstrated the induction of both cell-mediated and humoral immunity and efficacy in newborns cattle.

1.6.2. Cancer immunotherapy

The anticancer activity of CpG ODNs has been demonstrated in several preclinical murine tumor models, including hematologic malignancies, malignant melanoma, neuroblastoma, and renal carcinoma (Krieg, 2012; Adamus & Kortylewski, 2018). Based on these observations, CpG ODN-mediated activation of TLR9 signaling passway can result in the activation of NK cell–mediated tumor killing activity and promotion of tumor regression by cytotoxic T lymphocytes (Maher & Davies, 2004; Manuja, Manuja, Kaushik, Singha, & Singh, 2013; Jurk & Vollmer, 2007). Recent preclinical studies have reported that CpG ODNs can serve as an excellent candidate for supporting the immune checkpoint inhibitors utilized in the cancer therapy (Wang, et al., 2016; Adamus & Kortylewski, 2018). The intratumoral injection of CpG ODN combined with an anti-PD-1 (anti-programmed death 1) blockage into the anti–PD-1 nonresponding tumors resulted in the rapid activation, proliferation, and tumor infiltration with cytotoxic T cells and significant

expression of both IFN-γ and TNF-α in the mice model (Wang, et al., 2016). This immune stimulation resulted in the complete rejection of essentially all treated tumors, and generation of systemic immunity to combat the uninjected, distant-site tumors (Wang, et al., 2016).

1.6.3. Immunotherapy of allergy and asthma

Finally, a significant amount of data was generated to demonstrate the effectiveness of TLR9-based immunotherapy for prevention and treatment of asthma and allergy. CpG ODNs combined with allergens induces secretion of significant amounts of type I INFs and Th1 cytokines, which directly and indirectly promotes the differentiation of naïve T cells toward a Th1 phenotype (Fonseca & Kline, 2009; Li, et al., 2015). The intranasal and intradermal administration of CpG ODNs have significantly reversed the development of nose and lung pathologies, redirected the Th2 to the Th1 immune response, suppressed the secretion of Th2 cytokines, reduce the systemic levels of ovalbumin-specific IgE, and prevent the development of allergic lung inflammation in the murine model of allergic rhinitis and asthma syndrome (Fonseca & Kline, 2009; Li, et al., 2015).

1.7. Challenges in the current application of CpG ODNs

Even though the encouraging results were obtained from the numerous preclinical and clinical trials of CpG ODNs, their therapeutic application still faces several significant challenges (Hanagata, 2012; Zhang & Gao, 2017; Mutwiri, Nichani, Babiuk, & Babiuk, 2004). Firstly, the natural phosphodiester form of CpG ODNs is extremely susceptible to exonuclease degradation with a half-life of only 5 – 10 min, rendering them inactive in the free form shortly after administration (Mutwiri, Nichani, Babiuk, & Babiuk, 2004; Krieg, et al., 1995; Sands, et al., 1994). Hua et al. (1996) speculated that the natural form of CpG ODNs might be degraded even before the stimulation signals are totally delivered. They reported that CpG ODNs, synthesized with a

nuclease-resistant backbone, induced a marked B-cells proliferation and immunoglobulin secretion at more than 100-fold lower concentration than that of the unmodified CpG ODNs. Furthermore, Zimmermann et al. (2003) demonstrated lack of immunostimulatory activity of conventional CpG ODNs on spleen cells and RAW 264.7 macrophages, which was attributed to insufficient stability. Secondly, free CpG ODNs are characterized by unfavourable pharmacokinetics, and lack specificity towards the target APCs, which leads to the rapid absorption into the systemic circulation and insufficient cellular uptake (Mutwiri, Nichani, Babiuk, & Babiuk, 2004; Wilson, de Jong, & Tam, 2009; Zhang & Gao, 2017). Finally, irrespective of serum nuclease degradation and rapid systemic absorption, the constant negative charge is believed to limit the binding and internalization efficiency of CpG ODNs due to the electrostatic repulsion between the polyanion and the negatively charged cellular membrane (Hanagata, 2012).

These delivery challenges suggest a rather transient effect of CpG ODN-based immunotherapy, which may require an increase in the dosage and/or a repeated treatment administration to achieve the desired therapeutic effect (Mutwiri, Nichani, Babiuk, & Babiuk, 2004). To address these challenges and optimize the biological activity of CpG ODNs, researchers have focused on the development of new strategies for the chemical modification of the CpG ODNs, as well as the application of nanoscale delivery vehicles.

1.8. Strategies to enhance the biological activity of CpG ODNs

1.8.1. Modification of the CpG ODN backbone

The modification of the natural phosphodiester linkages by the substitution of one of the non-bridging Oxygen atoms with a Sulphur atom was reported to be reasonably effective in stabilizing CpG ODNs against nuclease degradation and modulating its pharmacokinetic properties (Kurreck, 2003; Wan & Punit, 2016; Krieg, Matson, & Fisher, 1996). Phosphorothioate

CpG ODN analogs demonstrated a considerable improvement in the *in vitro* and *in vivo* half-life stability (30 - 60 min) in plasma as compared with phosphodiester oligonucleotides (Agrawal & Zhao, 1998). Currently, the majority of CpG ODNs that have been studied for clinical applications has a complete or partial phosphorothioate backbone.

Generally, CpG ODNs with a phosphorothioate backbone were reported to be safe and well tolerated; however, frequent administration of phosphorothioate CpG ODNs at a high dosage may lead to the development of various adverse events (Bode, Zhao, Steinhagen, Kinjo, & Klinman, 2011; Heikenwalder, et al., 2004; Shirota & Klinman, 2014). For instance, daily administration of a fixed dosage (60 μg/mouse) of CpG ODN 1826 over a period of 2-20 days elicited dramatic alterations in morphology and functionality of murine lymphoid organs, as well as significant systemic toxicity (Heikenwalder, et al., 2004). Moreover, several safety concerns have been raised over the administration of CpG ODNs to humans, which are commonly described as local reactions at the injection site, including inflammation, induration, erythema, edema, and pain, as well as systemic flu-like symptoms, such as mild headache, nausea and fever (Wilson, et al., 2006; Shirota & Klinman, 2014; Krieg A. M., 2012). Additionally, administration of CpG ODN raised some safety concerns regarding a possible increase in the host's susceptibility to autoimmune disease (Krieg & Vollmer, 2007; Bode, Zhao, Steinhagen, Kinjo, & Klinman, 2011). CpG ODNs block the spontaneous apoptosis of stimulated B-cells and promote their proliferation and secretion of anti-double-stranded-DNA autoantibodies and proinflammatory cytokines in normal mice (Yi, Peckham, Ashman, & Krieg, 1999).

1.8.2. Self-assembled DNA nanostructures containing CpG motifs

To avoid the adverse effects of phosphorothioate CpG ODNs, a great number of self-assembled DNA nanostructures containing natural phosphodiester CpG motifs have been

developed. For instance, CpG ODNs with the phosphodiester backbone designed into the covalently closed dumbbell-like structures demonstrated resistance to the exonuclease degradation and enhanced immunomodulatory potential (Schmidt, Anton, Nordhaus, & Junghans, 2006). Recently, a dumbbell-like immunomodulator MGN1703 has entered a phase 3 clinical trial as a maintenance treatment following first-line chemotherapy in patients with metastatic colorectal carcinoma (Cunningham, et al., 2015). So far, MGN1703 appeared to be well tolerated and induced prolonged progression-free survival in patients (Wittig, Schmidt, Scheithauer, & Schmoll, 2015).

Nishikawa et al. (2008) and Mohri et al. (2015) investigated the influence of stereochemical properties of self-assembled nanostructures containing immunostimulatory CpG motifs on their immunostimulatory activity. The results demonstrated that the three CpG ODNs assembled into Y-shaped DNA structures have an outstanding cellular uptake efficiency and can generate significantly higher levels of proinflammatory cytokines compared to the double-stranded analogs. Mohri et al. (2015) investigated the immunostimulatory activity of DNA dendrimers formed from the several branched DNA units containing CpG motifs. This model demonstrated excellent cellular uptake and TNF-α and IL-6 cytokines secretion.

Furthermore, Zhang et al. (2015) developed a novel approach to enhance the activity of CpG ODNs by self-assembling elongated DNA building blocks, containing immunostimulatory CpG motifs, into multifunctional DNA nanoflowers. The dense packaging of CpG motifs prevented direct contact between the serum nucleases and the inner layers of the nanoflowers, which delayed its degradation. These formulations promoted a long-lasting immunostimulatory effect inducing a dramatic secretion of the proinflammatory cytokines (Zhang, et al., 2015).

1.8.3. Nanoparticle-based CpG ODN delivery

Development of gene delivery vehicles is another approach to address the instability of naked CpG ODNs in the body fluids, their insufficient targeting capacity and cellular uptake efficiency. Currently, all gene delivery vehicles are broadly classified as viral and non-viral vectors (Ramamoorth & Narvekar, 2015). Although viral systems have demonstrated a relatively high gene delivery efficiency, their clinical application is currently limited due to the high cytotoxicity and immunogenicity (Glover, Lipps, & Jans, 2005). Importantly, the first therapy-related fatality was attributed to the usage of the adenovirus gene delivery vector (Hollon, 2000). An additional concern over the use of viral vectors is related to the possibility of genotoxic events, linked to their integration into the host genome (David & Doherty, 2016). Thus, much effort has been made to develop safer CpG ODN delivery systems using non-viral vectors such as DNA nanotubes, inorganic nanoparticles, liposomes, and cationic polymers.

For instance, Sellner et al. (2015) assembled DNA nanotubes with a designed length of ~40 nm and a diameter of ~8 nm and investigated their CpG ODN delivery efficiency both *in vitro* and *in vivo*. Although the obtained CpG ODN-containing DNA nanotubes possessed a negative surface charge (-13.2 ± 0.4 mV), they were rapidly internalized by the tissue-resident macrophages and elicited a strong upregulation of the proinflammatory cytokines. Despite these potential advantages, the further therapeutic application of DNA nanotubes is still restricted due to the complexity of synthesis, an added preparation cost, the unknown uptake mechanism, and structure-uptake relationship (Angell, Xie, Zhang, & Chen, 2016).

Another strategy to achieve successful delivery of CpG ODNs involves its binding to inorganic nanoparticles (Chen, Zhang, Chinnathambi, & Hanagata, 2013; Chen, Zhang, Jia, Du, & Hanagata, 2015). Chen et al. (2015) developed chitosan-silica/CpG ODN nanohybrids with a

size of 100 – 200 nm, which promoted CpG ODN endocytosis and demonstrated its sustained release (Chen, Zhang, Chinnathambi, & Hanagata, 2013). Even though these functionalized nanohybrids were able to stimulate significantly higher IL-6 production compared to the control samples, the uncontrollable biodegradation of silica nanoparticles is still a limiting factor for their further *in vivo* application (Chen, Zhang, Chinnathambi, & Hanagata, 2013).

Furthermore, several attempts to deliver CpG ODNs using cationic liposomes were reported (de Jong, et al., 2007; Suzuki, et al., 2004). Although liposome-encapsulated CpG ODNs were successfully accumulated in macrophages and professional APCs following systemic administration, these liposomes tend to be rapidly eliminated from the bloodstream due to the large particle size, which lead to the inability to achieve a sustained drug delivery. Moreover, few studies reported cellular toxicity associated with the application of cationic liposomes (Cardarelli, et al., 2016; Knudsen, et al., 2015).

On the other hand, non-viral vectors based on cationic polymers demonstrated great potential for CpG ODN delivery, as they can easily form polyelectrolyte complexes via electrostatic interactions, protect CpG ODNs from premature nuclease degradation, and facilitate their intracellular uptake. Several cationic polymers have been investigated for CpG ODN delivery, including polyethyleneimine (PEI) (Cheng, Miao, Kai, & Zhang, 2018), gelatin (Zwiorek, et al., 2008), acetalated dextran (Peine, et al., 2013), poly (L-lysine) (Chen, Sun, Tran, & Shen, 2011), polystyrene (Kerkmann, et al., 2004), and chitosan (Chen S. , Zhang, Shi, Wu, & Hanagata, 2014). These systems have demonstrated a tremendous chemical diversity and vast potential for functionalization (Jeong, Kim, & Park, 2007; Mao, Guo, Shi, & Li, 2012). The modulation of their physicochemical properties provides an ability to regulate pharmacokinetics and tissue biodistribution of CpG ODN-complexes and helps to achieve a desired controlled

release. Moreover, polyelectrolyte complexes offer the possibility of unlimited gene packaging and multi-component loading, which is considered a significant advantage as CpG ODNs are often co-administrated with other immunoadjuvants and antigens (Jeong, Kim, & Park, 2007). Despite these advantages, polyelectrolyte complexes containing CpG ODNs have some limitations such as cytotoxicity, lack of biodegradability, insufficient biocompatibility and poor uptake efficiency, which have to be addressed to allow their application in the clinical environment.

1.9. Chitosan

Among all cationic polymers, chitosan has been identified as the most studied biomaterial for *in vitro* and *in vivo* gene-delivery (Techaarpornkul, et al., 2010; Mansouri, et al., 2004). Chitosan is a derivative of chitin, the second most abundant natural polysaccharide after cellulose (Elieh-Ali-Komi & Hamblin, 2016). Chitin is primarily isolated from crustacean shells, the abundant by-products of a seafood processing industry, which makes chitin an important renewable and commercially available recourse (Yan & Chen, 2015). Unfortunately, the chemical insolubility of chitin in water and organic solvents limits its biomedical application. The partial alkaline de-N-acetylation of chitin leads to the formation of chitosan, a linear polysaccharide composed of randomly distributed β-1,4-linked glucosamine and N-acetylglucosamine units (Figure 1-2). Every deacetylated glucosamine unit of chitosan contains a primary amine group with a pK_a value of about 6.5, making it soluble in weak acid solutions and insoluble at neutral and alkaline pH (Nimesh, Thibault, Lavertu, & Buschmann, 2010).

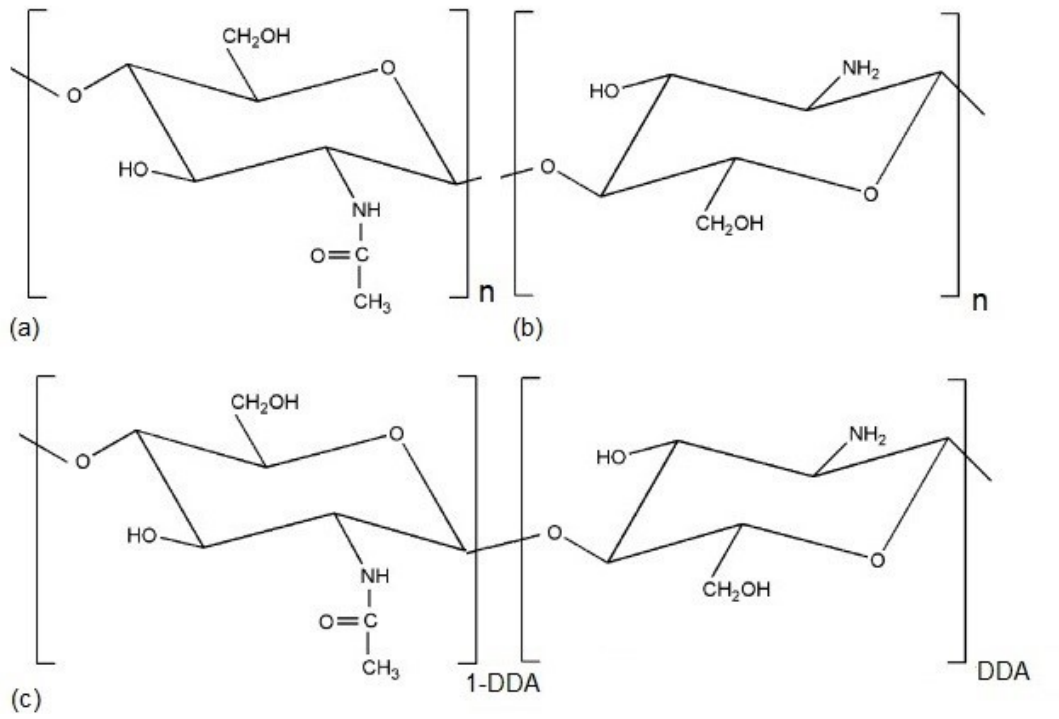

Figure 1-2. Chemical structure of (a) N-acetylglucosamine unit of chitin; (b) glucosamine unit of chitosan. (c) Chemical structure of a commercially available partially acetylated chitosan, which is a blend of N-acetylglucosamine and glucosamine units. The DDA refers to a proportion of deacetylated glucosamine units in relation to the N-acetylglucosamine units present on the chitosan backbone (Rinaudo, 2006; Alves & Mano, 2008).

Chitosan has several properties that are particularly advantageous for developing nano- and microparticles. These include ease of synthesis, low toxicity, excellent biodegradability, biocompatibility and huge potential for functionalization (Yin, et al., 2014). The pH-dependent nature of chitosan allows effective nucleic acid binding, facilitates its protection, and enables controlled release. Chitosan complexation minimises the potential damage of nucleic acids, as it occurs via electrostatic interactions and does not require any sonication or application of harsh organic solvents. Moreover, chitosan demonstrated the ability to integrate nucleic acids into small discrete particles with a low cellular toxicity and prolonged storage stability.

1.10. Properties of chitosan as a gene and drug delivery carrier

1.10.1. Biocompatibility and biodegradability

Chitosan displays several excellent biocompatibility and biodegradability, which makes it an appealing vector for drug and gene delivery (Cheung, Ng, Wong, & Chan, 2015). These properties become crucial features, when considering the vector long-term and acute toxicity, and are the mandatory requisites in securing its regulatory approval as a delivery system (Baldrick, 2010). This aims to eliminate the potential unwanted accumulation of the non-biodegradable materials in the living organs and tissues, causing various diseases and disorders (Rodrigues, Dionísio, López, & Grenha, 2012). Chitosan can be digested either by lysozymes or chitinases, which are available in all types of mucosal surfaces or produced by the normal intestinal flora (Mao, Guo, Shi, & Li, 2012; Ren, Yi, Wang, & Ma, 2005). Moreover, the chitosan degradation process results in the generation of non-toxic oligosaccharides, which end up being either incorporated into glycosaminoglycan and glycoprotein metabolic pathways or easily eliminated from the body via the urinary tract (Rodrigues, Dionísio, López, & Grenha, 2012; Ren, Yi, Wang, & Ma, 2005). Additionally, chitosan has good biocompatibility which implies the ability to properly function in the physiological environment without producing any undesirable toxic side effects or significant interactions with tissues (Rodrigues, Dionísio, López, & Grenha, 2012). The N-acetylglucosamine moiety of chitosan has structural similarities with mammalian glycosaminoglycans which are highly present in the surface of the cells and are the major component of the extracellular matrix. Therefore, the analogous structure of chitosan may lead to similar bioactivity and biocompatibility profile (Keong & Halim, 2009).

1.10.2. Mucoadhesion

Chitosan is also a mucoadhesive biopolymer (Bowman & Leong, 2006). Mucoadhesion is commonly defined as an attractive property of drug and gene delivery systems, as it can improve the adherence of the vector to the mucus membranes, leading to increased residence time and improved bioavailability of the encapsulated drug (Shaikh, Singh, Garland, Woolfson, & Donnelly, 2011). A mucus membrane or mucosa is a protective epithelial layer of cells that covers various tracts and cavities in the body and forms the primary barrier between the internal tissues and the external world. Some mucosal membranes secrete mucus, a gel-like fluid that consists primarily of water, mucins, inorganic salts, proteins, and muccopolysaccharides (Bowman & Leong, 2006). Mucins, the family of large glycoproteins, are the major component of the normal mucus. The high content of negatively charged sialic acid residues ($pK_a \sim 2.6$) in mucins confers a negative charge to mucus membranes at physiological conditions (Deacon, et al., 2000). Therefore, mucus could be defined as a physical barrier for the successful drug and gene delivery that simultaneously affects the drug permeability and uptake. The cationic nature of chitosan enables the electrostatic interactions with the negatively charged sialic acid moieties as well as the surfaces of the epithelial cells, conferring valuable mucoadhesive properties on the chitosan backbone (Bowman & Leong, 2006). Thus, chitosan-based nanoparticles are particularly appropriate for the mucosal route of administration, with their low toxicity, mucoadhesion and tunable physical properties. For instance, the oral administration of chitosan nanoparticles carrying a dominant peanut allergen gene (pCMVArah2) demonstrated modulation of the antigen-induced hypersensitivity and induction of protective immune responses against peanut allergy in the murine model (Roy, Mao, Huang, & Leong, 1999). Authors speculated that, due to the mucoadhesive properties of chitosan, the resulting nanoparticles were able to adhere to the gastrointestinal

epithelia, permeate the mucosal boundary, transfect the epithelial and/or immune cells, upregulate IgA secretion, and induce a mucosal immune response. In contrast, Roy, et al. (1999) demonstrated that the administration of naked pCMVArah2 has been mostly ineffective.

Chitosan derivatives are also known to retain good mucoadhesive properties (Chopra, et al., 2006). For instance, the chemical modification of chitosan to its quaternary derivatives resulted in the formation of polymers with a permanent cationic charge, improved aqueous solubility, and better mucoadhesive properties. The N, N, N-trimethyl chitosan is a chitosan derivative that has a persistent positive charge and one of the strongest mucoadhesive properties (Dewald, Hamman, & Kotze, 2003; Xu, Du, Huang, & Gao, 2003). Germershaus, et al. (2008) evaluated the *in vitro* uptake and transfection efficiency of chitosan and trimethyl chitosan/DNA polyplexes. Although trimethylation of chitosan significantly improved the uptake and transfection efficiency compared to the parental chitosan in the *in vitro* model, this derivative demonstrated increased cytotoxicity. Moreover, thiolated, amphiphilic, carboxylated, PEGylated, and lactose-modified chitosan are types of derivatives that also have been reported to possess good mucoadhesive properties (Ahmed & Aljaeid, 2016).

1.10.3. Drug and gene encapsulation and controlled release

The polycationic nature of chitosan makes it an attractive drug and gene delivery system with controlled release behaviour (Yuan, Shah, Hein, & Misra, 2010). At pH below the pK_a, the primary amine groups of chitosan become protonated conferring positive charges on the chitosan backbone (Ahmed & Aljaeid, 2016). This protonation allows chitosan to interconnect with various anionic compounds, leading to hydrogel formation with a 3-D network structure (Yuan, Shah, Hein, & Misra, 2010). Studies have reported the formation of hydrogel chitosan nanoparticles with numerous polyanions, including nucleic acids, hyaluronic acid, cellulose, heparin, sodium

tripolyphosphate (TPP), gellan gum, etc. (Roy, Mao, Huang, & Leong, 1999; He, et al., 2017; Siqueira, Picone, & Lopes Cunha, 2013). Moreover, resulting hydrogel structures demonstrated good potential for entrapment and controlled release of various bioactive compounds, including DNA, peptides, proteins, antigens, nucleic acids, and anti-cancer drugs.

The controlled drug and gene release from chitosan nanoparticles occurs through a number of mechanisms, including surface diffusion of the particle-adsorbed compound, diffusion of the compound from the polymer matrix, polymer degradation and erosion (Mohammed, Syeda, Wasan, & Wasan, 2017). Generally, this process depends on the chitosan molecular weight, charge density, particle size, preparation techniques, pH, and the presence of enzymes (Ahmed & Aljaeid, 2016). The initial release from the chitosan nanoparticles occurs due to the dissociation of the surface-bound bioactive compound. Then, the penetration of water into the nanoparticle structure results in the swelling of the polymer matrix, creating pores, and promotion of cargo diffusion.

Moreover, chitosan nanoparticles display a pH-dependent drug and gene release, which is related to the polymer solubility (Mohammed, Syeda, Wasan, & Wasan, 2017). At a pH below its pK_a, chitosan chains detangle, resulting in the swelling of the nanoparticle matrix and drug and gene release. At a pH above its pK_a, deprotonated, entangled and crosslinked chitosan chains form a physical barrier for the compound to diffuse through, which serves as a rate-limiting membrane for the drug and gene release (Ahmed & Aljaeid, 2016). The modification of the chitosan backbone can alter the tunable cargo release from the nanoparticles (Mohammed, Syeda, Wasan, & Wasan, 2017). Bozkir and Saka (2004) formulated chitosan- plasmid DNA (pDNA) nanoparticles using a complex coacervation method in the size range of 450–820 nm and a zeta potential of +9 to +18 mV. The obtained nanoparticles had a high encapsulation efficiency (~90%) and demonstrated a controlled release of encapsulated pDNA at pH 7.4, which was completed in 24 h.

Furthermore, chitosan is known to have good antimicrobial, antiviral, anti-inflammatory, and tumor inhibition activity (Islam, Rahman Bhuiyan, & Islam, 2017). Other researches have demonstrated evidence for its wound healing properties (Huang, et al., 2016). Thus, chitosan possesses a broad range of applications in the medical field outside gene delivery, such as wound dressing, tissue and blood vessel engineering, blood anticoagulant, cancer diagnostics, etc. (Islam, Rahman Bhuiyan, & Islam, 2017). It also has found some applications in the industrial field, mainly in cosmetic preparations, water treatment, paper making, and metal ion chelation (Cheung, Ng, Wong, & Chan, 2015).

1.11. Formation of chitosan-based nanoparticles for gene delivery

Different methods have been developed for the formulation of the chitosan-based nanoparticles for gene delivery, including simple complexation, complex coacervation, ionic gelation, emulsion cross-linking, emulsion-droplet coalescence, and reverse micellar method (Hembram, Prabha, Chandra, Ahmed, & Nimesh, 2014). The proper method selection depends on the nature of the active agent, the nanoparticle size and stability requirements, as well as the release kinetics and residual toxicity (Ahmed & Aljaeid, 2016). So far, the best-studied chitosan nanoparticles are produced by simple complexation, complex coacervation, and ionic gelation methods. Among many available methods, these techniques utilize milder aqueous reaction conditions, do not involve aggressive reagents and have a low energy consumption, which makes them suitable formulations for many biological applications.

A simple polyelectrolyte complexation method represents an easy technique to produce chitosan-DNA polyelectrolyte complexes (PECs) by self-assembly (Mao, Sun, & Kissel, 2010; Köping-Höggård, et al., 2001; Amaduzzi, et al., 2014). PEC formulation takes place due to the strong electrostatic interactions between the cationic chitosan and the anionic DNA, followed by

charge neutralization (Mao, Bakowsky, Jintapattanakit, & Kissel, 2006). When the polymer chains become closer, the partial charge neutralization occurs leading to decrease in hydrophilicity and separation of chitosan-DNA complexes from the solution. The PECs can be obtained in a size range of 50 to 700 nm. For instance, Katas and Alpar (2006) formulated chitosan complexes with small interfering RNA (siRNA) using the simple complexation method, which had a size lower than 500 nm and could be optimized with respect to the chitosan type, chain length, and its concentration. This method does not require the use of sonication or harsh organic solvents, therefore minimizing possible drug damage during the preparation process (Mao, Bakowsky, Jintapattanakit, & Kissel, 2006).

Several studies have demonstrated the formulation of chitosan-DNA nanoparticles by a simple coacervation/precipitation method using chitosan and sodium sulphate (Leong, et al., 1998; Mao, et al., 2001). This technique utilizes the process of spontaneous separation of a homogeneous polymer solution into two phases: a dense coacervate, the phase which is rich in chitosan content, and a dilute equilibrium phase with a low content of active compound (Pak, et al., 2016). Firstly, the complexes are formed when the positively charged amine groups of chitosan encounter the negatively charged phosphate groups of DNA. Then, sodium sulphate is used as a desolvating agent to trigger separation of coacervates from the supernatant (Leong, et al., 1998; Mao, et al., 2001). It has a good water affinity that facilitates the removal of water molecules associated with colloidal chains in the aqueous solution. Mao et al. (2001) reported the preparation of chitosan-DNA nanoparticles using the complex coacervation technique with sodium sulphate. Formulation of nanoparticles was optimised by adjusting the concentration of the components, buffer pH, temperature, and the molecular weights of chitosan and DNA. At a N/P charge of 3 - 8, nanoparticles demonstrated a narrow size in the 100–250 nm range. At pH 6.0, chitosan-DNA

nanoparticles possessed a slightly positive surface charge of +12 – 18 mV, which became nearly neutral at physiological pH.

An ionic gelation method is an alternative approach intended to formulate chitosan nanoparticles and entrap nucleic acids (Csaba, Köping-Höggård, & Alonso, 2009). This method is based on the ability of chitosan to form inter- and intramolecular bonds following the interaction with anionic compounds, leading to strong hydrogel formation (Calvo, Remuñán-López, Vila-Jato, & Alonso, 1997). Polyanions such as tripolyphosphate and poly (L-glutamic acid) have been widely used to facilitate this process (Rudzinski & Aminabhavi, 2010; Peng S. F., et al., 2009; Sreekumar, Goycoolea, Moerschbacher, & Rivera-Rodrigu, 2018). Csaba et al. (2009) were able to obtain nanoparticles with the size distribution between 93 and 336 nm depending on the chitosan molecular weight (Csaba, Köping-Höggård, & Alonso, 2009). Moreover, nanoparticles demonstrated an excellent gene encapsulation efficiency (almost 100%) and a well-defined spherical shape. The assembly of chitosan nanoparticles using the ionic gelation method offers not only a simple and mild preparation procedure but also an enhanced the gene encapsulation efficiency due to the formation of a nanoparticle hydrogel network structure (Csaba, Köping-Höggård, & Alonso, 2009).

1.12. Factors affecting the efficiency of chitosan nanoparticles as gene delivery vectors

1.12.1. Chitosan molecular weight (M_w)

The chitosan M_w is one of the most critical factors that modulate the physicochemical properties of chitosan, which later determine the physicochemical and morphological properties of chitosan-based nanoparticles (Katas & Alpar, 2006; Ahmed & Aljaeid, 2016). Subsequently, these factors determine the intracellular uptake efficiency of the nanoparticles and affect their distribution in the body (Katas & Alpar, 2006). Previous studies have shown that gene delivery

vectors with a size higher than 100 nm are more favourable for the internalization by APCs (Zhao, et al., 2011; Foged, Brodin, Frokjaer, & Sundblad, 2005). At the same time, nanoscale gene delivery vectors demonstrated a comparatively higher uptake efficiency than microparticles (Singh & Lillard, Jr., 2009). The size of chitosans nanoparticles was reported to be directly proportional to the chitosan M_w in the solution, where samples with the lower M_w yielded nanoparticles with a smaller particle size (Katas & Alpar, 2006; Alameh, et al., 2012). Furthermore, Köping-Höggård et al. (2002) suggested that the longer polymer chains can more easily form spherically shaped polyplexes at a lower charge ratio, which is highly favourable for the nanoparticle uptake and DNA transfection efficiency. Thus, the chitosan M_w could be regarded as a useful tool for optimization of physicochemical properties of chitosan-based nanoparticles.

The chitosan M_w also influences the stability of the gene-containing chitosan nanoparticles. An ideal gene delivery vector would provide a favourable protection of complexed nucleic acids against the serum nuclease degradation and their efficient release at the target site. For instance, Köping-Höggård et al. (2004) demonstrated that the chitosan-siRNA polyplexes formulated using chitosan oligomers (10 to 50 units of glucosamine units) dissociated more efficiently than ones formulated using chitosan with a high M_w (1000 units). The higher dissociation rates exhibited by the chitosan oligosaccharides could be attributed to the weaker nucleic acid binding valency and the loss of its the entanglement effect (Grigsby & Leong, 2010; Köping-Höggård, et al., 2004). On the other hand, chitosan oligosaccharides with a chain length less than 14 units could not form strong and stable polyplexes with pDNA. Although the longer chitosan chains demonstrated a much better ability to entangle and complex free pDNA, the *in vitro* application of chitosan-pDNA polyplexes formulated with smaller chains resulted in a higher gene release and, consequently, in higher levels of gene expression (Stranda, et al., 2010).

1.12.2. The degree of deacetylation (DDA)

The DDA is the second factor that determines the efficacy of chitosan as a gene delivery vector. The DDA (%) refers to a proportion of deacetylated glucosamine units in relation to the N-acetylglucosamine units present on the chitosan backbone. It controls the charge density or the number of protonable primary amines available for the electrostatic interaction with nucleic acids. The DDA of chitosan governs the nucleic acid binding ability, nanoparticle stability and its uptake efficiency, as well as intracellular release kinetics of the cargo.

Generally, chitosans with a high DDA (>65%) are used for gene delivery, as the higher charge density enables a better nucleic acid binding affinity, leading to the formation of more stable polyplexes and enhanced cellular uptake (Köping-Höggård, et al., 2001). Similarly, the decrease in the DDA reduces the strength of the electrostatic interactions and causes an easier polyplex dissociation, leading to a faster cargo release (Dehoussea, et al., 2010). Kiang et al. (2004) reported that pDNA/chitosan polyplexes, formulated with 62 and 72% DDA samples, demonstrated an overall lower stability in the presence of serum proteins compared to a 90 % DDA sample. Despite the polyplex instability and increased dissociation rates, these samples elicited elevated luciferase expression levels in a mouse model, which could be associated with a higher availability of pDNA to the surrounding tissues. Thus, an accurate balance between the DNA protection and release should be achieved to ensure the success of the chitosan polyplexes as gene delivery systems (Grigsby & Leong, 2010).

1.12.3. N/P charge ratio

A few studies have demonstrated that not only the chitosan molecular weight and the degree of deacetylation play a crucial role in defining properties of chitosan-DNA nanoparticles, but also the N/P charge ratio (Köping-Höggård, Mel'nikova, Vårum, Lindman, & Artursson, 2002; Liu, et al., 2007). The N/P charge ratio represents the ratio of moles of the primary amino groups (N) on the chitosan backbone to the phosphate groups (P) on the nucleic acid backbone. As an increase in the N/P ratio implies an increase in the chitosan quantities in the process of nanoparticle preparation, this parameter has a great impact on the size, morphology, and surface charge of nanoparticles (Mao, Sun, & Kissel, 2010). Nanoparticles formulated with a higher charge ratio had a higher zeta potential, which promoted the stability of the colloidal suspension and enhanced the cellular membrane binding efficiency (Köping-Höggård, Mel'nikova, Vårum, Lindman, & Artursson, 2002). Nevertheless, the N/P ratio must be optimized, as an insufficient charge ratio (N/P ~1) results in the loss of stability and aggregation of nanoparticles, while an overly high N/P ratio yields overly stable polyplexes that cannot release their cargo. Thus, an optimal charge ratio should be achieved to obtain required DNA protection and release (Alameh, et al., 2012; Ahmed & Aljaeid, 2016).

1.12.4. Ligand conjugation

Although chitosan possesses highly desirable biological properties for gene delivery, it lacks efficient APC targeting capacity. Generally, the cellular uptake of chitosan-based nanoparticles mostly occurs via a non-specific adsorptive endocytosis, which depends on the morphology and surface characteristics of nanoparticles (Choi, Nam, & Nah, 2016). Conjugation of chitosan with a specific ligand towards a particular receptor expressed on the surface of target cells results in preferential accumulation and intracellular uptake of the nanoparticles at the target

site of action (Mao, Sun, & Kissel, 2010). The APCs are known to express high levels of mannose recognition receptors that facilitate receptor-mediated endocytosis and phagocytosis of a variety of mannose-bearing antigens (Jiang, et al., 1995). Kim et al. (2006) prepared DNA-containing nanoparticles using mannosylated chitosan that exhibited a much greater gene delivery efficiency into APCs than chitosan itself. Similarly, Chu et al. (2015) prepared mannose-conjugated trimethyl chitosan-cysteine derivative with mannose ligand densities of 4, 13, and 21% for targeting macrophages. The obtained nanoparticles were finely dispersed with a mean particle size of ~150 nm, a good structural stability and siRNA protection ability. A mannose ligand density higher than 5% was reported to be necessary for the efficient nanoparticle uptake via the mannose recognition receptor and gene silencing. Since then, mannose conjugation has become a common approach for targeting APCs.

1.13. Summary of the key justifications for the research

Synthetic oligodeoxynucleotides containing unmethylated CpG motifs can mimic the immunostimulatory activity of bacterial and viral DNA (Krieg A. M., 2012). The mammalian immune system specifically recognizes the presence of CpG ODNs using a TLR9, a transmembrane pattern recognition receptor located in the endosomes and lysosomes of APCs (Shirota & Klinman, 2014). The stimulation of TLR9 triggers the production of numerous proinflammatory cytokines, which further direct the activation of adaptive immune responses (Hemmi, et al., 2000). This strong immunostimulatory activity of synthetic CpG ODNs suggests their promising therapeutic potential for the prevention and treatment of various viral, bacterial, and parasitic diseases (Krieg, 2012). Although there is ample evidence supporting the stimulatory activity of CpG ODNs, it is often transient due to the high susceptibility of naked CpG ODNs to serum nuclease degradation, poor targeting capacity, and inefficient cellular uptake (Hanagata,

2012; Zhang & Gao, 2017; Mutwiri, Nichani, Babiuk, & Babiuk, 2004). Several approaches have been made to address these challenges, including chemical modification of the CpG ODN backbone (Meng, Yamazaki, Yuuki, & Hanagata, 2011), self-assembly into DNA nanostructures (Mei, et al., 2015; Mohri, et al., 2015), and encapsulation within the inorganic, lipid and polymeric nanoparticles (Erikçi, Gursel, & Gürsel, 2011; Slütter, Bal, Ding, Jiskoot, & Bouwstra, 2011; Jung, Yu, & Mok, 2016; Chen S. , Zhang, Jia, Du, & Hanagata, 2015; Zhang, et al., 2017). These systems have demonstrated not only the ability to protect the CpG ODNs from premature serum nucleases degradation but also to promote the intracellular uptake efficiency and increase the immunostimulatory activity. Although some of those formulations represented promising delivery approaches, cationic polymer systems as safer and more cost-effective vectors offer several advantages over the others, including an immerse chemical diversity and a huge potential for functionalization (Yin, et al., 2014).

Chitosan, a naturally occurring cationic polysaccharide, has been identified as the most studied biomaterial for *in vitro* and *in vivo* gene delivery (Techaarpornkul, et al., 2010; Mansouri, et al., 2004). Chitosan has several advantageous properties for nanoparticle development that include high biocompatibility, good biodegradability, low toxicity, low immunogenicity, and huge potential for functionalization. Different methods have been employed for the preparation of nanoparticles with desired characteristics (Hembram, Prabha, Chandra, Ahmed, & Nimesh, 2014). Among all, preparation of chitosan nanoparticles using the ionic gelation method with poly (L-glutamic acid) as an anionic cross-linker offers simple and mild preparation conditions, which will minimize the damage to CpG ODNs, and enhanced gene encapsulation efficiency due to the formation of a hydrogel with a 3-D nanoparticle network structure, (Yuan, Shah, Hein, & Misra, 2010).

The structural and functional properties of chitosan are primarily determined by two fundamental parameters that include the DDA and M_w. Chitosan-based nanoparticles have been extensively studied for delivery of large pDNA. For this purpose, nanoparticles were formulated using chitosans with high DDA and large M_w, which promoted complex stability, protected pDNA against nuclease degradation and facilitated its cellular uptake (Scholz & Wagner, 2012; Lavertu, Méthot, Tran-Khanh, & Buschmann, 2006). The attempts to encapsulate small oligonucleotides using large polycations with high charge density resulted in the formation of overly stable complexes with low dissociation levels and diminished stimulatory activity (Gao, et al., 2005). Thus, the application of low molecular weight (LMW) chitosans has emerged as a possible strategy for the encapsulation of small oligonucleotides, as they can facilitate their dissociation from the carrier. Moreover, the stability of chitosan-based nanoparticles could be tailored by adjusting the DDA of chitosan, which governs the charge density on the chitosan backbone (Malmo, Sørgård, Vårum, & Strand, 2012). It was reported that the decrease in the charge density contributes to lower cytotoxicity and may facilitate the intracellular release of nucleic acids from the nanoparticles (Grigsby & Leong, 2010). Thus, the impact of both chitosan M_w and DDA on the physicochemical characteristics of nanoparticles should be evaluated in terms of the intracellular delivery of CpG ODNs.

Although chitosan provides a good basis for CpG ODN encapsulation, it may need some further modifications to meditate an efficient delivery to APCs (Asthana, Asthana, Kohli, & Vyas, 2014). Targeting mannose recognition receptors, selectively expressed on the surface of macrophages and DCs, is a conventional approach for modification of gene and drug delivery systems (Jiang, et al., 2008; Kim, Jin, Kim, Cho, & Cho, 2006; Dehaini, Fang, & Zhang, 2016). These receptors recognize and bind to mannosylated molecules, as well as mediate their

endocytosis (Stahl & Ezekowitz, 1998). Thus, the incorporation of a mannose moiety onto the chitosan backbone will be explored for its ability to enhance the delivery of CpG ODN containing nanoparticles to APCs.

1.14. Hypotheses and Objectives

The overall objective of this research was to develop a vector system based on ionically crosslinked chitosan nanoparticles (chitosan/ODN/PGA) suitable for the efficient CpG ODN delivery.

Based on the knowledge generated in the previous studies, this thesis research tested the following hypotheses:

1. The physiochemical properties of chitosan/ODN/PGA nanoparticles, such as Z-average particle size, poly dispersity index, zeta potential and encapsulation efficiency, stability can be improved by modulation of the chitosan M_w and DDA.
2. The *in vitro* uptake and internalization efficiency of chitosan/ODN/PGA nanoparticles can be improved through modulation of their particle size, zeta potential, and mannose ligand incorporation.
3. The extent of the *in vitro* immune response activation by the CpG ODN-loaded chitosan nanoparticles can be further improved by the incorporation of mannose moiety onto the chitosan backbone.

Therefore, our specific objectives are:

1. To investigate the impact of chitosan M_w, DDA and mannose grafting on the physiochemical properties of chitosan/ODN/PGA nanoparticles, such as Z-average particle size, polydispersity index, zeta potential, encapsulation efficiency, and stability.

2. To investigate the *in vitro* uptake and internalization efficiency of chitosan/ODN/PGA nanoparticles in relation to their particle size, zeta potential, and mannose ligand incorporation using macrophage-like RAW 264.7 cells.
3. To examine the *in vitro* immune response activation by the CpG ODN-loaded chitosan/PGA nanoparticles using macrophage-like RAW 264.7 cells.

The realization of this research project will advance our knowledge on the formulation of ionically cross-linked chitosan nanoparticles as a possible strategy for encapsulation and intracellular delivery of small unmethylated oligonucleotides containing CpG motifs. The impact of chitosan $M_{w,}$ DDA, and mannose grafting on the physiochemical characteristics of nanoparticles will be determined. Accordingly, the physiochemical properties of chitosan nanoparticles can be specifically tailored to achieve the desirable CpG ODNs encapsulation efficiency and provide enhanced immunostimulatory activity, which may open new routes for their therapeutic application. Further, this research will provide a valuable scientific basis for the intranasal administration of CpG ODN-loaded nanoparticles as a stand-alone treatment against infectious diseases such as the Bovine respiratory disease.

Chapter 2

Low molecular weight chitosan nanoparticles for CpG ODN 1826 delivery: impact of molecular weight, degree of deacetylation, and mannosylation on intracellular uptake and induction of TLR9-mediated cytokine secretion

2.1. Introduction

Synthetic oligonucleotides containing unmethylated cytosine-phosphate-guanosine motifs (CpG ODNs) have emerged as potent activators of innate and adaptive immune responses, exerting their activity through the stimulation of the endosomal Toll-like receptor 9 (TLR9) (Kawai & Akira, 2010; Krieg, 2006). Ligation of TLR9 leads to activation of MyD88-dependent NF-kB and MAPK signaling cascades, which ultimately initiates production of proinflammatory cytokines and chemokines, including tumor necrosis factor-α (TNF-α), interleukin-6 (IL-6), interleukin-10 (IL-10) and type I interferons (IFN) (Krieg, 2006; Hemmi, et al., 2000). Numerous preclinical and clinical studies have demonstrated a great potential of synthetic CpG ODNs as stand-alone immunostimulatory agents and as vaccine adjuvants for treatment and prevention of various infectious diseases, cancer and allergies (Shirota & Klinman, 2014; Hanagata, 2017; Krieg, 2012).

Although there is ample evidence supporting the stimulatory effect of CpG ODNs, this activity is often transient due to the susceptibility to serum nuclease degradation, poor targeting capacity, and inefficient cellular uptake (Mutwiri, Nichani, Babiuk, & Babiuk, 2004; Nichani, et al., 2004; Zhang & Gao, 2017). Therefore, there has been a great interest in developing strategies for optimizing the biological activity of CpG ODNs. One way to address this problem is a chemical modification of the natural phosphodiester backbone of CpG ODNs (Kurreck, 2003; Wan & Punit, 2016; Krieg, Matson, & Fisher, 1996). After the substitution of a non-bridging Oxygen in the phosphodiester linkage with Sulphur, the half-life of prepared phosphorothioate-based CpG ODN

analog was considerably improved (Agrawal & Zhao, 1998). The administration of CpG ODNs containing a full phosphorothioate backbone was reported to be generally safe and well tolerated; however, several safety concerns have been raised, including organ enlargement, destruction of lymphoid follicles and increased susceptibility to autoimmune disease (Bode, Zhao, Steinhagen, Kinjo, & Klinman, 2011; Heikenwalder, et al., 2004; Shirota & Klinman, 2014). In this regard, it is highly desirable to develop an efficient drug delivery system that could overcome these drawbacks, target the endosomal TLR9 receptors in antigen presenting cells (APCs), and enhance the immunostimulatory activity of CpG ODNs.

Chitosan, a naturally occurring cationic polysaccharide, has attracted significant attention as a potential candidate for the CpG ODN delivery due to its low toxicity, biocompatibility and good biodegradability (Techaarpornkul, et al., 2010; Mansouri, et al., 2004). Because of its polycationic nature, chitosan can easily integrate nucleic acids into finely dispersed nanoparticles (Nimesh, Thibault, Lavertu, & Buschmann, 2010). The degree of deacetylation (DDA) and molecular weight (M_w) of chitosan are the two primary parameters affecting its physiochemical properties, which, subsequently, play the crucial role in defining the physicochemical and morphological properties of chitosan nanoparticles.

A tremendous amount of data has been generated for large plasmid DNA (pDNA) delivery using chitosan-based nanoparticles, which were primarily designed to compact the large pDNA cargo into small polyplexes. Usually, they employ chitosans with high DDA and large M_w to promote nanoparticle stability and facilitate its intracellular uptake (Scholz & Wagner, 2012; Lavertu, Méthot, Tran-Khanh, & Buschmann, 2006). In contrast, oligonucleotides are already small molecules, and the attempts to encapsulate them using large polycations with high charge density resulted in the formation of overly stable complexes with low dissociation efficiency and

diminished stimulatory effect (Gao, et al., 2005). The application of low molecular weight (LMW) chitosans has emerged as a possible strategy for encapsulation of small oligonucleotides, as they can facilitate their dissociation from the carrier. Thus, this research aimed to develop a vector system based on chitosan nanoparticles suitable for the efficient CpG ODN encapsulation and its intracellular delivery, that will facilitate CpG ODN protection and enable release. Moreover, targeting the mannose recognition receptor, selectively expressed on the surface of APCs, appeared to be an effective strategy to enhance the delivery of CpG ODN-loaded nanoparticles to the endolysosomal TLR9 (Asthana, Asthana, Kohli, & Vyas, 2014).

The overall objective of this research was to develop a vector system based on chitosan nanoparticles suitable for the efficient CpG ODN delivery to target APCs, with minimal cellular toxicity. In particular, the impact of M_w, DDA and mannosylation of LMW chitosan on the properties of CpG ODN-loaded nanoparticles was investigated. Nanoparticles were prepared by ionic gelation method with poly (L-glutamic acid) using a well-defined LMW chitosan and its half N-acetylated and mannosylated derivatives. The obtained nanoparticles were morphologically and structurally characterized based on dynamic light scattering, laser Doppler velocimetry, transmission electron microscopy, and gel retardation. The nanoparticle-mediated cytotoxicity was evaluated in macrophage-like RAW264.7 cells. Also, the efficiency of this CpG ODN delivery system was determined based on quantification of CpG ODN uptake into RAW264.7 cells by multi-spectral imaging flow cytometry, as well as by assessing induction of IL-6 secretion by enzyme-linked immunosorbent assay (ELISA).

2.2. Materials and methods

2.2.1. Materials and cell culture

Chitosan (M_w ~200 kDa, DDA 77%), chitosanase from *Streptomyces griseus*, poly (L-glutamic acid) sodium salt (M_w ~1.5-5.5 kDa), acetic anhydride, α-D-Mannopyranosylphenyl isothiocyanate were purchased from MilliporeSigma (St. Louis, MO, USA). CpG ODN 1826 (5′-TCC ATG ACG TTC CTG ACG TT-3′) was purchased from Invivogen™ (San Diego, CA, USA). The cell culture-related reagents, including Dulbecco's modified Eagle's medium (DMEM), phosphate buffered saline (PBS, pH 7.4), Opti-MEM™ reduced serum media, and certified fetal bovine serum (FBS) were purchased from Gibco™ (Carlsbad, CA, USA). Lipofectamine 2000 Transfection Reagent and 3-[4,5-dimethylthiazol-2-yl]-2,5-diphenyltetrazolium bromide (MTT) ware obtained from Invitrogen™ (San Diego, CA, USA). All other reagents were of analytic grade.

RAW 264.7 (ATCC® TIB-71™) were purchased from American Type Culture Collection (ATCC) (Manassas, VA, USA). Cells were maintained in DMEM Medium supplemented with 10% (v/v) FBS at 37 °C h in the humidified atmosphere containing 5% CO_2. Every 48 to 56 h cells were subcultured according to the ATCC protocol without antibiotics.

2.2.2. Chitosan enzymatic hydrolysis

The LMW chitosan samples with M_w close to 5 and 15 kDa were prepared by enzymatic hydrolysis. Chitosan (2 g) was completely dissolved in 100 ml of 1% acetic acid (v/v). After adjusting pH to 5.5 with NaOH, the solution in the reaction vessel was placed in a water bath (50 °C). Then 5 U of Chitosanase from *Streptomyces griseus* were added to initiate the hydrolysis. The rate of hydrolysis was controlled by taking samples at regular intervals for analysis of the molecular weight by Size Exclusion Chromatography - High-Performance Liquid Chromatography (SEC-HPLC). When the desired molecular weight was achieved, the hydrolysis

was terminated by boiling the mixture for 10 min. Then the chitosan solution was cooled and filtered through 0.2 μm nylon membrane syringe filters (Merck Millipore Ltd., ON, Canada). The chitosan samples were further separated by ultrafiltration using Macrosep® advance centrifugal devices with 3, 10, and 30 kDa molecular weight cutoffs (MWCO) (Pall Filtron, Northborough, MA, USA). Then all fractions were adjusted to pH 9 with 0.5 M NaOH and dialyzed for 72 h against distilled water using a 3.5 – 5 kDa MWCO Spectra/Por® Biotech Cellulose Ester (CE) Membrane (Spectrum Laboratories Inc., Rancho Dominguez, CA, USA). Finally, samples were freeze-dried and grinded to generate fine powders.

2.2.3. Half reacetylation of LMWC

The N-acetylation reaction was performed following the procedure of Hu, et al. (2007) with some minor modifications. Briefly, 0.3 g of LMW chitosan samples obtained above were dissolved in 50 mL of 2% acetic acid (v/v). Then the desired amount of acetic anhydride was dissolved in 50 ml ethanol (corresponding to a molar ratio of 0.8 compared with glucosamine residue) and added slowly under vigorous stirring (1200 rpm) to the chitosan solution. After 4 h of continuous stirring (800 rpm) at room temperature, the solution was adjusted to pH 9, and chitosan was precipitated in 70 % ethanol. The precipitate was further washed with 100% ethanol and acetone to remove excess reactants. The obtained half N-acetylated chitosan samples ware dried at 35°C in the vacuum oven overnight. Then the dry powders were dissolved in 1% acetic acid (v/v) and dialyzed for 72 h against distilled water using the 3.5 – 5 kDa MWCO Spectra/Por® Biotech Cellulose Ester (CE) Membrane (Spectrum Laboratories Inc., Rancho Dominguez, CA, USA), and finally, obtained samples were freeze-dried. The DDA of half N-acetylated chitosans was determined by ^{1}H NMR spectroscopy.

2.2.4. Preparation of mannosylated LMW chitosan

Mannosylated LMW chitosans were synthesized according to a previously reported method with minor modifications (Kim, Jin, Kim, Cho, & Cho, 2006). The half N-acetylated LMW chitosan (50 mg) was dissolved in 5 ml Milli-Q® water and mixed with 10 mg α-D-Mannopyranosylphenyl isothiocyanate dissolved in 2 mL of Dimethyl Sulfoxide (DMSO). The polymer solution was stirred for 24 h at 700 rpm at 40 °C. The product was precipitated in isopropanol and centrifuged at 12000×g for 15 min at room temperature to collect the pellet. Then, the pellet was washed thoroughly with isopropanol and dried at 35°C in the vacuum oven overnight. The sugar substitution was confirmed and determined by ^{1}H NMR spectroscopy.

2.2.5. Characterization of chitosan

Chitosan number and weight average molecular weights (M_n and M_w) and the polydispersity index (M_w/M_n) were determined by SEC-HPLC using an Agilent 1200 Series HPLC System combined with an Agilent 1200 series refractive index detector (RID G1362A) (Agilent Technologies Inc., Mississauga, ON, Canada). The chromatographic analyses were carried out with an Ultrahydrogel guard column along with an Ultrahydrogel linear column (7.8 × 300 mm, blend) (Waters, MA, USA) following the methodology outlined in Gullón et al. (2016) with a slight modification. The temperature of the columns and refractive index detector was maintained at 30°C. Samples were eluted with 0.2 M acetic acid/0.1 M sodium acetate buffer (pH 4.3) at a flow rate of 0.6 ml/min. All samples were filtered using a 0.2 μm nylon membrane syringe filter (Merck Millipore Ltd., ON, Canada), and 50 μl of the sample solution was introduced in the HPLC system. The system was calibrated using pullulan standards with different molecular weights (0.3–800 kDa, Sigma, St. Louis, MO, USA) at a concentration of 2 mg/ml.

The Proton Nuclear Magnetic Resonance Spectroscopy (^{1}H NMR) was used to determine the DDA of chitosan samples (Lavertu, et al., 2003). Briefly, samples (10 mg) were dissolved in 1.96 ml D_2O and 0.04 ml DCl at room temperature overnight with stirring. 700 µl of the sample solution was then transferred to an NMR tube (Wilmad, 5 mm, 7" long). ^{1}H NMR spectra were acquired on an Agilent/Varian Inova 400 MHz two-channel spectrometer. The DDA was calculated using integrals of the peaks of proton H1 of both deacetylated (H1-D) and acetylated monomers (H1-A) using the following equation (1):

$$\mathrm{DDA} = \left(\frac{H1D}{H1D+H1A}\right) \times 100\% \quad (1)$$

2.2.6. Preparation of nanoparticles (NPs) using ionic gelation method

NPs were prepared based on the ionic gelation method at an N/P/C charge ratio of 20/1/6 as described elsewhere (Peng S. F., et al., 2009). The N/P/C charge ratio is expressed as the ratio of moles of the amino groups (N) on the chitosan backbone to the phosphate groups (P) on the CpG ODN 1826 and to the carboxyl groups (C) on poly (L-glutamic acid) (PGA). Chitosans were dissolved overnight on a rotary mixer in 0.05 % (v/v) acetic acid at a final concentration of 5 mg/ml. The pH value of polymer solutions was adjusted to 5.5 ± 0.1 with 0.01 M NaOH. The sterile filtered stock solutions of LMW, half N-acetylated, and mannosylated chitosans with M_w of 5 and 15 kDa were then diluted with RNAse free water to achieve a final concentration of 1.28, 1.94 and 2.78 mg/ml, for each pair of polymers, respectively. An aqueous CpG ODN 1826 (10 µg) was mixed with aqueous PGA (24 µg) with a final volume of 100 µl. NPs were spontaneously formulated upon the addition of the CpG ODN 1826 and PGA mixture into 100 µl of chitosan solution while vortexing for 60 s. Then the NPs were incubated at room temperature for at least 30 min to allow the nanoparticle formation.

2.2.7. Characterization of NPs

2.2.7.1. Mean particle size, size distribution, and zeta potential determination

NP size measurements were carried out using dynamic light scattering (DLS) with a Zetasizer Nano-ZS (Malvern Instruments, UK). The analysis was performed at 25 °C and at 90° scattering angle. The viscosity and the refractive index of distilled water were set at 0.88 MPa s and 1.33, respectively (Mao, et al., 2005). The mean hydrodynamic diameter of NPs and their size distribution were generated by the cumulant analysis. A zeta potential of NPs was determined using a laser Doppler velocimetry technique with the Zetasizer Nano-ZS. The zeta potential measurements were done using a standard capillary cell in the automatic mode. All measurements were done in triplicates with 3 consecutive runs to ensure reproducible results.

2.2.7.2. Transmission electron microscopy measurements

The morphological examination of freshly prepared NPs was performed using a transmission electron microscopy (TEM). The samples were placed on a copper grid, allowed to sit for 30 seconds and air-dry. Then they were negatively stained with 2% (w/v) uranyl acetate. TEM micrographs were obtained with a Philips/FEI (Morgagni) Transmission Electron Microscope with Gatan Digital Camera operating at 120 kV (Hillsboro, Oregon, USA).

2.2.7.3. Determination of CpG ODN 1826 encapsulation efficiency

To determine the encapsulation efficiency (EE) of CpG ODN, chitosan NPs were loaded with FITC-labelled CpG ODN 1826. The EE was calculated from the amount of non-entrapped or adsorbed CpG ODN remaining in the supernatant compared to the amount added during the encapsulation process. For this purpose, freshly prepared NPs were centrifuged at 13,000×g for 40 min. The concentration of FITC-labeled CpG ODN in the supernatant was quantified by

fluorescence intensity measurement using excitation/emission maxima of 495/520 nm in a SpectraMax® M3 microplate reader (Molecular Devices, California, USA). The supernatants of the corresponding NPs without FITC-labeled CpG ODN were used as a blank. The EE (%) of CpG ODN was calculated using the following equation (2):

$$EE\ (\%) = \frac{initial\ amount\ of\ CpG\ ODN - amount\ in\ the\ supernatant}{initial\ amount\ of\ \text{CpG ODN}} \times 100\% \quad (2)$$

2.2.8. Agarose gel electrophoresis

The 4% agarose gel electrophoresis was performed to monitor the complexation of CpG ODN 1826 to chitosan NPs. Samples of naked CpG ODN and CpG ODN-loaded into the chitosan NPs were mixed with the 6× DNA loading dye (Thermo Scientific, San Jose, CA) in a 6:1 proportion and loaded on the gel. The TrackIt™ 1 Kb Plus DNA Ladder (Invitrogen, Carlsbad, CA) was used as a tracking marker in all gels. The electrophoresis was performed at a constant voltage of 50 V for 30 min in 0.05 M Citric Acid – Sodium Citrate Buffer at pH 5.0, 5.5, and 5.9. Subsequently, gels were stained with 1× dilution of SYBR Gold Nucleic Acid Gel Stain (Invitrogen, Carlsbad, CA) in 1× Tris-acetate-EDTA (TAE) buffer for 30 min. The migration of CpG ODN was visualized using a UV illuminator (Azure c200, Azure Biosystems).

2.2.9. *In vitro* experiments

2.2.9.1. Cytotoxicity of chitosan/PGA NPs

The cytotoxicity of the chitosan/PGA NPs as carriers for CpG ODN 1826 was evaluated using a quantitative MTT assay. Macrophage-like RAW 264.7 cells were seeded in 96 well plates at a density of 5×10^3 cells/well in 100 µl volume of full culture medium (DMEM medium supplemented with 10% FBS) and allowed to attach overnight. After the incubation, the culture medium was removed, and fresh full growth medium containing different chitosan/PGA NPs at a final concentration of 0.2, 0.1 and 0.05 mg/mL was added to each well. Cells treated only with the

full culture medium served as a control. RAW 264.7 cells were further incubated for 24 h at 37°C. Following the incubation, the medium containing chitosan samples was removed, cells were washed once with 100 µl of PBS, and 100 µl of MTT solution (1 mg/mL) in full growth medium was then introduced into each well. After 4h of incubation at 37°C, the MTT containing medium was discarded, and the resultant formazan crystals formed in live cells were dissolved in DMSO (100 µl). Finally, the absorbance intensity at 570 nm was measured using a SpectraMax® M3 microplate reader (Molecular Devices, USA). The relative cell viability was calculated as a percentage of viable cells compared with that of untreated cells as shown in the equation (3):

$$Cell\ viability\ (\%) = \frac{OD570\ sample}{OD570\ control} \times 100\%, \quad (3)$$

where OD570 sample represents the absorbance measurement of treated cells, and OD570 control represents the absorbance measurement from cells that did not receive any treatment.

2.2.9.2. Cellular uptake assay

To monitor cellular uptake of chitosan NPs, samples loaded with FITC-labelled CpG ODN 1826 as a fluorescent marker were used. RAW 264.7 cells were seeded on the MatTek glass bottom dishes (P35G-1.5-14-C, MatTek Corp., USA) at a density of 1×10^5 cells/dish in a 2 ml volume and incubated overnight. Prior to the uptake study, the growth medium was discarded, and the cells were washed 3 times and pre-incubated at 37 °C for 1 h with 2 ml of pre-warmed Opti-MEM®. Cells were treated with NPs containing FITC-labeled CpG ODNs at a concentration corresponding to 400 nM. Cells treated with naked FITC-labeled CpG ODNs served as a control. After 4 h of incubation at 37°C, the uptake process was terminated by discarding the NP-containing medium and rinsing cells three times with pre-warmed PBS and fixing them with 4% paraformaldehyde (w/v in PBS) for 15 min. Then the paraformaldehyde solution was aspirated, and cells were gently rinsed three times with PBS. Following the fixation step, cell membranes and nuclei were stained

with Wheat Germ Agglutinin-Texas Red®-X conjugates (5 ug/ml in HBSS, 15 min) and DAPI (0.1 ug/ml in PBS, 15 min), respectively. Cells were kept in PBS until analysis with a Confocal laser scanning microscope Zeiss LSM 710 Meta (Carl Zeiss Jena GmbH, Jena, Germany). The fluorescence was observed using a blue diode (excitation at 405 nm), multi-line Argon laser (excitation at 458, 488, 514 nm), and a solid-state laser (excitation at 561 nm). An oil immersion objective was used to visualize samples. Images were processed with ZEN 2009LE software (Carl Zeiss MicroImgaing GmbH, Germany).

2.2.9.3. Cellular internalization assay

The cellular internalization of NPs was quantitatively analyzed by Multi-Spectral Imaging Flow Cytometry (MIFC) (Phanse, et al., 2012). RAW 264.7 cells were seeded in 6-well plates at a density of 0.5×10^6/well in a 2 ml volume and incubated overnight to allow attachment. Cells were pre-incubated with Opti-MEM® and transfected with NPs containing FITC-labeled CpG ODN as well as naked FITC-labeled CpG ODN at a concentration corresponding to 40 nM. After 4 h of incubation at 37°C, the experiment was terminated. Cells were detached from the surface of the culture vessels with Versene solution. Cells were washed once, resuspended in 0.1 ml of FACS buffer (2% FBS in PBS) and transferred to microtubes for further analysis.

The internalization of FITC-labeled CpG ODN 1826 and its median fluorescence intensity (MFI) levels were determined using the ImageStreamX® Mark II imaging flow cytometer (Amnis/EMD Millipore, Seattle, WA) equipped with dual cameras and three excitation lasers (405, 488, 642 nm). All samples were acquired at ×40 magnification with a 0.75 numerical aperture objective giving a 60 × 256 µm field of view. A minimum of 5000 events in focus were collected for each sample. MIFC data was collected only from the relevant channels including Channel 01 (Ch01, bright field camera 1), Channel 02 (Ch02, FITC fluorescence, 488 nm blue laser power of

40 mV), Ch06 (side scatter), and Ch09 (bright field camera 2). No compensation was required as only one fluorescence channel was used.

The IDEAS® 4.0 software was used to analyze the MIFC data. Masks (regions of interest within the fluorescent image) coupled with features (calculations that contain quantitative and positional information about the image) were used to obtain the quantitative measurements of the acquired images (Phanse, et al., 2012). Mainly, the default mask (M01) of the brightfield was used to identify singlets and cells in the focus. Then, the Erode mask (M01,4) was created to specify only the intracellular region of the cell by eroding the default mask (M01) by 4 pixels around. The IDEAS features Area and Aspect ratio of the brightfield image (M01) were used to limit the analysis to a single cell and eliminate debris and doublets. The Gradient RMS feature was used to locate all cells in focus. The Max Pixel and the Intensity features were used to quantify the percentage of FITC fluorescence positive cells. To quantify internalized FITC labelled CpG ODNs from surface bound CpG ODNs a histogram of the Internalization feature was generated, which compares the FITC fluorescent intensity inside the cell to the whole cell intensity.

2.2.10. Cytokine release from RAW 264.7 cells

RAW 264.7 cells were used to evaluate the ability of CpG ODN 1826 containing chitosan NPs to induce the proinflammatory cytokine secretion. RAW 264.7 cells were seeded in 6-well plates at a density of 0.5×10^6/well in a 2 ml volume and incubated overnight to allow attachment. After the incubation, cells were washed and pre-incubated with Opti-MEM® for 1 h. Cells were stimulated with NPs containing CpG ODNs and free CpG ODNs at a concentration corresponding to 40 nM. Cells stimulated with CpG ODNs complexed with Lipofectamine™ 2000 were used as a positive control. Following a 24 h incubation at 37°C, the media were collected and centrifuged at 120 × g for 10 min at 4 °C. The supernatants were stored at -20°C until use. The levels of IL-6

secretion in cell culture supernatants were determined by enzyme-linked immunosorbent assay (ELISA) assay using protocols recommended by the manufacturer (eBiosciences, Vienna, Austria).

2.2.11. Statistical analysis

The half N-acetylated and mannosylated chitosan derivatives were prepared from the same batch of LMW chitosan of 5 and 15 kDa molecular weight. In graphs, all data are present as a mean ± standard deviation (SD). A one-way ANOVA combined with a Tukey–Kramer tests was carried out to examine the difference between groups. GraphPad Prism version 7.00 for Windows software (GraphPad Software Inc., La Jolla, CA, USA) was used to perform all statistical analyses and construct the graphs. A two-sided P value less than 0.05 was considered statistically significant.

2.3. Results and discussion

2.3.1. Preparation of chitosan samples

Chitosan was first enzymatically hydrolyzed with chitosanase from *Streptomyces griseus* at pH 5.5 at the temperature of 50 ℃. LMW chitosan hydrolysates with narrow molecular weight distribution were obtained using ultrafiltration membranes of various molecular weight cut-offs. In the second step, the LMW chitosan samples were half N-acetylated using acetic anhydride in the acetic acid–water–ethanol complex solvent system. The obtained half N-acetylated products, with about 50% DDA, were fully soluble in pure water due to the random distribution of the N-acetyl groups which is consistent with previously reported results (Kubota, Tatsumoto, Sano, & Toya, 2000). The SEC-HPLC chromatograms of chitosan, LMW, and partially N-acetylated chitosan samples are shown in Figure 2-1. The final M_w (weight average molecular weight), M_n (number average molecular weight), and the M_n/M_w (polydispersity index) of samples were

calculated based on the SEC-HPLC data and are demonstrated in Table 2-1. The data shows that the M_w of each hydrolysate declined from 200 kDa to around 5 and 15 kDa as a result of enzymatic hydrolysis. After the N-acetylation reaction, the M_w of samples was not modified appreciably due to the mild reaction conditions that protect the integrity of chitosans against degradation (Kiang, Wen, Lim, & Leong, 2004). The DDA of untreated chitosan and the 5 and 15 kDa hydrolysates was calculated to be 76.9%, 74.4% and 76.1%, respectively, using the ^{1}H NMR spectroscopy (Figure A2-1). The enzymatic hydrolysis reaction with chitosanase had a rather evident effect on chitosan depolymerization with no alteration of the DDA. After the N-acetylation reaction, the DDA of 5 kDa and 15 kDa samples were decreased to 49.5% and 51.2 %, respectively. The ^{1}H NMR spectrum of the partially N-acetylated chitosan is shown in Figure A2-2.

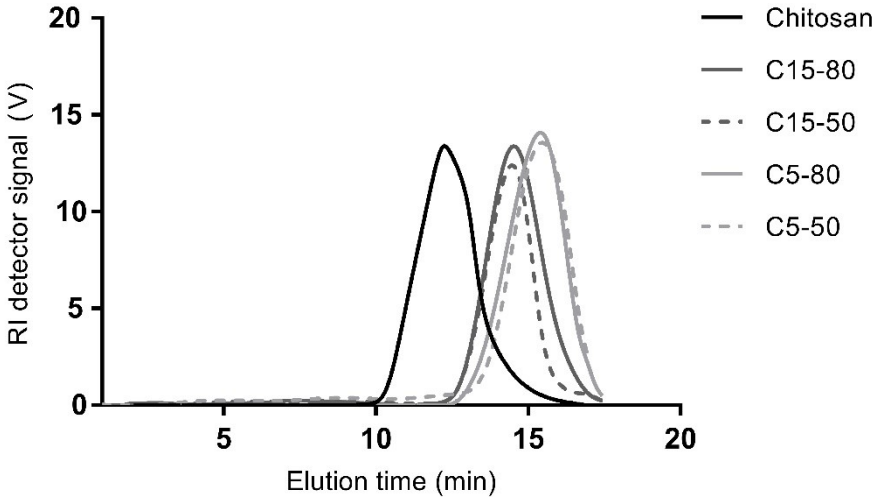

Figure 2-1. HPLC-SEC chromatography of chitosan and its LMW hydrolysates and half N-acetylated samples with different M_w and DDA. Samples are denoted as C M_w – DDA, where the M_w denotes the weight-average molecular weight, DDA – degree of deacetylation. For instance, C15-80 sample possess M_w of 15 kDa and the DDA 80%.

Table 2-1. Molecular weight and DDA of chitosan and the LMW and half N-acetylated chitosan derivatives.

Samples	M_w (kDa)	M_n (kDa)	M_w/M_n	DDA (%)
Chitosan	201.8	179.0	1.13	76.9
C5-80	7.05	6.23	1.12	76.1
C15-80	15.01	13.56	1.11	74.4
C5-50	6.54	5.63	1.16	49.5
C15-50	18.36	16.67	1.10	51.2

M_w: weight average molecular weight; M_n: number average molecular weight; M_n/M_w: polydispersity index; DDA: degree of deacetylation.

2.3.2. Synthesis of mannose grafted LMW chitosan

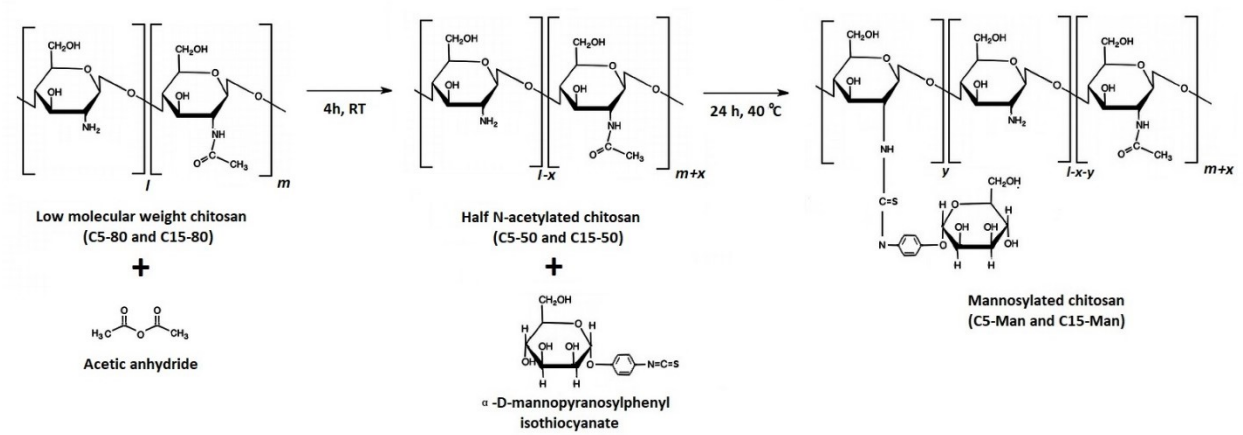

Figure 2-2. Proposed reaction scheme for the preparation of mannosylated LMW chitosan.

To obtain mannosylated LMW chitosan, the half N-acetylated LMW samples were mannosylated with α-D-mannopyranosylphenyl isothiocyanate (Figure 2-2). The direct thiourea linkage reaction between the electrophilic isothiocyanate group of α-D-Mannopyranosylphenyl isothiocyanate and the primary amine group of LMW chitosan typically require an unprotonated form of amine to ensure its nucleophilic behavior (Ravin, 2014). Thus, preparation of the half N-acetylated LMW chitosan with good water solubility had facilitated the mannose grafting on the primary amine groups. The synthesized polymers were analyzed using ^{1}H NMR, and the chemical

shifts of proton peaks are shown in Figure A2-3. The proton peaks at 7.0-7.4 ppm were assigned to the protons of the benzene (-CH-) in α-D-Mannopyranosylphenyl isothiocyanate, confirming the mannose conjugation onto the half N-acetylated LMW chitosan backbone. The degree of mannose substitution was calculated by comparing DDAs of samples prior and after this modification and ware determined to be 13.2% and 17.9% for 5 kDa and 15 kDa samples, respectively. Mannosylated chitosan samples are denoted as C M_w – Man, where the M_w denotes the weight-average molecular weight, Man – the presence of mannose ligand. For instance, C15-Man – a mannosylated 15 kDa chitosan sample.

2.3.3. Formation and physicochemical characterization of chitosan/ODN/PGA NPs

In this study, CpG ODN – loaded NPs based on LMW chitosan and its derivatives were prepared using an ionic gelation method with poly (L-glutamic acid) (PGA) as a crosslinking agent in an aqueous medium. The pK_a values of chitosan and PGA are 6.5 and 4.9, respectively (Nimesh, Thibault, Lavertu, & Buschmann, 2010; Cheng & Corn, 1999; Peng S. F., et al., 2009). At the current experimental conditions (pH 5.5), both chitosan and PGA are ionized. CpG ODN 1826 has a constant negative charge over the studied pH range, as the pK_a value of its phosphate groups is approximately 1 (Ma, Lavertu, Winnin, & Buschmann, 2009). Driven by electrostatic interactions between the positively charged amino groups ($-NH_3^+$) on the chitosan backbone and the negatively charged posthaste groups ($-PO_4^-$) on CpG ODN and carboxyl groups ($-COO^-$) on PGA backbones, ionized polymer chains can be cross-linked to form nanoparticles. This process results in the gelation of chitosan and generation of a 3-D network matrix in the form of spherical and homogeneous NPs (Csaba, Köping-Höggård, & Alonso, 2009) (Figure 2-3). The CpG ODN

release from the chitosan nanoparticle is likely to occur though the diffusion mechanism and degradation of the polymer matrix (Mohammed, Syeda, Wasan, & Wasan, 2017).

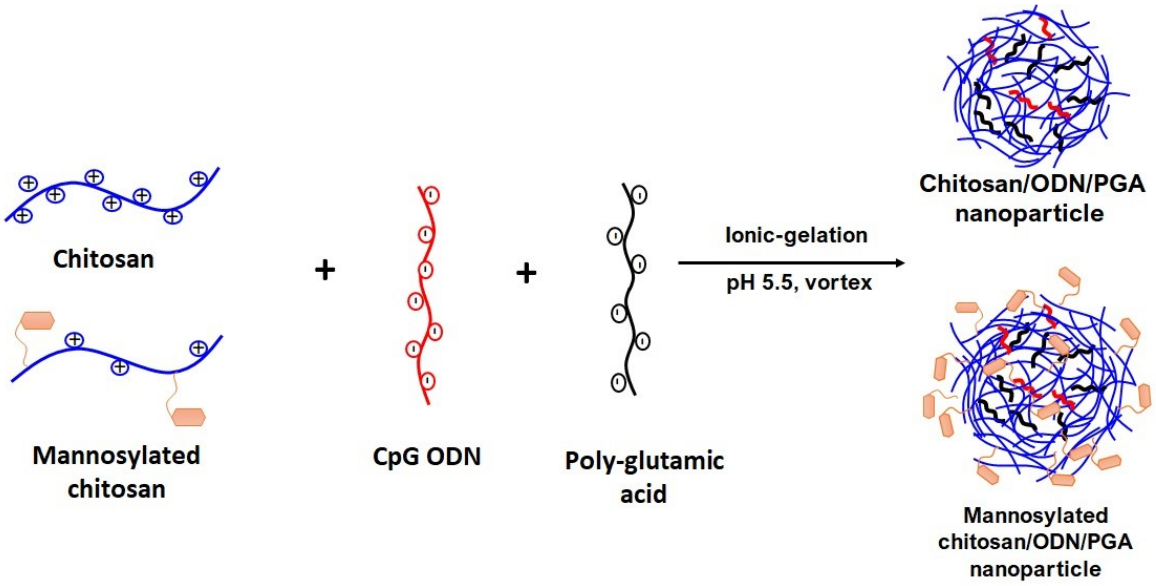

Figure 2-3. Schematic illustration of the formation of CpG ODN 1826 – loaded NPs using an ionic gelation method of chitosan and mannosylated chitosan samples.

The particle surface charge, size, and morphology can greatly influence the *in vitro* and *in vivo* performance of the polymeric NPs (Fröhlich, 2012; Agirre, Zarate, Puras, Ojeda, & Pedraz, 2015; Song, Zhou, van Drunen Littel-van den Hurk, & Chen, 2014). These factors determine particle stability in the suspension and its intracellular uptake; thereby, they affect the intensity of CpG ODN-induced cytokine secretion and immune response activation. NPs with a near-neutral or weak surface charge tend to form aggregates and agglomerates faster, which can significantly alter their *in vitro* and *in vivo* behaviour. The stronger the charge on the surface of NPs the better is the stability of the colloid system, and hence the longer is the shelf life (Bhattacharjee, 2016). Moreover, the positive surface charge of NPs appears to improve binding with negatively charged cellular membranes via electrostatic interactions, which allows DNA to overcome the electrostatic

repulsion and permeate into the cell (Fröhlich, 2012). Previous studies have shown that the gene delivery vectors in the nanometer size demonstrated a relatively higher uptake efficiency compared to microparticles (Singh & Lillard, Jr., 2009). At the same time, particles with a size higher than 100 nm are particularly favorable for the cellular uptake by the APCs via endocytosis (Zhao, et al., 2011; Foged, Brodin, Frokjaer, & Sundblad, 2005; Panyam & Labhasetwar, 2003). Finally, it was reported that the spherical NPs are being endocytosed easier and faster compared to the rod and fiber-like NPs (Gatoo, et al., 2014). Thus, in order to obtain chitosan NPs with desired characteristics, samples of different size and charge were prepared. Moreover, various N/P/C charge ratios of moles of the amino groups (N) on the chitosan backbone to phosphate groups (P) on CpG ODN to the carboxyl groups (C) on PGA were evaluated. In this study, the N/P/C ratio of 20/1/6 was selected based on preliminary trials (data not shown), yielding the formation of small, spherical and finely dispersed NPs with a net positive surface charge.

The mean particle size and the size distribution of the CpG ODN – loaded NPs was measured by the DLS method. Table 2-2 shows that the resulted NPs were finely dispersed with a relatively narrow size distribution as reflected by PDI values lower than 0.200. Under the N/P/C charge ratio of 20/1/6, the mean hydrodynamic diameter of NPs ranged from 101.8 to 185.05 nm. Generally, lowering the M_w from 15 kDa to 5 kDa resulted in the formation of NPs with the smaller size (Katas & Alpar, 2006). C5-80 and C15-80 samples demonstrated a formation of the most compact NPs with a mean particle size of 101.8 and 116.3 nm, respectively. The half N-acetylated and mannosylated chitosans yielded NP of larger mean size than the parent polymer, which could be associated with a higher concentration of those polymers in the mixture to reach the N/P/C charge ratio of 20/1/6. Thus, C5-50 and C15-50 samples formed NPs with the mean particle size of 126.1 and 153.86 nm, respectively. This size growth could also be related to the steric hindrance

caused by the higher number of bulky acetyl groups on their backbones (Kiang, Wen, Lim, & Leong, 2004). After the mannose grafting, the size of NPs was further increased and reached 146.19 and 185.05 nm for C5-Man and C15-Man samples, respectively. The increase in the mean particle size of C5-Man and C15-Man chitosans might be also related to the re-orientation of the uncharged and hydrophilic mannose moieties full of hydroxyl groups towards the surface of NPs. Moreover, they are prone to crosslink between each other and tent to create a form of a corona structure, which could also lead to the size incensement (Chu, Tang, & Yin, 2015).

The zeta potential of CpG ODN – loaded NPs is summarized in Table 2-2. The values ranged from + 20.1 to + 30.1 mV, suggesting that the NPs possessed a net positive surface charge due to excess amount of chitosan. The zeta potential of NPs depended on the DDA of chitosan samples, which governs the charge density on the polymer backbone (Alameh, et al., 2018; Fröhlich, 2012). Thus, the half-N acetylation and mannosylation of parent LMW chitosan decreased the DDA values from 76.1% for C5-80 to 49.5% for C5-50 and 13.2% for the C5-Man, which resulted in a decrease of corresponding zeta potentials from + 29.9 to +23.8 and +20.1 mV, respectively. The same trend was observed for the 15 kDa samples. The M_w of the samples did not show any noticeable influence on the zeta potential of prepared NPs.

The morphology of the CpG ODN-loaded NPs formulated at the charge ratio of 20/1/6 was visualized by the TEM. As demonstrated in Figure 2-4, all NPs appeared to be approximately spherical with a relatively homogeneous size distribution. TEM images also revealed a homogeneous dispersion of NPs due to their positive surface charge resulting in the electrostatic repulsion between colloidal nanoparticles. Thus, the results of DLS and TEM studies confirm the formation of the nanosized cationic NPs with a positive surface charge.

Table 2-2. Average particle size, polydispersity index (PDI), zeta potential, and encapsulation efficiency (EE) of chitosan NPs cross-linked with CpG ODN 1826 and PGA at 20/1/6 charge ratios.

Sample	Size, nm	PDI	Zeta potential, mv	EE, %
C5-80	101.84 ± 4.49	0.147 ± 0.032	29.93 ± 2.90	97.34 ± 1.54
C5-50	126.1 ± 7.585	0.098 ± 0.010	23.78 ± 1.34	88.84 ± 1.56
C5-Man	146.19 ± 5.637	0.075 ± 0.021	20.14 ± 1.32	88.09± 2.40
C15-80	116.26 ± 10.88	0.129 ± 0.031	30.10 ± 2.41	96.78 ± 1.91
C15-50	153.86 ± 8.77	0.132 ± 0.015	27.98 ± 0.91	91.97 ± 3.15
C15-Man	185.05 ± 12.01	0.166 ± 0.017	22.50 ± 0.87	89.60± 1.89

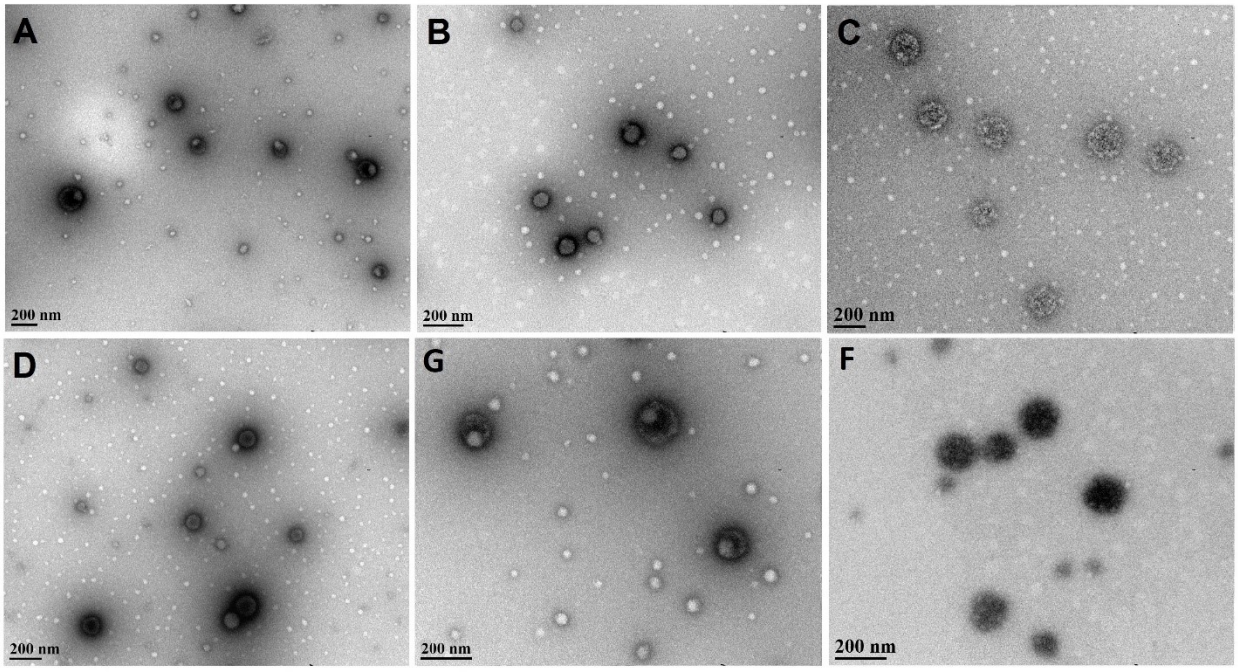

Figure 2-4. TEM images of CpG ODN 1826 loaded NPs at an N/P/C charge ratio of 20/1/6: (A) C5-80/ODN/PGA; (B) C5-50/ODN/PGA; (C) C5-Man/ODN/PGA; (D) C15-80/ODN/PGA; (E) C15-50/ODN/PGA; (F) C15-Man/ODN/PGA.

2.3.4. CpG ODN encapsulation efficiency (EE)

Table 2-2 shows that the levels of CpG ODN encapsulation by C5-80 and C15-80 samples had reached 97.34 ± 1.54 % and 96.78 ± 1.91 %, respectively. This could be attributed to the higher cationic charge density of parenting LMW samples that facilitated a better entrapment of anionic CpG ODN. Nevertheless, this study showed high degrees of CpG ODN encapsulation (over 88%) for both half N-acetylated and mannosylated derivatives, which suggests that the half N-acetylation and mannosylation of the chitosan backbone did not alter the CpG ODN assembling process to a great extend (P=0.0766).

2.3.5. Agarose gel electrophoresis

An effective gene delivery vector should be able to form compact complexes with negatively charged DNA molecules to provide the packaging that protects genetic material against enzymatic degradation by serum nucleases. To evaluate the ability of chitosan NPs to effectively encapsulate CpG ODN 1826, the agarose gel electrophoresis was performed. Figure 2-5 demonstrates the influence of chitosan M_w, DDA and mannose grafting on its ability to complex CpG ODN 1826 at different pH values.

Firstly, the obtained results suggest that the chitosan DDA and its protonation degree played a predominant role in the CpG ODN 1826 encapsulation process (Alameh, et al., 2018; Ma, Lavertu, Winnin, & Buschmann, 2009). Since, CpG ODN 1826 and PGA both have a constant negative charge over the investigated pH range, the variation of solution pH only influenced the degree of ionization of chitosan (Alameh, et al., 2018; Liu, et al., 2007; Nimesh, Thibault, Lavertu, & Buschmann, 2010; Kiang, Wen, Lim, & Leong, 2004). Thus, the increase of the pH of the solution led to the partial reduction of the chitosan's cationic charge density and, subsequently, the CpG ODN encapsulation efficiency (Figure 2-5).

On the other hand, the DDA of chitosan influences the CpG ODN 1826 binding affinity (Kiang, Wen, Lim, & Leong, 2004; Alameh, et al., 2018). Since, the increase in the DDA leads to the increase in the charge density on the chitosan backbone, a lower number of C5-80 and C15-80 was required to electrostatically bind CpG ODN (Ma, Lavertu, Winnin, & Buschmann, 2009). Thus, C5-80 and 15-80 showed a nearly complete retardation of CpG ODN migration at the entire range of tested pH values with a minor release at pH 5.9 (Figure 2-5. A, B, C, lanes 3, 4). In contrast, the half N-acetylated and mannosylated chitosan samples with the DDA of about 50 and 35% demonstrated a noticeable CpG ODN release associated with the pH increase (Figure 2-5. A, B, C, lanes 5, 6, 7, 8). Although, the total number of protonated glucosamine residues was maintained constant at the charge ratio of 20/1/6, half N-acetylated and mannosylated chitosans with the lower DDA had to contribute more chains to achieve the same retardation effect as parental LMW samples. Moreover, the increased content of more bulky acetyl and mannose groups on their backbones created steric hindrance leading to the decreased CpG ODN binding efficiency (Kiang, Wen, Lim, & Leong, 2004). At the same time, the increased number of entangled and cross-linked chitosan chains might form a physical barrier for CpG ODNs to diffuse through, which serves as a rate-limiting membrane for the CpG ODN release (Fig. 2-5. A, B, C, lanes 5, 6, 7, 8) (Alameh, et al., 2018; Ma, Lavertu, Winnin, & Buschmann, 2009; Ahmed & Aljaeid, 2016).

Analysis by agarose gel electrophoresis indicated that chitosan samples with an M_w of 15 kDa displayed a stronger retardation effect on the CpG ODNs migration behavior in comparison to the 5 kDa samples (Figure 2-5). It was previously reported that chitosans with a higher M_w have longer and more flexible chains, whereas polymers with a lower M_w have shorter and stiffer chains (Köping-Höggård, et al., 2004; Alameh, et al., 2018). Thus, a decrease in the ability of shorter chitosan samples to bind anionic phosphate groups of CpG ODNs could be attributed to the loss

of the chain entanglement effect exhibited by the longer polymers (Kiang, Wen, Lim, & Leong, 2004). The 15 kDa chitosans can more easily entangle free CpG ODNs after the initial electrostatic interaction and create an additional non-ionic, knot-like network structure, which limits the diffusion of CpG ODNs (Figure 2-5. A, B, C, lanes 4, 6, 8) (Grigsby & Leong, 2010). In contrast, the decreased ability of shorter C5-80, C5-50, and C5-Man samples to physically entangle free CpG ODN led to its noticeable release associated with the pH increase (Figure 2-5. A, B, C, lanes 3, 5, 7). This suggests that smaller chitosan chains even with the 80% DDA cannot completely entrap CpG ODNs into stable and dense nanoparticles.

However, this trend was not observed when chitosans with comparable M_w and DDA were used to complex plasmid DNA (pDNA). NPs prepared with fully deacetylated chitosan samples with a M_w of 4.7 kDa were able to completely condense and retard the mobility of pDNA even at the N/P charge ratio of 5/1 (Köping-Höggård, Mel'nikova, Vårum, Lindman, & Artursson, 2002). The much smaller size of oligonucleotides compared to pDNA could possibly explain the stronger interactive forces exhibited by pDNA molecules (Scholz & Wagner, 2012). Generally, pDNA have a size of several kilo base pairs (bp), whereas synthetic CpG oligonucleotides have only about 18-25 bases and thus carry a fewer number of negative charges on their backbone (Krieg, 2006; Scholz & Wagner, 2012). Therefore, it is not surprising that CpG ODN 1826 would need a much higher density of chitosan to initiate the electrostatic interaction and assemble NPs. Moreover, the large pDNA molecules can be condensed into much smaller nanostructures in the size range of 30 to 100 nm due to the negative charge neutralization following the electrostatic interaction with the cationic polymer (Scholz & Wagner, 2012). In contrast, CpG ODN 1826 is already a small molecule, thus the main priority for its delivery is the formation of a stable and dense nanoparticle network structure to facilitate a good protection against nuclease degradation.

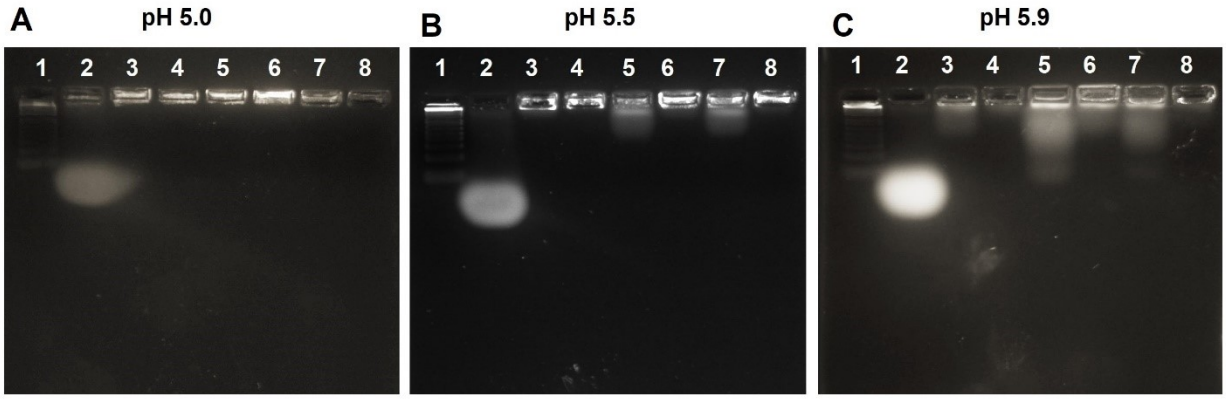

Figure 2-5. Evaluation of the effect of chitosan M_w and DDA and mannose grafting on the encapsulation efficiency of chitosan/ODN/PGA NPs at N/P/C ratio of 20/1/6 using native 4% agarose gel electrophoresis. Lane 1: 1 Kb Plus DNA Ladder; Lane 2: Naked CpG ODN 1826; Lane 3: C5-80/ODN/PGA; Lane 4: C15-80/ODN/PGA; Lane 5: C5-50/ODN/PGA; Lane 6: C15-50/ODN/PGA; Lane 7: C5-Man/ODN/PGA; Lanes 8: C15-Man/ODN/PGA.

2.3.6. Cytotoxicity of chitosan/PGA NPs

A low cytotoxicity of drug/gene delivery vehicles is considered to be one of the major requirements for the successful *in vivo* application. Although the positive charge of NPs appears to improve the uptake efficiency of cationic NPs, they have demonstrated profound cellular toxicity associated with disruption/modulation of the cellular membrane integrity leading to the cell death (Garnett & Kallinteri, 2006; Fröhlich, 2012). In this study, the potential cytotoxicity of cationic NPs formulated using LMW, half N-acetylated and mannosylated chitosan samples as delivery vehicles for CpG ODN 1826 was investigated. The macrophage-like RAW 264.7 cells were incubated with various NPs for 24 h at 37°C. The viability of treated cell relative to the untreated control cell was determined using an MMT assay.

As shown in Figure 2-6, the cationic NPs did not exhibit any significant cytotoxicity under experimental concentrations ranging from 0.05 – 0.2 mg/ml. RAW 264.7 cells treated with chitosan/PGA formulations at a concentration lower than 0.1 mg/ml demonstrated a comparable metabolic activity to the cells in the control group. Moreover, NPs formulated with mannosylated

chitosan samples revealed a significant decrease in cytotoxicity in comparison to the LMW chitosan at concentrations lower than 0.1 mg/ml ($P<0.05$), which could be attributed to the reduction of the cationic surface charge. Generally, reducing the M_w of the chitosan samples from 15 to 5 kDa displayed no alteration in cell viability under experimental concentrations, which was in agreement with the findings reported by Huang, Khor, & Lim (2004). The cell viability rates higher than 100% may be caused by the increased enzymatic activity in the treated cells. These data suggest that the chitosan/PGA NPs are relatively safe and biocompatible vectors for CpG ODN 1826 delivery.

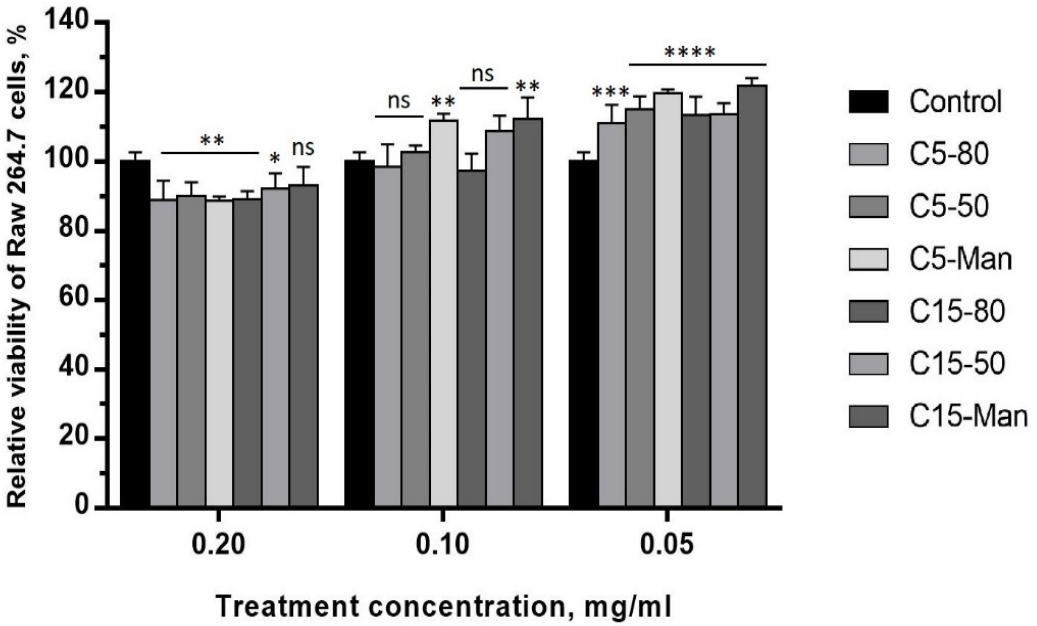

Figure 2-6. *In vitro* cytotoxicity of chitosan/PGA NPs measured by the MTT assay. RAW 264.7 cells were treated with the indicated concentrations of chitosan NPs for 24 h. The relative cell viability is expressed as the percentage of living cells relative to the untreated control cells. Results represent the mean ± S.D (n = 4). *P < 0.05, **P < 0.01, ***P<0.001, and ****P<0.0001 compared with the control.

2.3.7. Cellular uptake of NPs

The present knowledge of CpG ODN recognition indicates that its intracellular delivery is necessary to initiate activation of the TLR9-mediated immune response (Mutwiri, Nichani, Babiuk, & Babiuk, 2004). Moreover, because TLR9 receptors are localized in the endolysosomes of APCs, a delivery system for CpG ODNs requires a specific design strategy to achieve a successful cellular uptake and retention in the endolysosomal compartments of APCs for a prolonged period of time (Krieg, 2002; Chen S. , Zhang, Chinnathambi, & Nobutaka Hanagata, 2013; Hanagata, 2012). Therefore, the cellular uptake efficiency of CpG ODN - loaded NPs formulated using LMW, half N-acetylated and mannosylated chitosan samples was investigated using macrophage-like RAW 264.7 cells. Cells were incubated with different NPs containing FITC-labeled CpG ODN 1826 for 4 h at 37 °C. Cells incubated with naked FITC-CpG ODN 1826 were used as a control. To monitor the cellular uptake, cell membranes were stained red with Wheat Germ Agglutinin-Texas Red®-X conjugates and the cell nuclei were stained blue with DAPI.

Figure 2-7 shows the resultant confocal laser scanning microscope images. As illustrated, the expression of a green fluorescence signal emitted by the FITC-labeled CpG ODN was observed throughout the cytoplasm of all treated cells, indicating successful intracellular delivery. RAW 264.7 cells treated with NPs emitted a significantly brighter green fluorescence signal when compared to the control cells treated with CpG ODN alone (Figure 2-7). These results suggest that the cationic surface charge and nano-scale size of chitosan/ODN/PGA can facilitate the interaction with anionic plasma membranes and, therefore, promote the intracellular uptake via endocytosis (Hanagata, 2012). The lower fluorescent intensity emitted by control cells treated with CpG ODNs alone could be associated with the electrostatic repulsion between the negatively charged CpG

ODN backbone and the anionic plasma membrane that could affect its attachment (Hanagata, 2012).

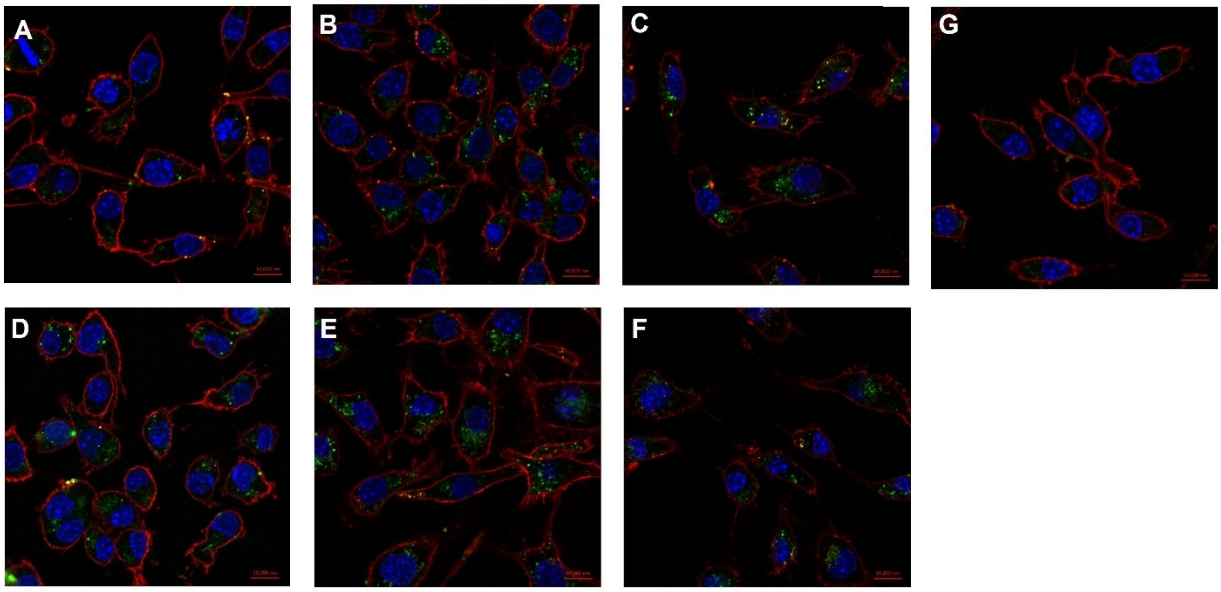

Figure 2-7. Confocal laser scanning microscope images of RAW 264.7 cells exposed for 4 h to: (A) C5-80/ODN/PGA; (B) C5-50/ODN/PGA; (C) C5-Man/ODN/PGA; (D) C15-80/ODN/PGA; (E) C15-50/ODN/PGA; (F) C15-Man/ODN/PGA; (G) naked CpG ODN.

2.3.8. Quantification of the cellular internalization of NPs

Quantification of the fluorescence intensity of FITC-labeled CpG ODN 1826 loaded into chitosan NPs by traditional flow cytometry or fluorescent microscopy is not possible, as NPs may have a different subcellular localization (Jenner, Ducker, Clark, Prior, & Rowland, 2016). The conventional low-resolution flow cytometry technologies lack the ability to distinguish the internalized CpG ODNs from the cell surface-bound. On the other hand, fluorescence microscopy permits recording of enhanced spatial resolution images, but it is a relatively time-consuming technique with a limited capability to analyze large data sets (Phanse, et al., 2012). In contrast, the multi-spectral imaging flow cytometry (MIFC), combined with the IDEAS® software, has advantages of both techniques. This allows a rapid examination of cellular morphology, using

bright field images and patterns of multi-color fluorescent staining, and quantification of the fluorescence at different cellular localizations (Dominical, Samsel, & McCoy Jr., 2017).

To determine whether the nanoparticle encapsulation can enhance the ability of the macrophage-like RAW 264.7 cells to internalize FITC – labelled CpG ODN 1826, the Internalization feature and the Erode Mask was employed. Figure 2-8 demonstrates that this technique can be successfully utilized to distinguish cells with surface-bound (left panel) or internalized (right panel) CpG ODNs using the representative C15-80/ODN/PGA NPs and naked CpG ODNs (Phanse, et al., 2012; Jenner, Ducker, Clark, Prior, & Rowland, 2016). Throughout the study, the percentage of cells with intracellular FITC-labeled CpG ODNs reached almost 100% with no significant difference between all nanoparticle formulations and naked CpG ODNs (Figure 2-9). All samples were able to successfully penetrate the cellular membrane and did not agglomerate on the cell surface. The rapid and efficient uptake of CpG ODN - loaded NPs could be attributed to the positive surface charge of the prepared NPs that potentially can promote the anionic membrane bounding and following cellular internalization process. Interestingly, cells treated with free CpG ODNs demonstrated a comparable internalization rate to cells treated with encapsulated CpG ODN, which might be explained by potential involvement of surface pattern recognition receptors facilitating the CpG ODN uptake. Recently, Lahoud, et al. (2011) provided some evidence that the DEC-205 receptor, expressed by a variety of immune cells, can facilitate the uptake of B class CpG ODNs and promote their internalization and trafficking to the early endolysosomes.

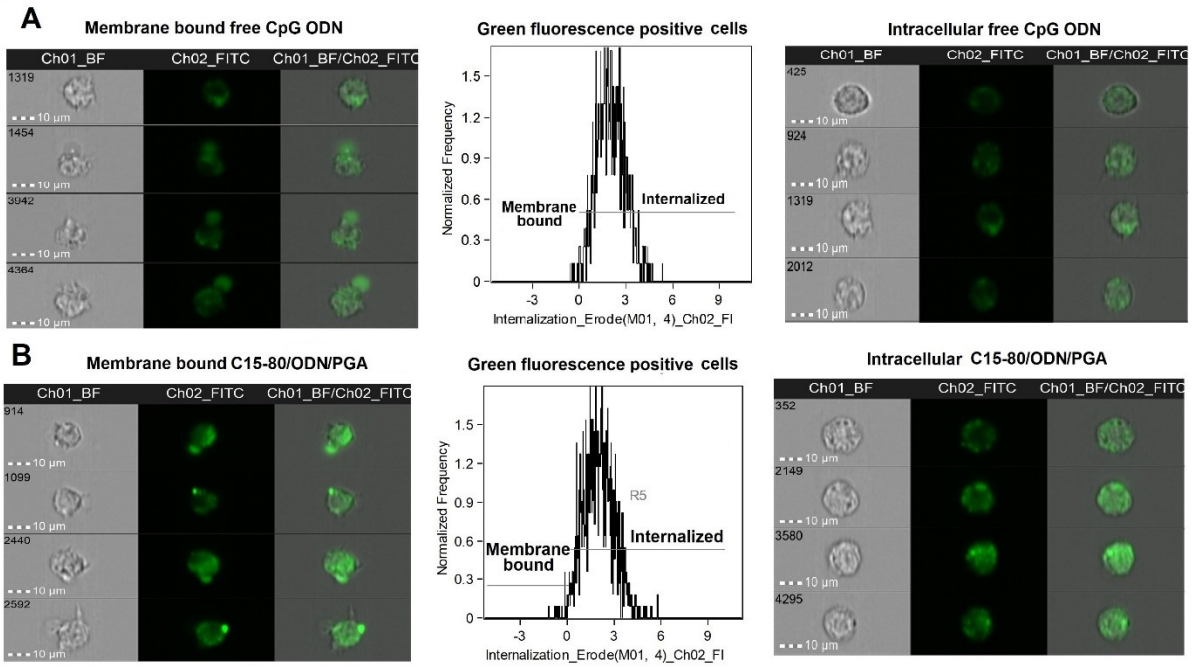

Figure 2-8. Representative images of RAW 264.7 cell with internalized and surface-bound free and nanoparticle encapsulated FITC-labeled CpG ODN 1826: (A) the membrane bound free CpG ODN 1826 (left panel) and fully internalized CpG ODN 1826 (right panel); (B) the membrane bound C15-80/ODN/PGA NPs (left panel) and fully internalized C15-80/ODN/PGA NPs (right panel). Cells were incubated with different formulations for 4h, harvested and analyzed by multispectral imaging flow cytometry using the Internalization feature and the Erode Mask. For each sample 5000 events were collected.

.

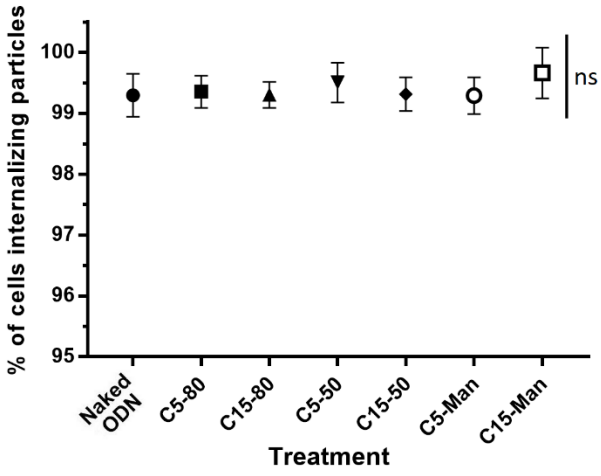

Figure 2-9. Internalization of the free and nanoparticle encapsulated FITC-labeled CpG ODN 1826 into RAW 264.7 cells. Cells were incubated with different formulations for 4h, harvested and analyzed by multispectral imaging flow cytometry to quantify the percentage of cells internalizing particles using the Internalization feature and the Erode Mask. For each sample 5000 events were collected. Data are expressed as the mean ± SD.

To accurately compare the uptake efficiency of NPs, a gross medium fluorescence intensity (MFI) given off from every single cell in the population of FITC-positive cells was quantified. The gross MFI is a measure of the total fluorescence intensity which includes both surface-bounded and intracellular fluorescence signals (Jenner, Ducker, Clark, Prior, & Rowland, 2016). This parameter was determined using the Max Pixel feature (brightest pixel in the picture) versus Intensity feature. It is represented as a normalized MFI (nMFI), where the MFI of the stained sample was normalized to the MFI of the control (Figure A2-4).

As shown in Figure 2-10, RAW 264.7 cells treated with NPs demonstrated significantly higher nMFI levels compared to cells treated with the CpG ODN alone (P<0.05) with one exception. In particular, no significant difference was observed in the normalized FITC fluorescence intensity levels expressed by cells treated with C5-50/ODN/PGA. The limited efficacy of the C5-50 chitosan might be attributed to its physicochemical properties. The above experiments suggest that chitosans with smaller chain length and lower charge density tend to

dissociate prematurely and partially release their cargo, which might have compromised their efficacy as a vector for the CpG ODNs delivery (Dehoussea, et al., 2010). On the other hand, RAW 264.7 cells exposed to C15-80/ODN/PGA NPs generated the highest fluorescence signal among all samples (P<0.05). This can be explained by the higher zeta potential expressed by the C15-80 NPs, which was previously correlated with the increased cellular membrane binding and uptake (Köping-Höggård, et al., 2004; Huang, Fong, Khor, & Lim, 2005). C5-Man and C15-Man demonstrated significantly higher nMFI levels compared to naked CpG ODNs (P<0.05), which could be attributed to the nanoparticle recognition via the mannose receptor-mediated endocytosis (Chu, Tang, & Yin, 2015).

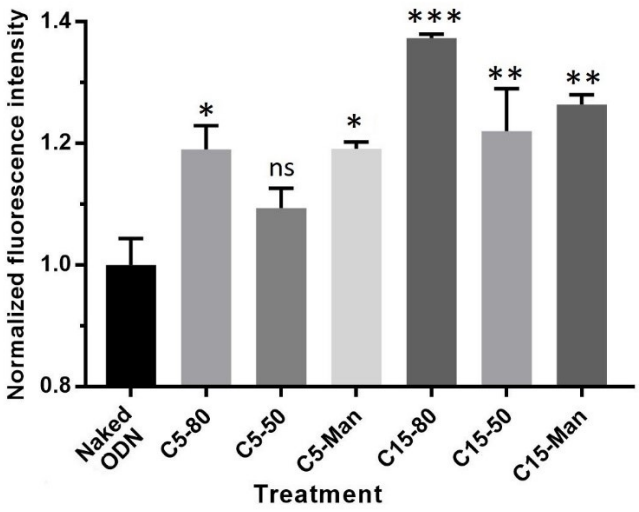

Figure 2-10. Quantification of the median FITC fluorescence intensity (MFI) exhibited by RAW264.7 cells treated with the free and nanoparticle encapsulated FITC-labeled CpG ODN 1826 for 4 h, harvested and analyzed by multispectral imaging flow cytometry using the Max Pixel feature (brightest pixel in the picture) versus Intensity feature from the population of cells positive for the FITC fluorescence. For each sample 5000 events were collected. The data are expressed as the normalized MFI levels (nMFI) relative to the naked CpG ODNs. Results represent the mean ± S.D, *P < 0.05, **P < 0.01, and ***P<0.001.

2.3.9. Interleukine-6 induction in RAW 264.7 cells

The *in vitro* stimulation of APCs such as macrophages, monocytes and dendritic cells using CpG ODNs triggers the activation of the TLR9 signaling pathway and induces a secretion of proinflammatory cytokines and chemokines (Hanagata, 2012; Krieg, 2006). To determine the extent of the cytokine induction by naked CpG ODNs and CpG ODN-loaded NPs in the macrophage-like RAW264.7 cells, the amounts of interleukin-6 (IL-6) secreted into the supernatant media were quantitatively measured by ELISA. Lipofectamine 2000 (LF)-encapsulated CpG ODN was used as a "gold standard" to evaluate the efficiency of the chitosan NP preparations (Cardarelli, et al., 2016; Song, Zhou, van Drunen Littel-van den Hurk, & Chen, 2014).

As shown in Figure 2-11, cells treated with half N-acetylated and mannosylated samples demonstrated a significantly higher IL-6 secretion levels compared to the naked CpG ODNs ($P<0.05$). Although C5-80 and C15-80 samples promoted the CpG ODN cellular uptake (Figure 2-10), they did not induce significant changes in the levels of IL-6 secretion. It was previously reported that the successful intracellular gene delivery depends both on strong DNA protection and efficient intracellular unpacking (Grigsby & Leong, 2010). Thus, the limited efficacy of C5-80 and C15-80 vectors might be explained by the higher CpG ODN-binding valency and its insufficient release inside of the endolysosomal compartments due to the high positive charge density of chitosan. In contrast, the acetylation and mannosylation of chitosan primary amine groups decreased its charge density and diminished the CpG ODN binding affinity. We may speculate that the diminished CpG ODN binding affinity can promote the endolysosomal release of CpG ODNs and mediate a high level of interaction with TLR9 leading to the downstream initiation of an intracytoplasmic signaling pathway and cytokine secretion. Surprisingly, the

significantly lower levels of IL-6 secretion following the CpG ODN– LF treatment (P<0.05), could be associated with increased cellular cytotoxicity of the cationic liposomes having a relatively high surface charge (Song, Zhou, van Drunen Littel-van den Hurk, & Chen, 2014).

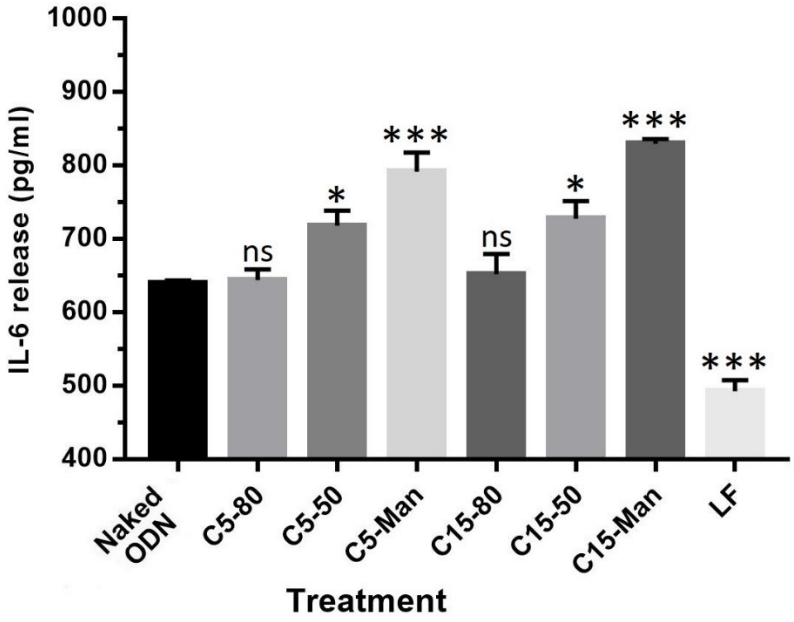

Figure 2-11. Detection of IL-6 secreted by RAW264.7 cells treated with naked CpG ODN 1826, CpG ODN-loaded chitosan NPs or CpG ODN in Lipofectamine (LF). Cells were incubated with different formulations for 24h, harvested and analyzed by ELISA. Data are expressed as the mean ± SD, *P < 0.05, **P < 0.01, and ***P<0.001.

2.3.10. Conclusion

NPs were prepared by ionic gelation of well-defined low molecular weight, half N-acetylated and mannosylated chitosan samples with poly (L-glutamic acid) and evaluated as a potential CpG ODN 1826 delivery systems. Obtained NPs were finely dispersed (PDI < 0.2) with a mean size ranging from 101.8 to 184.5 nm and a zeta potential from +20.1 to +30.1 mV. High CpG ODN encapsulation efficiency was achieved (≥ 88%) in all formulations.

The cellular toxicity, intracellular uptake and cytokine release of the CpG ODN-loaded nanoparticles was studied *in vitro* using RAW 264.7 cells. The results suggest that all nanoparticles

are relatively safe with cell viability over 89%, and both the nanoparticle physiological properties and *in vitro* immunostimulatory activity are dependent on the chitosan M_w and DDA. The mean nanoparticle size was significantly narrowed by lowering the M_w of chitosan from 15 to 5 kDa. Samples with a higher DDA and larger M_w exhibited a better CpG ODN binding ability and chain entanglement effect and were able to form more stable nanoparticles. The high DDA and larger M_w also promoted the cell binding and uptake. Nevertheless, the most efficient immunostimulatory effect was observed while using 50% acetylated and mannosylated chitosan samples, as demonstrated by the highest IL-6 release. The decreased charge density on the chitosan backbone resulted in enhanced intracellular CpG ODN release, which promoted cytokine secretion *in vitro*. Overall, these findings will promote the application of chitosan-based nanoparticles as vectors for the intracellular delivery of CpG ODNs. Further collaboration with the livestock industry may lead to the development of a new CpG ODN delivery system for the Bovine respiratory disease immunotherapy to reduce disease morbidity and mortality.

Chapter 3

General Discussions and Conclusion

3.1. Summary and conclusions

Immunotherapy is a promising treatment and prevention strategy to combat various pathological conditions, including cancer, allergies, asthma and infection diseases. The relatively recent understanding of mechanisms for awakening and enhancing immune responses has fueled immunotherapies to search for novel, safe and effective immunostimulatory agents that can be applied as a stand-alone treatment, a vaccine adjuvant, and successfully co-administrated with other immunoadjuvants and antigens. Recently, synthetic oligonucleotides containing unmethylated CpG motifs (CpG ODNs) have emerged as potent activators of innate and adaptive immune responses, exerting their activity through the stimulation of the endolysosomal Toll-like receptor 9 (TLR9) expressed by the antigen presenting cells (APCs). However, due to the limited stability in the physiological fluids, rapid absorption into the systemic circulation, and insufficient cellular uptake, there is a great interest in developing reliable delivery vehicles for CpG ODNs to enhance their bioavailability and optimize biological activity to achieve the desired therapeutic effect. The overall objective of this research was to develop a vector system based on chitosan nanoparticles suitable for the efficient CpG ODN delivery to the target APCs.

In this work, the influence of chitosan molecular weight, the degree of deacetylation and mannose grafting on the physicochemical properties and *in vitro* immunostimulatory activity of CpG ODN-loaded nanoparticles was investigated. Chitosan samples with the molecular weights of 5 and 15 kDa and the degree of deacetylation of 50 and 80 % were prepared. Additionally, mannosylated chitosans with a substitution degree of 15% were synthesized. Chitosan samples were assembled into nanoparticles by ionic gelation method using poly (L-glutamic acid) as a

cross-linking agent. Obtained nanoparticles had average sizes in a range of 101.8 - 184.5 nm, surface charge values ranged from +20.1 to 30.1 mV, and good encapsulation efficiency (over 88%).

The mean nanoparticle size was significantly narrowed by lowering the molecular weight of chitosan from 15 to 5 kDa. The half N-acetylated and mannosylated samples yielded nanoparticles with a larger size than parent chitosans probably due to the increased concentration of polymers on the solutions and steric hindrance of their backbones caused by the increased number of bulky acetyl and mannose groups. The gel retardation assay demonstrated that the chitosan samples with the molecular weight of 5 kDa had a limited ability to physically entangle CpG ODNs compared to 15 kDa samples, which resulted in the unfavourable nanoparticle dissociation and the premature CpG ODNs release. Simultaneously, increasing the degree of deacetylation facilitated the formation of nanoparticles with a smaller size and a higher surface charge due to the increased cationic charge density on the chitosan backbone. Also, samples with a higher degree of deacetylation exhibited a better CpG ODNs and poly (L-glutamic acid) binding ability and were able to assemble into more stable nanoparticles.

Importantly, chitosan nanoparticles did not exhibit any significant cytotoxicity under experimental concentrations ranging from 0.05 – 0.2 mg/ml, suggesting their applicability as relatively safe and biocompatible carriers for CpG ODN 1826 delivery. Subsequently, the *in vitro* uptake efficiency of nanoparticles was evaluated in relation to the particle size, zeta potential, and mannose grafting. All nanoparticles exhibited mean hydrodynamic diameters higher than 100 nm and positive net zeta potential values, which were reported to be favourable for the cellular uptake via endocytosis by APCs (Zhao, et al., 2011; Foged, Brodin, Frokjaer, & Sundblad, 2005). Chitosans with 80% degree of deacetylation and 15 kDa molecular weight improved the

intracellular uptake of free CpG ODNs by 37.3% due to the high positive charge at the nanoparticle surface. Moreover, the mannose ligand grafting on the chitosan backbone promoted the uptake of nanoparticles by 27% through the mannose receptor-mediated recognition and uptake. Finally, the most efficient immunostimulatory effect was observed while using 50% deacetylated and mannosylated chitosan samples with the molecular weight of 15 kDa. The decreased charge density of the chitosan backbone resulted in the enhanced intracellular CpG ODN release, which promoted *in vitro* cytokine secretion. These findings support the application of half N-acetylated and mannosylated chitosans with the molecular weight of 15 kDa as promising vectors for the intracellular delivery of CpG ODNs and reveal the importance of chitosan structures for the optimization of the immunostimulatory activity of CpG ODNs.

3.2. Significance of this research

This research has extended the application of chitosan-based nanoparticles as efficient vectors for the intracellular delivery of CpG ODNs to the target antigen presenting cells. Currently, the most investigated cationic polymer vectors for the CpG ODN delivery employ polyethyleneimine (PEI) (Cheng, Miao, Kai, & Zhang, 2018), gelatin (Zwiorek, et al., 2008), acetalated dextran (Peine, et al., 2013), poly (L-lysine) (Chen, Sun, Tran, & Shen, 2011), and polystyrene (Kerkmann, et al., 2004), which could have low encapsulation efficiency, poor storage stability, fast cargo release, and lack of biodegradability (Petkar, Chavhan, Agatonovik-Kustrin, & Sawant, 2011). In contrast, chitosan is a renewable, biocompatible, biodegradable, and mucoadhesive natural polymer. Due to its polycationic nature, chitosan can effectively encapsulate nucleic acids, facilitate their protection against the nuclease degradation, and enable the controlled release. Moreover, preparation of chitosan nanoparticle using a simple and mild ionic-gelation method offers the minimal damage to CpG ODNs as well as an enhanced gene encapsulation

efficiency. Thus, chitosan-based nanoparticles have shown to be an easy-to-use and cost-effective CpG ODN delivery vectors.

A tremendous amount of studies has described physicochemical properties of chitosan favorable for the large plasmid DNA (pDNA) delivery. Usually, these vectors employ chitosans with the large molecular weight and the high degree of deacetylation to facilitate the complexation of pDNA into small nanoparticles, promote their stability, and enhance intracellular uptake (Scholz & Wagner, 2012; Lavertu, Méthot, Tran-Khanh, & Buschmann, 2006). In contrast, the encapsulation of small oligonucleotides using these chitosans resulted in the formation of the overly stable nanoparticles that exhibit poor gene release behaviour and diminish their therapeutic effect (Gao, et al., 2005). Thus, this research aimed to develop a vector system based on chitosan nanoparticles suitable for the efficient CpG ODN encapsulation and its intracellular delivery, that will facilitate CpG ODN protection and enable release. Moreover, targeting the mannose recognition receptor appeared to be an effective strategy to mediate the efficient delivery of CpG ODN-loaded nanoparticles to the endolysosomal TLR9 of APCs (Asthana, Asthana, Kohli, & Vyas, 2014).

This study has better elucidated the influence of the chitosan molecular weight, the degree of deacetylation and mannose grafting on the ability of chitosan nanoparticles to efficiently encapsulate and deliver small CpG ODN 1826 in the *in vitro* model of macrophage-like cells. The modulation of chitosan molecular structures and the nanoparticle physicochemical properties (e.g. size, surface charge, mannose grafting) provided the ability to enhance the CpG ODN encapsulation efficiency as well as the nanoparticle uptake and cytokine secretion.

This research provided a valuable scientific basis for development of immune modulators as a stand-alone treatment or a vaccine adjuvant for a number of pathogenic diseases. The

established innate immune response activation, demonstrated by the CpG ODN-loaded chitosan nanoparticles, may be advantageous in providing the opportunity to limit the spread of infectious agents and prevent the development of a full-scale disease before the generation of the proper adaptive immunity by a host. One possible application could be the intranasal administration of CpG ODNs as an effective strategy to mitigate the spread of Bovine respiratory disease in cattle through the rapid boost of innate immunity.

Lastly, although this work was focused on the development of chitosan-based nanoparticles suitable for the efficient CpG ODN intracellular delivery, this technique can be adapted for the delivery of other small pharmaceuticals and bioactive compound. It will be particularly interesting to explore the feasibility of obtained nanoparticles for the delivery of antisense oligonucleotides, siRNA and RNAi (double-stranded RNA-mediated interference). Moreover, the applicability of obtained nanoparticles could be explored for the delivery of other bioactive compounds such as vitamins, minerals, phytochemicals, phytochemicals, etc. The fundamental knowledge gained from this study will facilitate the rational design and fabrication of chitosan-based nanoparticles for the drug and gene delivery by modulating physicochemical properties of chitosan in order to treat and prevent various pathological conditions including cancer, infections, genetic disorders and other chronic abnormal conditions.

3.3. Recommendations for future work

This research demonstrated that the *in vitro* delivery efficiency of CpG ODN-loaded nanoparticles could be tailored by altering the physicochemical properties of chitosan, such as the molecular weight, the degree of deacetylation, and mannose grafting. Although nanoparticles formulated with the half N-acetylated and mannosylated chitosan samples and longer molecular chains demonstrated the most efficient immunostimulatory activity in a model of macrophage-like

cells, the *in vivo* performance is a much more complicated and challenging process, which is affected by the interaction with the endogenous negatively charged molecules. Thus, in the next step, the ability of CpG ODN-loaded nanoparticles to conserve their immunostimulatory activity *in vivo* should be investigated.

The levels of proinflammatory cytokine secretion should be measured following the intranasal administration of CpG ODN-loaded nanoparticles into mice. Consequently, the immunoprotective effect of nanoparticles should be evaluated in the challenge study using a lethal dose of Pneumonia Virus of Mice (PVM). Furthermore, the immunostimulatory activity of CpG ODN-laded nanoparticles should be investigated in cattle using a Bovine herpes virus-1 or a Bovine viral diarrhea virus model. This study will assess potential of CpG ODNs as standalone immunotherapy for the Bovine respiratory disease treatment and prevention.

Moreover, CpG ODN-loaded nanoparticles were prepared at the constant N/P/C charge ratio using the ionic gelation method. While the influence of physicochemical properties of chitosan, such as the molecular weight, the degree of deacetylation and mannose grafting, were evaluated in terms of the *in vitro* delivery efficiency of CpG ODNs, the N/P/C charge ratio was not addressed. It would be beneficial to examine the impact of this parameter on the *in vitro* and *in vivo* delivery efficiency of CpG ODNs and the immunostimulatory activity.

Furthermore, the storage stability of the CpG ODN-loaded nanoparticles should be investigated. Chitosan is known to undergo the gradual chain degradation upon storage, which is associated with destruction of functional groups leading to the loss of physicochemical properties (Szymańska & Winnicka, 2015). Thus, the effect of both intrinsic (degree of deacetylation, molecular weight, purity, etc.) and extrinsic (storage conditions, preparation conditions,

sterilization, acid dissolution, etc.) factors on storage stability of CpG ODN-loaded chitosan nanoparticles should be acknowledged.

References

Adamus, T., & Kortylewski, M. (2018). The revival of CpG oligonucleotide-based cancer immunotherapies. *Contemporary Oncology, 22*(1A), 56-60. doi:10.5114/wo.2018.73887

Agirre, M., Zarate, J., Puras, G., Ojeda, E., & Pedraz, J. L. (2015). Improving transfection efficiency of ultrapure oligochitosan/DNA polyplexes by medium acidification. *Drug Delivery, 22*(1), 100-110. doi:10.3109/10717544.2013.871373

Agrawal, S., & Zhao, Q. (1998). Antisense therapeutics. *Current Opinion in Chemocal Biology, 2*(4), 519-528. doi:10.1016/S1367-5931(98)80129-4

Ahmed, T. A., & Aljaeid, B. M. (2016). Preparation, characterization, and potential application of chitosan, chitosan derivatives, and chitosan metal nanoparticles in pharmaceutical drug delivery. *Drug design, development and therapy, 10*, 483–507. doi:10.2147/DDDT.S99651

Alameh, M., DeJesus, D., Jean, M., Darras, V., Thibault, M., Lavertu, M., . . . Merzouki, A. (2012). Low molecular weight chitosan nanoparticulate system at low N:P ratio for nontoxic polynucleotide delivery. *International Journal of Nanomedicine, 7*, 1399-1414. doi:10.2147/IJN.S26571

Alameh, M., Lavertu, M., Tran-Khanh, N., Chang, C.-Y., Lesage, F., Bail, M., . . . Buschmann, M. D. (2018). siRNA Delivery with Chitosan: Influence of Chitosan Molecular Weight, Degree of Deacetylation, and Amine to Phosphate Ratio on in Vitro Silencing Efficiency, Hemocompatibility, Biodistribution, and in Vivo Efficacy. *Biomacromolecules, 19*, 112-131. doi:10.1021/acs.biomac.7b01297

Alexander, C., & Rietschel, E. T. (2001). Bacterial lipopolysaccharides and innate immunity. *Journal of Endotoxin Research, 7*(3), 167-202.

Alves, N., & Mano, J. (2008). Chitosan derivatives obtained by chemical modifications for biomedical and environmental applications. *International Journal of Biological Macromolecules, 43*(5), 401-414. doi:10.1016/j.ijbiomac.2008.09.007

Amaduzzi, F., Bomboi, F., Boninco, A., Bordi, F., Casciardi, S., Chronopoulou, L., . . . Sennato, S. (2014). Chitosan–DNA complexes: Charge inversion and DNA condensation. *Colloids and Surfaces B: Biointerfaces, 114*(1), 1-10. doi:0.1016/j.colsurfb.2013.09.029

Angell, C., Xie, S., Zhang, L., & Chen, Y. (2016). DNA Nanotechnology for Precise Control over Drug Delivery and Gene Therapy. *Small, 12*(9), 1117-1132. doi:10.1002/smll.201502167

Asthana, G. S., Asthana, A., Kohli, D. V., & Vyas, S. P. (2014). Mannosylated Chitosan Nanoparticles for Delivery of Antisense Oligonucleotides for Macrophage Targeting. *BioMed Research International, 3*(526391). doi:10.1155/2014/526391

Baldrick, P. (2010). The safety of chitosan as a pharmaceutical excipient. *Regulatory Toxicology and Pharmacology, 56*(3), 290-299. doi:10.1016/j.yrtph.2009.09.015

Bhattacharjee, S. (2016). DLS and zeta potential – What they are and what they are not? *Journal of Controlled Release, 235*, 337-351. doi:10.1016/j.jconrel.2016.06.017

Bode, C., Zhao, G., Steinhagen, F., Kinjo, T., & Klinman, D. M. (2011). CpG DNA as a vaccine adjuvant. *Expert Rev Vaccines, 10*(4), 499-511. doi:10.1586/erv.10.174.

Bowman, K., & Leong, K. W. (2006). Chitosan nanoparticles for oral drug and gene delivery. *International Journal of Nanomedicine, 1*(2), 117-128.

Bozkir, A., & Saka, O. M. (2004). Chitosan Nanoparticles for Plasmid DNA Delivery: Effect of Chitosan Molecular Structure on Formulation and Release Characteristics. *Drug Delivery, 11*(2), 107-112. doi:10.1080/10717540490280705

Brubaker, S. W., Bonham, K. S., Zanoni, I., & Kagan, J. C. (2015). Innate Immune Pattern Recognition: A Cell Biological Perspective. *Annu Rev Immunol, 33*, 257-290. doi:10.1146/annurev-immunol-032414-112240

Calvo, P., Remuñán-López, C., Vila-Jato, J. L., & Alonso, M. J. (1997). Novel hydrophilic chitosan–polyethylene oxide nanoparticles as protein carriers. *Journal of Applied Polymer Science, 63*, 125-132. doi:10.1002/(SICI)1097-4628(19970103)63:1<125::AID-APP13>3.0.CO;2-4

Cardarelli, F., Digiacomo, L., Marchini, C., Amici, A., Salomone, F., Fiume, G., . . . Caracciol, G. (2016). The intracellular trafficking mechanism of Lipofectamine-based transfection reagents and its implication for gene delivery. *Scientific Reports, 6*, 25879. doi:10.1038/srep25879

Chen, H. C., Sun, B., Tran, K. K., & Shen, H. (2011). Effects of particle size on toll-like receptor 9-mediated cytokine profiles. *Biomaterials, 32*(6), 1731-1737. doi:10.1016/j.biomaterials.2010.10.059

Chen, S., Zhang, H., Chinnathambi, S., & Nobutaka Hanagata. (2013). Synthesis of novel chitosan–silica/CpG oligodeoxynucleotide nanohybrids with enhanced delivery efficiency. *Materials Science and Engineering: C, 33*(6), 3382-3388. doi:10.1016/j.msec.2013.04.017

Chen, S., Zhang, H., Shi, X., Wu, H., & Hanagata, N. (2014). Microfluidic generation of chitosan/CpG oligodeoxynucleotide nanoparticles with enhanced cellular uptake and immunostimulatory properties. *Lab Chip, 14*, 1842-1849. doi:10.1039/c4lc00015c

Chen, S., Zhang, Q., Jia, L., Du, X., & Hanagata, N. (2015). A facilely controlled length, cytotoxicity, length-dependent and cell type-dependent cellular uptake of silica nanotubes and their applications in the delivery of immunostimulatory CpG oligodeoxynucleotides. *Journal of Materials Chemistry B, 3*, 7246-7254. doi:10.1039/C5TB01270H

Cheng, T., Miao, J., Kai, D., & Zhang, H. (2018). Polyethylenimine-Mediated CpG Oligodeoxynucleotide Delivery Stimulates Bifurcated Cytokine Induction. *ACS Biomaterials Science & Engineering, 4*(3), 1013-1018. doi:10.1021/acsbiomaterials.8b00049

Cheng, Y., & Corn, R. M. (1999). Ultrathin Polypeptide Multilayer Films for the Fabrication of Model Liquid/Liquid Electrochemical Interfaces. *Journal of Physical Chemistry B, 103*(41), 8726–8731. doi:10.1021/jp9920693

Cheung, R. C., Ng, T. B., Wong, J. H., & Chan, W. Y. (2015). Chitosan: An Update on Potential Biomedical and Pharmaceutical Applications. *Marine Drugs, 13*(8), 5156-5186. doi:10.3390/md13085156

Choi, C., Nam, J.-P., & Nah, J.-W. (2016). Application of chitosan and chitosan derivatives as biomaterials. *Journal of Industrial and Engineering Chemistry, 35*(25), 1-10. doi:10.1016/j.jiec.2015.10.028

Chopra, S., Mahdi, S., Kaur, J., Iqbal, Z., Talegaonkar, S., & Ahmad, F. J. (2006). Advances and potential applications of chitosanderivatives as mucoadhesive biomaterials in moderndrug delivery. *Journal of Pharmacy and Pharmacology, 58*, 1021–1032. doi:10.1211/jpp.58.8.0002

Christmas, P. (2010). Toll-Like Receptors: Sensors that Detect Infection. *Nature Education, 3*(9), 85.

Chu, S., Tang, C., & Yin, C. (2015). Effects of mannose density on in vitro and in vivo cellular uptake and RNAi efficiency of polymeric nanoparticles. *Biomaterials, 52*, 229-239. doi:10.1016/j.biomaterials.2015.02.044

Csaba, N., Köping-Höggård, M., & Alonso, M. J. (2009). Ionically crosslinked chitosan/tripolyphosphate nanoparticles for oligonucleotide and plasmid DNA delivery. *International Journal of Pharmaceutics, 382*(1-2), 205-214. doi:10.1016/j.ijpharm.2009.07.028

Cunningham, D., Zurlo, A., Salazar, R., Ducreux, M., Waddell, T. S., Stein, A., . . . Arnold, D. (2015). THE RANDOMIZED PHASE 3 IMPALA STUDY: IMMUNOMODULATORY MAINTENANCE THERAPY WITH TLR-9 AGONIST MGN1703 IN PATIENTS WITH METASTATIC COLORECTAL CARCINOMA. *Journal of Clinical Oncology, 33*. doi:10.1200/jco.2015.33.3_suppl.tps791

David, R. M., & Doherty, A. T. (2016). Viral Vectors: The Road to Reducing Genotoxicity. *Toxicological Sciences, 155*(2), 315-325. doi:10.1093/toxsci/kfw220

de Jong, S., Chikh, G., Sekirov, L., Raney, S., Semple, S., Klimuk, S., . . . Tam, Y. (2007). Encapsulation in liposomal nanoparticles enhances the immunostimulatory, adjuvant and anti-tumor activity of subcutaneously administered CpG ODN. *Cancer Immonology, Immunotherapy, 56*(8), 1251-1264. doi:10.1007/s00262-006-0276-x

Deacon, M. P., McCgurk, S., Rober, C. J., Williams, P. M., Tendler, S. J., Davies, M. C., . . . Harding, S. E. (2000). Atomic force microscopy of gastric mucin and chitosan mucoadhesive systems. *Biochemical Journal, Pt 3*, 557–563.

Dehaini, D., Fang, R. H., & Zhang, L. (2016). Biomimetic strategies for targeted nanoparticle delivery. *Bioengineering & Translational Medicine, 1*(1), 30-46. doi:10.1002/btm2.10004

Dehoussea, V., Garbacki, N., Jaspart, S., Castagnea, D., Piel, G., Colige, A., & Evrard, B. (2010). Comparison of chitosan/siRNA and trimethylchitosan/siRNA complexes behaviour in vitro. *International Journal of Biological Macromolecules, 46*, 342-349. doi:10.1016/j.ijbiomac.2010.01.010

Dewald, S., Hamman, J. H., & Kotze, A. F. (2003). Evaluation of the mucoadhesive properties of N-trimethyl chitosan chloride. *Drug Development and Industrial Pharmacy, 29*(1), 61-69. doi: 10.1081/DDC-120016684

Dominical, V., Samsel, L., & McCoy Jr., P. J. (2017). Masks in imaging flow cytometry. *Methods, 112*(1), 9-17. doi:10.1016/j.ymeth.2016.07.013

Elieh-Ali-Komi, D., & Hamblin, M. R. (2016). Chitin and Chitosan: Production and Application of Versatile Biomedical Nanomaterials. *International Journal of Advanced Research (Indore), 4*(3), 411-426.

Erikçi, E., Gursel, M., & Gürsel, İ. (2011). Differential immune activation following encapsulation of immunostimulatory CpG oligodeoxynucleotide in nanoliposomes. *Biomaterials, 32*(6), 1715-1723. doi:10.1016/j.biomaterials.2010.10.054

Foged, C., Brodin, B., Frokjaer, S., & Sundblad, A. (2005). Particle size and surface charge affect particle uptake by human dendritic cells in an in vitro model. *International Journal of Pharmaceutics, 298*(2), 315-322. doi:10.1016/j.ijpharm.2005.03.035

Fonseca, D. E., & Kline, J. N. (2009). Use of CpG oligonucleotides in treatment of asthma and allergic disease. *Advanced Drug Delivery Reviews, 61*(3), 256-262. doi:10.1016/j.addr.2008.12.007

Fröhlich, E. (2012). The role of surface charge in cellular uptake and cytotoxicity of medical nanoparticles. *International Journal of Nanomedicine, 7*, 5577—5591. doi:10.2147/IJN.S36111

Gao, S., Chen, J., Donga, L., Ding, Z., Yang, Y.-h., & Zhang, J. (2005). Targeting delivery of oligonucleotide and plasmid DNA to hepatocyte via galactosylated chitosan vector. *European Journal of Pharmaceutics and Biopharmaceutics, 60*(3), 327-334. doi:10.1016/j.ejpb.2005.02.011

Garnett, M. C., & Kallinteri, P. (2006). Nanomedicines and nanotoxicology: some physiological principles. *Occupational Medicine, 56*(5), 307-311. doi:10.1093/occmed/kql052

Gatoo, M. A., Naseem, S., Arfat, M. Y., Dar, A. M., Qasim, K., & Zubair, S. (2014). Physicochemical Properties of Nanomaterials: Implication in Associated Toxic Manifestations. *BioMed Research International, 2014*, 498420. doi:10.1155/2014/498420

Germershaus, O., Mao, S., Sitterberg, J., Bakowsky, U., & Kissel, T. (2008). Gene delivery using chitosan, trimethyl chitosan or polyethylenglycol-graft-trimethyl chitosan block copolymers: Establishment of structure–activity relationships in vitro. *Journal of Controlled Release, 125*, 145-154. doi:10.1016/j.jconrel.2007.10.013

Glover, D. J., Lipps, H. J., & Jans, D. A. (2005). Towards safe, non-viral therapeutic gene expression in humans. *Nature Reviews Genetics, 6*(4), 299-310. doi:10.1038/nrg1577

Gomis, S., Babiuk, L., Allan, B., Willson, P., Waters, E., Ambrose, N., & Potter, A. (2004). Protection of Neonatal Chicks Against a Lethal Challenge of Escherichia coli Using DNA Containing Cytosine-Phosphodiester-Guanine Motifs. *Avian Diseases, 48*(4), 813-822. doi:10.1637/7194-041204R

Goonewardene, K. B., Popowich, S., Gunawardana, T., Gupta, A., Kurukulasuriya, S., Karunarathna, R., . . . Gomis, S. (2017). Intrapulmonary Delivery of CpG-ODN Microdroplets Provides Protection Against Escherichia coli Septicemia in Neonatal Broiler Chickens. *Avian Diseases, 61*(4), 503-511. doi:10.1637/11684-060617-Reg.1

Griebel, P. J., Brownlie, R., Manuj, A., Nichani, A., Mookherjee, N., Popowych, Y., . . . Babiuk, L. A. (2005). Bovine toll-like receptor 9: A comparative analysis of molecular structure, function and expression. *Veterinary Immunology and Immunopathology, 108*(1-2), 11-16. doi:10.1016/j.vetimm.2005.07.012

Grigsby, C. L., & Leong, K. W. (2010). Balancing protection and release of DNA: tools to address a bottleneck of non-viral gene delivery. *Journal of the Royal Society Interface, 7*, S67–S82. doi:10.1098/rsif.2009.0260

Gullón, B., Montenegro, M. I., Ruiz-Matute, A. I., Cardelle-Cobas, A., Corzo, N., & Pintado, M. E. (2016). Synthesis, optimization and structural characterization of a chitosan–glucose derivative obtained by the Maillard reaction. *Carbohydrate Polymers, 137*(10), 382-389. doi:org/10.1016/j.carbpol.2015.10.075

Häcker, G., Redecke, V., & Häcker, H. (2002). Activation of the immune system by bacterial CpG-DNA. *Immunology, 105*(3), 245-251. doi:10.1046/j.0019-2805.2001.01350.x

Hanagata, N. (2012). Structure-dependent immunostimulatory effect of CpG oligodeoxynucleotides and their delivery system. *International journal of nanomedicine*(7), 2181–2195. doi:0.2147/IJN.S30197

Hanagata, N. (2017). CpG oligodeoxynucleotide nanomedicines for the prophylaxis or treatment of cancers, infectious diseases, and allergies. *International Journal of Nanomedicine, 12*, 515-531. doi:10.2147/IJN.S114477

He, Z., Santos, J. L., Tian, H., Huang, H., Hu, Y., Liu, L., . . . Mao, H.-Q. (2017). Scalable fabrication of size-controlled chitosan nanoparticles for oral delivery of insulin. *Biomaterials, 130*, 28-41. doi:10.1016/j.biomaterials.2017.03.028

Heikenwalder, M., Polymenidou, M., Junt, T., Sigurdson, C., Wagner, H., Akira, S., . . . Aguzzi, A. (2004). Lymphoid follicle destruction and immunosuppression after repeated CpG oligodeoxynucleotide administration. *NATURE MEDICINE, 10*(2), 187-192. doi:10.1038/nm987

Hembram, K. C., Prabha, S., Chandra, R., Ahmed, B., & Nimesh, S. (2014). Advances in preparation and characterization of chitosan nanoparticles for therapeutics. *Artificial Cells, 44*(1), 1-10. doi:10.3109/21691401.2014.948548

Hemmi, H., Takeuchi, O., Kawai, T., Kaisho, T., Sato, S., Sanjo, H., . . . Take, K. (2000). A Toll-like receptor recognizes bacterial DNA. *Nature, 408*, 740-745.

Hollon, T. (2000). Researchers and regulators reflect on first gene therapy death. *Nature Medicine, 6*(1), 6.

Hu, Y., Du, Y., Yang, J., Tang, Y., Li, J., & Wang, X. (2007). Self-aggregation and antibacterial activity of N-acylated chitosan. *Polymer, 48*(11), 3098-3106. doi:10.1016/j.polymer.2007.03.063

Hua, L., Nishioka, Y., Reich, C. F., Pisetsky, D. S., & Lipsky, P. E. (1996). Activation of human B cells by phosphorothioate oligodeoxynucleotides. *The Journal of clinical investigation, 98*(5), 1119-1129. doi:10.1172/JCI118894

Huang, M., Fong, C.-W., Khor, E., & Lim, L.-Y. (2005). Transfection efficiency of chitosan vectors: Effect of polymer molecular weight and degree of deacetylation. *Journal of Controlled Release, 106*(3), 391-406. doi:10.1016/j.jconrel.2005.05.004

Huang, M., Khor, E., & Lim, L.-Y. (2004). Uptake and Cytotoxicity of Chitosan Molecules and Nanoparticles: Effects of Molecular Weight and Degree of Deacetylation. *Pharmaceutical Research, 21*(2), 344-353.

Huang, W., Wang, Y., Chen, Y., Zhao, Y., Zhang, Q., Zheng, X., . . . Zhang, L. (2016). Strong and Rapidly Self-Healing Hydrogels: Potential Hemostatic Materials. *Advanced Healthcare Material, 5*(21), 2813-2822. doi:10.1002/adhm.201600720

Hyer, R., McGuire, D. K., Xing, B., Jackson, S., & Janssen, R. (2018). Safety of a two-dose investigational hepatitis B vaccine, HBsAg-1018, using a toll-like receptor 9 agonist adjuvant in adult. *Vaccine, 36*(19), 2604-2611. doi:10.1016/j.vaccine.2018.03.067

Islam, S., Rahman Bhuiyan, M., & Islam, M. (2017). Chitin and Chitosan: Structure, Properties and Applications in Biomedical Engineering. *Journal of Polymers and the Environment, 25*(3), 854-866. doi:10.1007/s10924-016-0865-5

Ivory, C. P., Prystajecky, M., Jobin, C., & Chadee, K. (2008). oll-Like Receptor 9-Dependent Macrophage Activation by Entamoeba histolytica DNA. *Infection and Immunity, 76*(1), 289-297. doi:10.1128/IAI.01217-07

Jelinski, M., & Janzen, E. (2016, May 16). *Bovine respiratory disease*. Retrieved from http://www.beefresearch.ca/research-topic.cfm/bovine-respiratory-disease-38.

Jenner, D., Ducker, C., Clark, G., Prior, J., & Rowland, C. A. (2016). Using Multispectral Imaging Flow Cytometry to Assess an In Vitro Intracellular Burkholderia thailandensis Infection Model. *Cytometry Part A, 89*(4), 328-337. doi:10.1002/cyto.a.22809

Jeong, J. H., Kim, S. W., & Park, T. G. (2007). Molecular design of functional polymers for gene therapy. *Progress in Polymer Science, 32*(11), 1239–1274. doi:10.1016/j.progpolymsci.2007.05.019

Jiang, H.-L., Kang, M.-L., Quan, J.-S., Kang, S. G., Akaike, T., Yoo, H. S., & Cho, C. S. (2008). The potential of mannosylated chitosan microspheres to target macrophage mannose receptors in an adjuvant-delivery system for intranasal immunization. *Biomaterials, 29*(12), 1931-1939. doi:j.biomaterials.2007.12.025

Jiang, W., Swiggard, W. J., Heuf, C., Peng, M., Mirza, A., Steinman, R. M., & Nussenzweig, M. C. (1995). The receptor DEC-205 expressed by dendritic cells and thymic epithelial cells is involved in antigen processing. *Nature, 375*, 151-155. doi:10.1038/375151a0

Jung, H., Yu, G., & Mok, H. (2016). CpG oligonucleotide and α-d-mannose conjugate for efficient delivery into macrophages. *Applied Biological Chemistry, 59*(5), 759–763. doi:10.1007/s13765-016-0223-2

Jurk, M., & Vollmer, J. (2007). Therapeutic Applications of Synthetic CpG Oligodeoxynucleotides as TLR9 Agonists for Immune Modulation. *Biodrugs, 21*(6), 387-401. doi:1173-8804/07/0006-0387/$44.95/0

Jurk, M., Schulte, B., Kritzler, A., Noll, B., Eugen , U., Wader, T., . . . Vollmer, J. (2004). C-Class CpG ODN: sequence requirements and characterization of immunostimulatory activities on mRNA level. *Immunobiology, 209*(1-2), 141-154. doi:oi.org/10.1016/j.imbio.2004.02.006

Katas, H., & Alpar, H. (2006). Development and characterisation of chitosan nanoparticles for siRNA delivery. *Journal of Controlled Release, 115*(2), 216-225. doi:0.1016/j.jconrel.2006.07.021

Kawai, T., & Akira, S. (2010). The role of pattern-recognition receptors in innate immunity: update on Toll-like receptors. *Nature Immunology, 11*, 373-384. doi:10.1038/ni.1863

Kawai, T., & Akira, S. (2011). Toll-like Receptors and Their Crosstalk with Other Innate Receptors in Infection and Immunity. *Immunity, 34*(5), 637-650. doi:10.1016/j.immuni.2011.05.006

Kawasaki, T., & Kawai, T. (2014). Toll-Like Receptor Signaling Pathways. *Frontiers in Immunology, 5*(461). doi:10.3389/fimmu.2014.00461

Keong, L. C., & Halim, A. S. (2009). n Vitro Models in Biocompatibility Assessment for Biomedical-Grade Chitosan Derivatives in Wound Management. *International Journal of Molecular Sciences, 10*(3), 1300-1313. doi:10.3390/ijms10031300

Kerkmann, M., Costa, L. T., Richter, C., Rothenfusser, S., Battiany, J., Hornung, V., . . . Hartmann, G. (2004). Spontaneous Formation of Nucleic Acid-based Nanoparticles Is Responsible for High Interferon-α Induction by CpG-A in Plasmacytoid Dendritic Cells*. *The Journal of Biological Chemistry*, 8086-8093. doi:10.1074/jbc.M410868200

Kiang, T., Wen, J., Lim, H. W., & Leong, K. W. (2004). The effect of the degree of chitosan deacetylation on the efficiency of gene transfection. *Biomaterials, 25*(22), 5293-5301. doi:10.1016/j.biomaterials.2003.12.036

Kim, T. H., Jin, H., Kim, H. W., Cho, M.-H., & Cho, C. S. (2006). Mannosylated chitosan nanoparticle–based cytokine gene therapy suppressed cancer growth in BALB/c mice bearing CT-26 carcinoma cells. *Molecular Cancer Therapeutics, 5*(7), 1723–1732. doi:10.1158/1535-7163.MCT-05-0540

Kim, T. H., Nah, J. W., Cho , M.-H., Park, T. G., & Cho, C. S. (2006). Receptor-Mediated Gene Delivery into Antigen Presenting Cells Using Mannosylated Chitosan/DNA Nanoparticles. *Journal of Nanoscience and Nanotechnology, 9*(10), 2798-2803. doi:10.1166/jnn.2006.434

Klaschik, S., Tross, D., & Klinman, D. M. (2009). Inductive and suppressive networks regulate TLR9-dependent gene expression in vivo. *Journal of Leukocyte Biology, 85*(5), 788–795. doi:10.1189/jlb.1008671

Klima, C. L., Zaheer, R., Cook, S. R., Booker, C. W., Hendrick, S., Alexander, T. W., & McAllister, T. A. (2014). Pathogens of Bovine Respiratory Disease in North American Feedlots Conferring Multidrug Resistance via Integrative Conjugative Elements. *Journal of Clinical Microbiology, 52*(2), 438-448. doi:10.1128/JCM.02485-13

Klinman, D. M. (2004). Immunotherapeutic uses of CpG oligodeoxynucleotides. *Nature Reviews Immunology, 4*, 249–259. doi:10.1038/nri1329

Klinman, D. M., Yi, A.-K., Beaucage, S. L., Conover, J., & Krieg, A. M. (1996). CpG motifs present in bacteria DNA rapidly induce lymphocytes to secrete interleukin 6, interleukin 12, and interferon gamma. *Proceedings of the national academy of sciences*, 2879–2883.

Knudsen, K. B., Northeved, H., Kumar, P., Permin, A., Gjetting, T., Andresen, T., . . . Roursgaard, M. (2015). In vivo toxicity of cationic micelles and liposomes. *Nanomedicine: Nanotechnology, Biology and Medicine, 11*(2), 467-477. doi:10.1016/j.nano.2014.08.004

Köping-Höggård, M., Mel'nikova, Y. S., Vårum, K. M., Lindman, B., & Artursson, P. (2002). Relationship between the physical shape and the efficiency of oligomeric chitosan as a gene delivery system in vitro and in vivo. *The journal of gene medicine, 5*(2), 130–141. doi:10.1002/jgm.327

Köping-Höggård, M., Tubulekas, I., Guan, H., Edwards, K., Nilsson, M., Vårum, K. M., & Artursson, P. (2001). Chitosan as a nonviral gene delivery system. Structure–property relationships and characteristics compared with polyethylenimine in vitro and after lung administration in vivo. *Gene Therapy, 8*, 1108-1121. doi:10.1038/sj.gt.3301492

Köping-Höggård, M., Vårum, K., Issa, M., Danielsen, B., Christensen, B., Stokke, B., & Artursson, P. (2004). Improved chitosan-mediated gene delivery based on easily dissociated chitosan polyplexes of highly defined chitosan oligomers. *Gene therapy, 11*(19), 1441-1452. doi:1038/sj.gt.3302312

Krieg, A. M. (2002). CpG motifs in bacterial DNA and their immune effects. *Annual review of immunology, 20*(1), 709-760. doi:10.1146/annurev.immunol.20.100301.064842

Krieg, A. M. (2006). Therapeutic potential of Toll-like receptor 9 activation. *Nature Reviews Drug Discovery, 5*, 471- 484. doi:10.1038/nrd2059

Krieg, A. M. (2012). CpG Still Rocks! Update on an Accidental Drug. *Nucleic Acid Ther.*, 77-89. doi:10.1089/nat.2012.0340

Krieg, A. M., Matson, S., & Fisher, E. (1996). Oligodeoxynucleotide Modifications Determine the Magnitude of Cell Stimulation by CpG Motifs. *ANTISENSE & NUCLEIC ACID DRUG DEVELOPMENT, 6*(2), 133-139. doi:10.1089/oli.1.1996.6.133

Krieg, A. M., Yi, A.-K., Matson, S., Waldschmidt, T. J., Bishop, G. A., Teasdale, R., . . . Klinman, D. M. (1995). CpG motifs in bacterial DNA trigger direct B-cell activation. *Nature*, 546–549.

Kumar, H., Kawai, T., & Akira, S. (2009). Pathogen recognition in the innate immune response. *Biochemical Journal, 1*, 1-16. doi:10.1042/BJ20090272

Kurreck, J. (2003). Antisense technologies. Improvement through novel chemical modifications. *European Journal of Biochemistry, 270*, 1628-1644. doi:10.1046/j.1432-1033.2003.03555.x

Lahoud, M. H., Ahmet, F., Zhang, J.-G., Meuter, S., Policheni, , A. N., Kitsoulis, S., . . . Caminschi, I. (2011). DEC-205 is a cell surface receptor for CpG oligonucleotides. *Proceedings of the National Academy of Sciences, 109*(40), 16270-16275. doi:10.1073/pnas.1208796109

Lavertu, M., Méthot, S., Tran-Khanh, N., & Buschmann, M. D. (2006). High efficiency gene transfer using chitosan/DNA nanoparticles with specific combinations of molecular weight and degree of deacetylation. *Biomaterials, 27*(27), 4815-4824. doi:10.1016/j.biomaterials.2006.04.029

Lavertu, M., Xia, Z., Serreqi, A. N., Berrada, M., Rodrigues, A., Wang, D., . . . Gupta, A. (2003). A validated 1H NMR method for the determination of the degree of deacetylation of chitosan. *Journal of Pharmaceutical and Biomedical Analysis*, 1149-1158. doi:10.1016/S0731-7085(03)00155-9

Leong, K., Mao, H.-Q., Truong-Le, V., Roy, K., Walsh, S., & August, J. (1998). DNA-polycation nanospheres as non-viral gene delivery vehicles. *Journal of Controlled Release, 53*(1-3), 183-193. doi:10.1016/S0168-3659(97)00252-6

Li, H.-T., Zhang, T.-T., Chen, Z.-g., Ye, J., Liu, H., Zou, X.-l., . . . Yang, H.-l. (2015). Intranasal administration of CpG oligodeoxynucleotides reduces lower airway inflammation in a murine model of combined allergic rhinitis and asthma syndrome. *International Immunopharmacology, 28*(1), 390-398. doi:10.1016/j.intimp.2015.06.028

Liang, R., van den Hurk, J. V., Babiuk, L. A., & van Drunen Littel-van den Hurk, S. (2006). Priming with DNA encoding E2 and boosting with E2 protein formulated with CpG oligodeoxynucleotides induces strong immune responses and protection from Bovine viral diarrhea virus in cattle. *Journal of General Virology, 87*, 2971-2982. doi:10.1099/vir.0.81737-0

Lipford, G. B., Sparwasser , T., Bauer, M., Zimmermann, S., Koch, E.-S., He, K. H., & Wagner, H. (1997). Immunostimulatory DNA: sequence-dependent production of potentially harmful or useful cytokines. *The European Journal of Immunology, 27*(14), 3420-3426. doi:10.1002/eji.1830271242

Liu, X., Howard, K. A., Dong, M., Andersen, M. Ø., Rahbek, U. L., Johnsen, M. G., . . . Kjems, J. (2007). The influence of polymeric properties on chitosan/siRNA nanoparticle formulation and gene silencing. *Biomaterials, 28*(6), 1280-1288. doi:10.1016/j.biomaterials.2006.11.004

Ma, P. L., Lavertu, M., Winnin, F. M., & Buschmann, M. D. (2009). New insights into chitosan-DNA interactions using isothermal titration microcalorimetry. *Biomacromolecules, 10*(6), 1490-1499. doi:10.1021/bm900097s

MacKinnon, K. M., He, H., Swaggerty, C. L., McReynolds, J. L., Genovese, K. J., Duke, S. E., . . . Kogut, M. H. (2009). In ovo treatment with CpG oligodeoxynucleotides decreases colonization of Salmonella enteriditis in broiler chickens. *Veterinary Immunology and Immunopathology, 127*(3-4), 371-375. doi:10.1016/j.vetimm.2008.10.001

Maher, J., & Davies, E. T. (2004). Targeting cytotoxic T lymphocytes for cancer immunotherapy. *British Journal of Cancer, 91*, 817-821. doi:10.1038/sj.bjc.6602022

Malmo, J., Sørgård, H., Vårum, K. M., & Strand, S. P. (2012). siRNA delivery with chitosan nanoparticles: Molecular properties favoring efficient gene silencing. *Journal of Controlled Release, 158*(2), 261-268. doi:10.1016/j.jconrel.2011.11.012

Mansouri, S., Lavigne, P., Corsi, K., Benderdour, M., Beaumont, E., & Fernandes, J. C. (2004). Chitosan–DNA nanoparticles as non-viral vectors in gene therapy: Strategies to improve

transfection efficacy. *European Journal of Pharmaceutics and Biopharmaceutics., 57*(1), 1-8. doi:10.1016/S0939-6411(03)00155-3

Manuja, A., Manuja, B. K., Kaushik, J., Singha, H., & Singh, R. K. (2013). Immunotherapeutic potential of CpG oligodeoxynucleotides in veterinary species. *Immunopharmacology and Immunotoxicology, 35*(5), 535-544,. doi:10.3109/08923973.2013.828743

Mao, H.-Q., du Roya, K., Troung-Le, V. L., Janesa, K. A., Lin, K. Y., Wang, Y., . . . Leong, K. W. (2001). Chitosan-DNA nanoparticles as gene carriers: synthesis, characterization and transfection efficiency. *Journal of Controlled Release, 70*(3), 399-421. doi:10.1016/S0168-3659(00)00361-8

Mao, S., Bakowsky, U., Jintapattanakit, A., & Kissel, T. (2006). Self-Assembled Polyelectrolyte Nanocomplexes between Chitosan Derivatives and Insulin. *Journal of Pharmaceutical Sciences, 95*(5), 1035-1048. doi:10.1002/jps.20520

Mao, S., Guo, C., Shi, Y., & Li, L. C. (2012). Recent advances in polymeric microspheres for parenteral drug delivery—part 2. *Expert Opinion on Drug Delivery, 9*(10), 1209-1223. doi:10.1517/17425247.2012.717926

Mao, S., Shu, X., Florian , U., Wittmar, M., Xie, X., & Kissel, T. (2005). Synthesis, characterization and cytotoxicity of poly(ethylene glycol)-graft-trimethyl chitosan block copolymers. *Biomaterials, 26*(32), 6343-6356. doi:10.1016/j.biomaterials.2005.03.036

Mao, S., Sun, W., & Kissel, T. (2010). Chitosan-based formulations for delivery of DNA and siRNA. *Advanced Drug Delivery Reviews, 61*(1), 12-27. doi:10.1016/j.addr.2009.08.004

Mei, L., Zhu, G., Qiu, L., Wu, C., Chen, H., Liang, H., . . . Tan, W. (2015). Self-assembled multifunctional DNA nanoflowers for the circumvention of multidrug resistance in targeted anticancer drug delivery. *Nano Research, 8*(11), 3447–3460. doi:10.1007/s12274-015-0841-8

Meng, W., Yamazaki, T., Yuuki, N., & Hanagata, N. (2011). Nuclease-resistant immunostimulatory phosphodiester CpG oligodeoxynucleotides as human Toll-like receptor 9 agonists. *BMC Biotechnology, 11*(88). doi:10.1186/1472-6750-11-88

Messina, J., Gilkeson, G., & Pisetsky, D. (1991). Stimulation of in vitro murine lymphocyte proliferation by bacterial DNA. *The Journal of Immunology, 147*(6), 1759-1764.

Mifsud, E. J., Tan, A. C., & Jackson, D. C. (2014). TLR Agonists as Modulators of the Innate Immune Response and Their Potential as Agents Against Infectious Disease. *Frontiers in Immunology, 5*(79), 1-10. doi:10.3389/fimmu.2014.00079

Miyake, K., Shibata, T., Ohto, U., Shimizu, T., Saitoh, S.-I., Fukui, R., & Murakam, Y. (2018). Mechanisms controlling nucleic acid-sensing Toll-like receptors. *International Immunology, 30*(2), 43–51. doi:10.1093/intimm/dxy016

Mogensen, T. H. (2009). Pathogen Recognition and Inflammatory Signaling in Innate Immune Defenses. *Clinical Microbiology Reviews, 22*(2), 240-273. doi:10.1128/CMR.00046-08

Mohammed, M. A., Syeda, J. T., Wasan, K. M., & Wasan, E. K. (2017). An Overview of Chitosan Nanoparticles and Its Application in Non-Parenteral Drug Delivery. *Pharmaceutics, 9*(53), 1-26. doi:10.3390/pharmaceutics9040053

Mohri, K., Kusuki, E., Ohtsuki, S., Takahashi, N., Endo, M., Hidaka, K., . . . Nishikawa, M. (2015). Self-Assembling DNA Dendrimer for Effective Delivery of Immunostimulatory CpG DNA to Immune Cells. *Biomacromolecules, 16*(4), 1095-1101. doi:DOI: 10.1021/bm501731f

Mutwiri, G. K., Nichani, A. K., Babiuk, S., & Babiuk, L. A. (2004). Strategies for enhancing the immunostimulatory effects of CpG oligodeoxynucleotides. *Journal of Controlled Release, 97*(1), 1-17. doi:10.1016/j.jconrel.2004.02.022

Neujahr, D. C., Reich, C. F., & Pisetsky, D. S. (1999). Immunostimulatory properties of genomic DNA from different bacterial species. *Immunobiology, 200*(1), 106-119. doi:10.1016/S0171-2985(99)80036-9

Nichani, A., Mena, A., Popowych, Y., Dent, D., Townsend, H., Mutwiri, G., . . . Griebel, P. (2004). In vivo immunostimulatory effects of CpG oligodeoxynucleotide in cattle and sheep. *Veterinary Immunology and Immunopathology, 98*, 17-29. doi:10.1016/j.vetimm.2003.10.001

Nimesh, S., Thibault, M. M., Lavertu, M., & Buschmann, M. D. (2010). Enhanced Gene Delivery Mediated by Low Molecular Weight Chitosan/DNA Complexes: Effect of pH and Serum. *Mol Biotechnology, 46*(2), 182–196. doi:10.1007/s12033-010-9286-1

Nishikawa, M., Matono, M., Rattanakiat, S., Matsuoka, N., & Takakura, Y. (2008). Enhanced immunostimulatory activity of oligodeoxynucleotides by Y-shape formation. *Immunology, 124*(2), 247-255. doi:10.1111/j.1365-2567.2007.02762.x

Pak, C. W., Kosno, M., Holehouse, A. S., Padrick, S. B., Mittal, A., Ali, R., . . . Rosen, M. K. (2016). Sequence Determinants of Intracellular Phase Separation by Complex Coacervation of a Disordered Protein. *Molecular Cell, 63*(1), 72-85. doi:10.1016/j.molcel.2016.05.042

Panyam, J., & Labhasetwar, V. (2003). Biodegradable nanoparticles for drug and gene delivery to cells and tissue. *Advanced Drug Delivery Reviews, 55*(3), 329-347. doi:10.1016/S0169-409X(02)00228-4

Peine, K. J., Bachelder, E. M., Vangun, Z., Papenfuss, T., Brackman, D. J., Gallovic, M. D., . . . Ainslie, K. M. (2013). Efficient Delivery of the Toll-like Receptor Agonists Polyinosinic:Polycytidylic Acid and CpG to Macrophages by Acetalated Dextran Microparticles. *Molecular Pharmaceutics, 10*(8), 2849-2857. doi:10.1021/mp300643d

Peng, S. F., Yang, M.-J., Su, C.-J., Chen, H.-L., Lee, P.-W., Wei, M.-C., & Sung, H.-W. (2009). Effects of incorporation of poly(g-glutamic acid) in chitosan/DNA complex nanoparticles on cellular uptake and transfection efficiency. *Biomaterials*, 1797–1808. doi:10.1016/j.biomaterials.2008.12.019

Petkar, K., Chavhan, S., Agatonovik-Kustrin, S., & Sawant, K. (2011). Nanostructured Materials in Drug and Gene Delivery: A Review of the State of the Art. *Critical Reviews™ in Therapeutic Drug Carrier Systems, 28*(2), 101-164. doi:10.1615/CritRevTherDrugCarrierSyst.v28.i2.10

Phanse, Y., Ramer-Tait, A. E., Friend, S. L., Carrillo-Conde, B., Lueth, P., Oster, C. J., . . . Bellaire, B. H. (2012). Analyzing Cellular Internalization of Nanoparticles and Bacteria by Multi-spectral Imaging Flow Cytometry. *Journal of Visualized Experiments, 64*(3884). doi: 10.3791/3884

Pohar, J., Kužnik Krajnik, A., Jerala, R., & Benčina, M. (2015). Minimal Sequence Requirements for Oligodeoxyribonucleotides Activating Human TLR9. *The Journal of Immunology, 194*(8), 3901-3908. doi:10.4049/jimmunol.1402755

Polewicz, M., Gracia, A., Garlapati, S., Kessel, J., Strom, S., Halperin, S. A., . . . Gerdts, V. (2013). Novel vaccine formulations against pertussis offer earlier onset of immunity and provide protection in the presence of maternal antibodies. *Vaccine, 31*(31), 3148-3155. doi:0.1016/j.vaccine.2013.05.008

Ramamoorth, M., & Narvekar, A. (2015). Non Viral Vectors in Gene Therapy- An Overview. *Journal of Clinical and Diagnostic Research, 9*(1), GE01–GE06. doi:10.7860/JCDR/2015/10443.5394

Rankina, R., Pontarolloa, R., Gomisa, S., Karvonen, B., Willsona, P., Loehra, B., . . . Babiuk, L. (2002). CpG-containing oligodeoxynucleotides augment and switch the immune responses of cattle to bovine herpesvirus-1 glycoprotein D. *Vaccine, 20*(23-24), 3014-3022. doi:10.1016/S0264-410X(02)00216-5

Rathinam, V. A., & Fitzgerald, K. A. (2011). Innate Immune sensing of DNA viruses. *Virology, 411*(2), 153-162. doi:10.1016/j.virol.2011.02.003

Ravin, N. (Ed.). (2014). *Chemistry of Bioconjugates: Synthesis, Characterization, and Biomedical Applications.* Hoboken, NJ: John Wiley & Sons, Inc.

Ray, N. B., & Krieg, A. M. (2003). Oral Pretreatment of Mice with CpG DNA Reduces Susceptibility to Oral or Intraperitoneal Challenge with Virulent Listeria monocytogenes. *Infection and Immunity, 71*(8), 4398-4404. doi:10.1128/IAI.71.8.4398-4404.2003

Ren, D., Yi, H., Wang, W., & Ma, X. (2005). The enzymatic degradation and swelling properties of chitosan matrices with different degrees of N-acetylation. *Carbohydrate Research, 340*(15), 2403-2410. doi:10.1016/j.carres.2005.07.022

Rinaudo, M. (2006). Chitin and chitosan: Properties and applications. *Progress in Polymer Science, 31*(7), 603-632. doi:10.1016/j.progpolymsci.2006.06.001

Roberts, T. L., Dunn, J. A., Terry, T. D., Jennings, M. P., Hume, D. A., Sweet, M. J., & Stacey, K. J. (2005). Differences in macrophage activation by bacterial DNA and CpG-containing oligonucleotides. *175*(6), 3569-3576. doi:org/10.4049/jimmunol.175.6.3569

Rodrigues, S., Dionísio, M., López, C. R., & Grenha, A. (2012). Biocompatibility of Chitosan Carriers with Application in Drug Delivery. *Journal of Functional Biomaterials, 3*(3), 615-641. doi:10.3390/jfb3030615

Roers, A., Hiller, B., & Hornung, V. (2016). Recognition of Endogenous Nucleic Acids by the Innate Immune System. *Immunity, 44*(4), 739-754. doi:10.1016/j.immuni.2016.04.002

Roy, K., Mao, H.-Q., Huang, S.-K., & Leong, K. W. (1999). Oral gene delivery with chitosan–DNA nanoparticles generates immunologic protection in a murine model of peanut allergy. *Nature Medicine, 5*, 387-391. doi:10.1038/7385

Rudzinski, W. E., & Aminabhavi, T. M. (2010). Chitosan as a carrier for targeted delivery of small interfering RNA. *International Journal of Pharmaceutics, 399*(1-2), 1-11. doi:10.1016/j.ijpharm.2010.08.022

Samulowitz, U., Weber, M., Weeratna, R., Uhlmann, E., Noll, B., Krieg, A. M., & Vollmer, J. (2010). A novel class of immune-stimulatory CpG oligodeoxynucleotides unifies high potency in type I interferon induction with preferred structural properties. *Oligonucleotides, 20*(2), 93-101. doi:10.1089/oli.2009.0210

Sands, H., Gorey-Feret, L. J., Cocuzza, A. J., Hobbs, F. W., Chidester, D., & Trainor, G. L. (1994). Biodistribution and metabolism of internally 3H-labeled oligonucleotides. I. Comparison of a phosphodiester and a phosphorothioate. *Molecular Pharmacology, 45*(5), 932-943.

Scheiermann, J., & Klinman, D. M. (2014). Clinical evaluation of CpG oligonucleotides as adjuvants for vaccines targeting infectious diseases and cancer. *Vaccine, 32*(48), 6377–6389. doi:10.1016/j.vaccine.2014.06.065

Schmidt, M., Anton, K., Nordhaus, C., & Junghans, C. (2006). Cytokine and Ig-production by CG-containing sequences withphosphorodiester backbone and dumbbell-shape. *Allergy, 61*(1), 56-63. doi:10.1111/j.1398-9995.2005.00908.x

Scholz, C., & Wagner, E. (2012). Therapeutic plasmid DNA versus siRNA delivery: Common and different tasks for synthetic carriers. *Journal of Controlled Release, 161*, 554-565. doi:10.1016/j.jconrel.2011.11.014

Sellner, S., Kocabey, S., Nekolla, K., Krombach, F., Liedl, T., & Rehberg, M. (2015). DNA nanotubes as intracellular delivery vehicles in vivo. *Biomaterials, 53*, 453-463. doi:10.1016/j.biomaterials.2015.02.099

Shaikh, R., Singh, T. R., Garland, M. J., Woolfson, A. D., & Donnelly, R. F. (2011). Mucoadhesive drug delivery systems. *Journal of Pharmacy And Bioallied Sciences, 3*(1), 89-100. doi:10.4103/0975-7406.76478

Shirota, H., & Klinman, D. M. (2014). Recent progress concerning CpG DNA and its use as a vaccine adjuvant. *Expert Rev. Vaccines, 13*(2), 299-312. doi:10.1586/14760584.2014.863715

Singh, R., & Lillard, Jr., J. W. (2009). Nanoparticle-based targeted drug delivery. *Experimental and Molecular Pathology, 86*(3), 215-223. doi:10.1016/j.yexmp.2008.12.004

Siqueira, C., Picone, F., & Lopes Cunha, R. (2013). Chitosan–gellan electrostatic complexes: Influence of preparation conditions and surfactant presence. *Carbohydrate Polymers, 95*(1), 695-703. doi:10.1016/j.carbpol.2013.01.092

Slütter, B., Bal, S. M., Ding, Z., Jiskoot, W., & Bouwstra, J. A. (2011). Adjuvant effect of cationic liposomes and CpG depends on administration route. *Journal of Controlled Release, 154*(2), 123-130. doi:10.1016/j.jconrel.2011.02.007

Snider, M., Garg, R., Brownlie, R., van den Hurk, J. V., & van Drunen Littel-van den Hurk, S. (2014). The bovine viral diarrhea virus E2 protein formulated with a novel adjuvant induces strong, balanced immune responses and provides protection from viral challenge in cattle. *Vaccine, 32*(50), 6758-6754. doi:0.1016/j.vaccine.2014.10.010

Song, Y., Zhou, Y., van Drunen Littel-van den Hurk, S., & Chen, L. (2014). Cellulose-based polyelectrolyte complex nanoparticles for DNA vaccine delivery. *Biomaterials Science, 2*, 1440-1449. doi:10.1039/C4BM00202D

Song, Y.-C., & Liu, S.-J. (2015). A TLR9 agonist enhances the anti-tumor immunity of peptide and lipopeptide vaccines via different mechanisms. *Scientific Reports, 5*(12578). doi:10.1038/srep12578

Sreekumar, S., Goycoolea, F. M., Moerschbacher, B. M., & Rivera-Rodrigu, G. R. (2018). Parameters influencing the size of chitosan-TPP nano- and microparticles. *Scientific Reports, 8*, 4695. doi:10.1038/s41598-018-23064-4

Stahl, P. D., & Ezekowitz, R. B. (1998). The mannose receptor is a pattern recognition receptor involved in host defense. *Current Opinion in Immunology, 10*(1), 50-55. doi:10.1016/S0952-7915(98)80031-9

Stranda, S. R., Lelu, S., Reitan, N. K., de Lange Davies, C., Artursson, P., & Våru, K. M. (2010). Molecular design of chitosan gene delivery systems with an optimized balance between polyplex stability and polyplex unpacking. *Biomaterials, 31*(5), 975-987. doi:10.1016/j.biomaterials.2009.09.102

Suzuki, Y., Wakita, D., Chamoto, K., Narita, Y., Tsuji, T., Takesh, T., . . . Nishimura, T. (2004). Liposome-Encapsulated CpG Oligodeoxynucleotides as a Potent Adjuvant for Inducing Type 1 Innate Immunity. *Cancer Research, 64*(23), 8754-8760. doi:10.1158/0008-5472.CAN-04-1691

Szymańska, E., & Winnicka, K. (2015). Stability of Chitosan—A Challenge for Pharmaceutical and Biomedical Applications. *Marine Drugs, 13*(4), 1819-1847. doi:10.3390/md13041819

Takeda, K., Kaisho, T., & Akira, S. (2003). TOLL-like receptors. *Annu. Rev. Immunol., 21*, 335–376. doi:10.1146/annurev.immunol.21.120601.141126

Techaarpornkul, S., Wongkupasert, S., Opanasopit, P., Apirakaramwong, A., Nunthanid, J., & Ruktanonchai, U. (2010). Chitosan-Mediated siRNA Delivery In Vitro: Effect of Polymer Molecular Weight, Concentration and Salt Forms. *AAPS PharmSciTech, 11*(1), 64-72. doi:10.1208/s12249-009-9355-6

Tokunaga, T., Yamamoto, H., Shimada, S., Abe, H., Fukuda, T., Fujisawa, Y., . . . Suganuma, T. (1984). Antitumor Activity of Deoxyribonucleic Acid Fraction From Mycobacterium bovis BCG. I. Isolation, Physicochemical Characterization, and Antitumor Activity. *JNCI: Journal of the National Cancer Institute, 72*(4), 955–962. doi:10.1093/jnci/72.4.955

Vollmer, J., & Krieg, A. M. (2009). Immunotherapeutic applications of CpG oligodeoxynucleotide TLR9 agonists. *Advanced Drug Delivery Reviews, 61*, 195-204. doi:10.1016/j.addr.2008.12.008

Vollmer, J., Weeratna, R., Payette, P., Jurk, M., Schetter, C., Laucht, M., . . . Krieg, A. M. (2004). Characterization of three CpG oligodeoxynucleotide classes with distinct immunostimulatory activities. *European journal of immunology, 34*(1), 251-262. doi:10.1002/eji.200324032

Wan, B. W., & Punit, S. P. (2016). The Medicinal Chemistry of Therapeutic Oligonucleotides. *Journal of Medicinal Chemistry, 59*(21), 9646-9667. doi:10.1021/acs.jmedchem.6b00551

Wang, S., Campos, J., Gallotta, M., Gong, M., Crain, C., Naik, E., . . . Guiducci, C. (2016). Intratumoral injection of a CpG oligonucleotide reverts resistance to PD-1 blockade by expanding multifunctional CD8+ T cells. *PNAS, 113*(46), 7240-7249. doi:0.1073/pnas.1608555113

Wei, M., Chen, N., Li, J., Yin, M., Liang, L., He, Y., . . . Huang, Q. (2012). Polyvalent Immunostimulatory Nanoagents with Self-Assembled CpG Oligonucleotide-Conjugated Gold Nanoparticles. *Angewandte Chemie International Edition, 51*, 1202 –1206. doi:10.1002/anie.201105187

Wittig, B., Schmidt, M., Scheithauer, W., & Schmoll, H.-J. (2015). MGN1703, an immunomodulator and toll-like receptor 9 (TLR-9) agonist: From bench to bedside. *Critical Reviews in Oncology/Hematology, 94*(1), 31-44. doi:10.1016/j.critrevonc.2014.12.002

Xu, Y., Du, Y., Huang, R., & Gao, L. (2003). Preparation and modification of N-(2-hydroxyl) propyl-3-trimethyl ammonium chitosan chloride nanoparticle as a protein carrier. *Biomaterials, 24*(27), 5015-5022. doi:10.1016/S0142-9612(03)00408-3

Yan, N., & Chen, X. (2015). Sustainability: Don't waste seafood waste. *Nature, 524*(7564), 155-157. doi:10.1038/524155a.

Yi, A.-K., Peckham, D. W., Ashman, R. F., & Krieg, A. M. (1999). CpG DNA rescues B cells from apoptosis by activating NFκB and preventing mitochondrial membrane potential

disruption via a chloroquine-sensitive pathway. *International Immunology, 11*(12), 2015–2024. doi:10.1093/intimm/11.12.2015

Yin, H., Kanasty, R. L., Eltoukhy, A. A., Vegas, A. J., Dorkin, J. R., & Anderson, D. G. (2014). Non-viral vectors for gene-based therapy. *Nature Reviews Genetics, 15*, 541-555. doi:10.1038/nrg3763

Yuan, Q., Shah, J., Hein, S., & Misra, R. (2010). Controlled and extended drug release behavior of chitosan-based nanoparticle carrier. *Acta Biomaterialia, 6*(3), 1140-1148. doi:10.1016/j.actbio.2009.08.027

Zhang, H., & Gao, X.-D. (2017). Nanodelivery systems for enhancing the immunostimulatory effect of CpG oligodeoxynucleotides. *Materials Science and Engineering: C, 70*(2), 935-946. doi:10.1016/j.msec.2016.03.045

Zhang, H., Yan, T., Xu, S., Feng, S., Huang, D., Fujita, M., & Gao, X.-D. (2017). Graphene oxide-chitosan nanocomposites for intracellular delivery of immunostimulatory CpG oligodeoxynucleotides. *Materials Science and Engineering C, 73*, 144-151. doi:10.1016/j.msec.2016.12.072

Zhang, L., Zhu, G., Mei, L., Wu, C., Qiu, L., Cui, C., . . . Tan, W. (2015). Self-Assembled DNA Immunonanoflowers as Multivalent CpG Nanoagents. *ACS applied materials & interfaces, 7*(43), 24069-24074. doi:10.1021/acsami.5b06987

Zhao, F., Zhao, Y., Liu, Y., Chang, X., Chen, C., & Zhao, Y. (2011). Cellular Uptake, Intracellular Trafficking, and Cytotoxicity of Nanomaterials. *Nanotechnology with Soft Matter, 7*(10), 1322-1337. doi:10.1002/smll.201100001

Zimmermann, S., Heeg, K., & Dalpke, A. (2003). Immunostimulatory DNA as adjuvant: efficacy of phosphodiester CpG oligonucleotides is enhanced by 3′ sequence modifications. *Vaccine, 21*(9-10), 990-995. doi:10.1016/S0264-410X(02)00550-9

Zwiorek, K., Bourquin, C., Battiany, J., Winter, G., Endres, S., Hartmann, G., & Coester, C. (2008). Delivery by Cationic Gelatin Nanoparticles Strongly Increases the Immunostimulatory Effects of CpG Oligonucleotides. *Pharmaceutical Research, 25*(3), 551-562. doi:10.1007/s11095-007-9410-5

Suplementary information

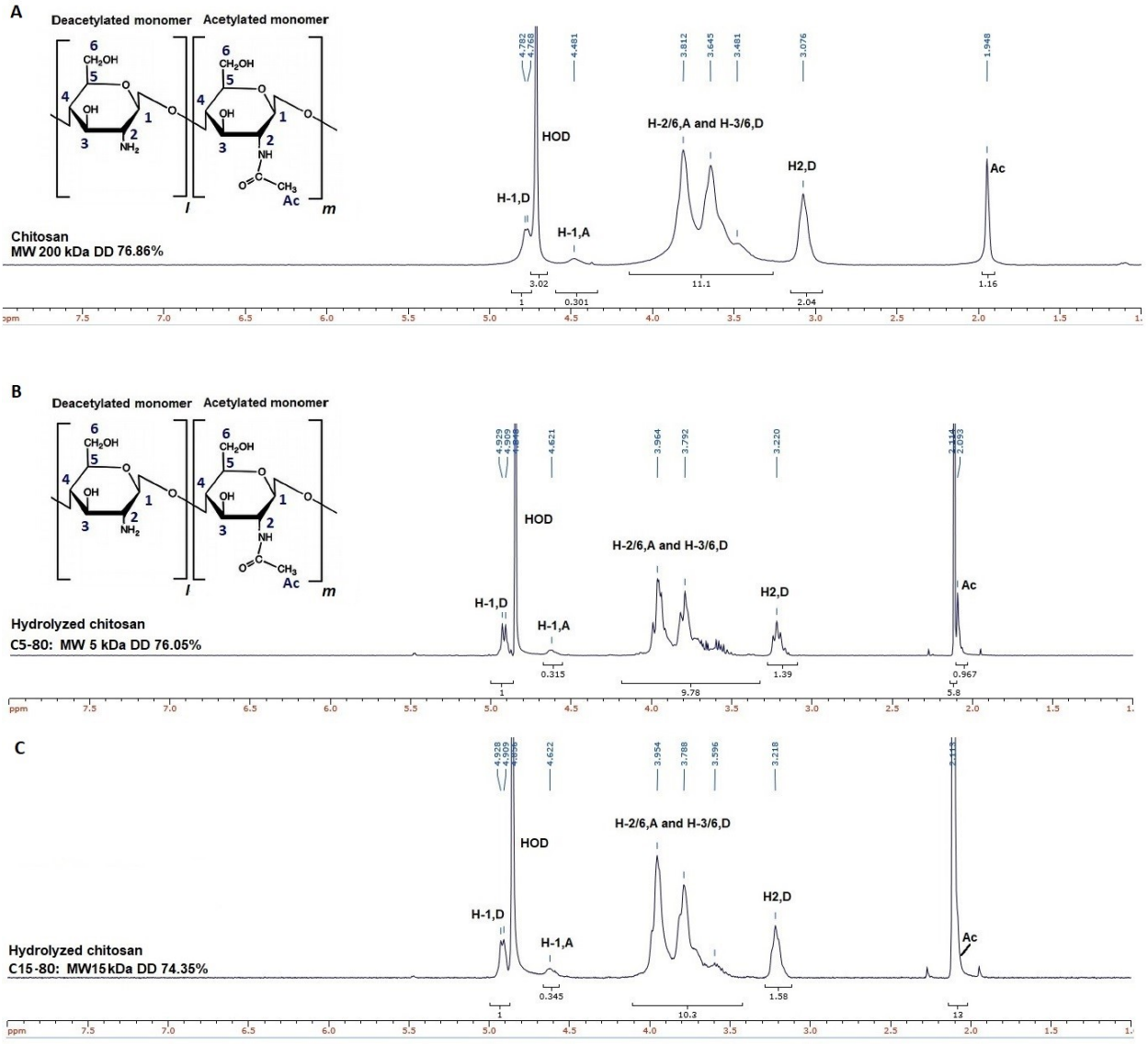

Figure A2-1. The ^{1}H NMR spectrum of (A) parental LMW chitosan, (B) C5-80, and (C) C15-80 samples.

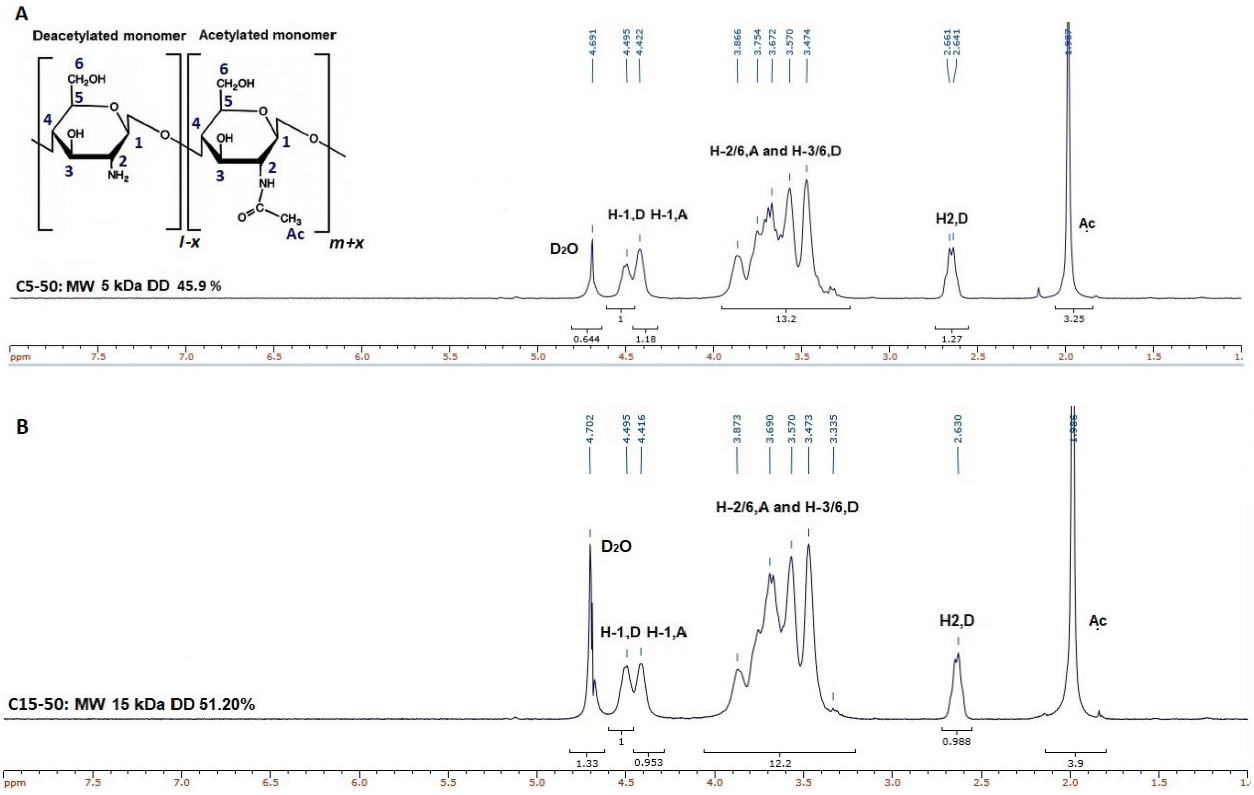

Figure A2-2. The ^{1}H NMR spectrum of (A) C5-50 and (B) C15-50, partially N-acetylated LMW chitosan samples.

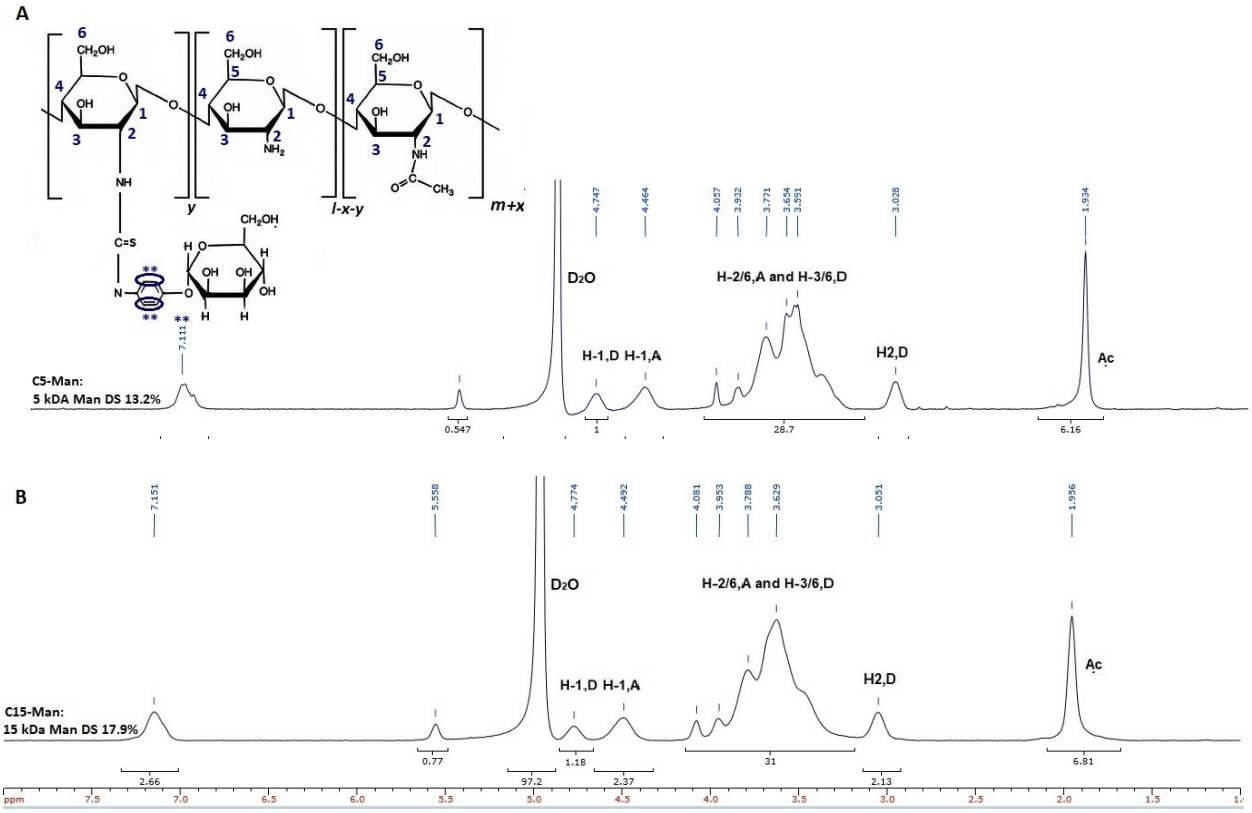

Figure A2-3. The ^{1}H NMR spectrum of (A) C5-Man and (B) C15-Man, mannosylated LMW chitosan samples.

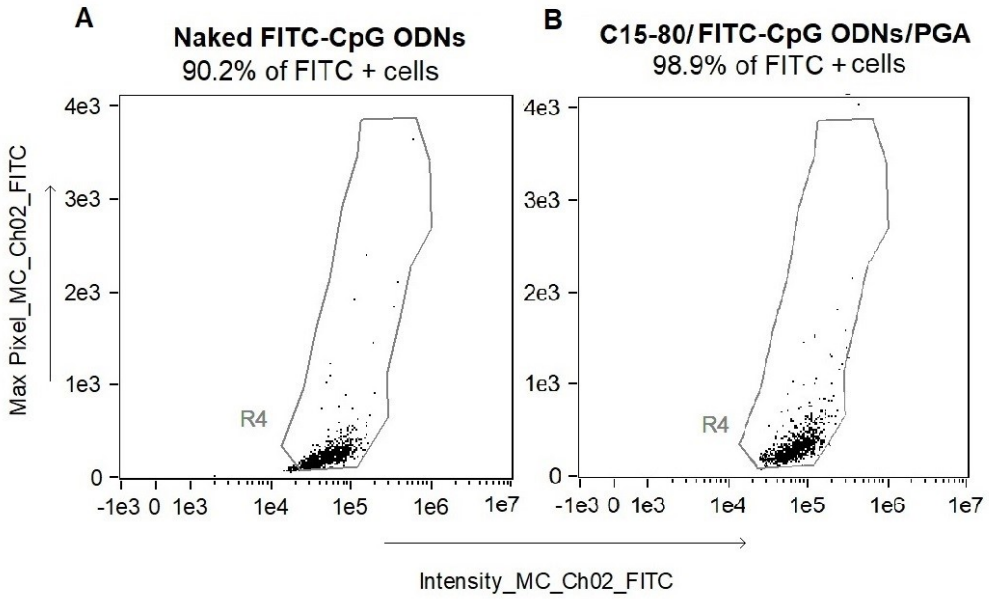

Figure A2-4. Identification of RAW 264.7 cells positive for FITC fluorescence using the Max Pixel and the Intensity feature. (A) Cells exposed to naked FITC-CpG ODNs for 4 h. (B) Cells exposed to the C18-80/ PGA/ FITC-CpG ODN for 4 h.